

104

SQR

# A Reproduced Copy OF

(NASA-CR-133100) INFRARED SPECTRA OF  
GROUP III A METAL OXIDES (Case Western  
Reserve Univ.) 138 p. CSCL 07D

N73-26102

G3/06    Unclass  
          07416

Reproduced for NASA

*by the*

**NASA Scientific and Technical Information Facility**

Reproduced by  
**NATIONAL TECHNICAL  
INFORMATION SERVICE**  
US Department of Commerce  
Springfield, VA. 22151

PRICES SUBJECT TO CHANGE



FFNo 672 Aug 65

138

FRED J. KOHL

INFRARED SPECTRA OF GROUP III A METAL OXIDES

*by*

Denis Aloysius Lynch, Jr.

*Department of Chemistry*

*CASE WESTERN RESERVE UNIVERSITY*

*June 1972*

*i*

# Infrared Spectra of Group III A Metal Oxides

by

Denis Aloysius Lynch, Jr.

## ABSTRACT

The primary molecules produced in the vaporization of the group III A metals and their solid sesquioxides are the suboxide species  $M_2O$ . However, other metal-oxides, such as  $MO$ ,  $M_2O_2$ , and in specific instances  $MO_2$  and  $M_4O_2$ , have also been shown to exist in minor concentrations. Very little structural data is available for these oxides since most investigations have been limited by the great preponderance of the suboxide molecule in the vapor phase. This latter species has been studied over the past ten years with only a moderate degree of success.

Infrared analyses of the suboxides have been contradictory. The  $\nu_3$  asymmetric stretching mode had been observed by both gas phase and matrix isolation spectroscopy. However, it was not until 1971 that the  $\nu_1$  symmetric stretching mode for  $Tl_2O$  was detected. Later the same year both the  $\nu_1$  stretching and  $\nu_2$  bending modes for all the suboxides were reported. Unfortunately, the results of the two investigations were not in agreement other than to indicate that the previous  $\nu_3$  assignments were correct and that the suboxides possess  $C_{2v}$  symmetry.

The experiments and analyses described in this dissertation were undertaken to measure the infrared frequencies of metal-oxygen

species which could be formed in the matrix and to investigate with an oxygen -18 enrichment study the controversy on the vibrational assignments for the suboxide. In the course of this research several new molecules,  $\text{Al}_3\text{O}_2$ ,  $\text{Ga}_3\text{O}$ ,  $\text{In}_3\text{O}$ ,  $\text{In}_4\text{O}_2$ ,  $\text{InTaO}$ ,  $\text{InTaO}_2$ , and  $\text{In}_2\text{WO}_4$ , were found by mass spectrometric sampling to exist in extremely minor concentrations in the vapor phase. The latter three species were formed by reaction with the crucible materials and were unimportant for an infrared analysis.

The infrared spectroscopic measurements were obtained by the matrix isolation technique of molecular beam sampling. In the first set of experiments, the  $\text{MO}_2$  species were formed by direct reaction between metal and  $\text{O}_2$  in the matrix. A  $\text{C}_{2v}$  structure and an O-M-O bond angle near  $40^\circ$  was favored for these molecules by analogy with a similar investigation of the alkali metals. The following vibrational frequencies were determined:  $\nu_1 = 1116.0 \text{ cm}^{-1}$  ( $\text{AlO}_2$ );  $\nu_1 = 1088.4 \text{ cm}^{-1}$ ;  $\nu_2 = 383.3 \text{ cm}^{-1}$  ( $\text{GaO}_2$ );  $\nu_1 = 1082.3 \text{ cm}^{-1}$ ;  $\nu_2 = 332.2 \text{ cm}^{-1}$ ;  $\nu_3 = 456.4 \text{ cm}^{-1}$  ( $\text{InO}_2$ );  $\nu_1 = 1082.1 \text{ cm}^{-1}$ ;  $\nu_2 = 295.9 \text{ cm}^{-1}$ ;  $\nu_3 = 432.9 \text{ cm}^{-1}$  ( $\text{TlO}_2$ ).

The second set of experiments with oxygen -18 enriched samples definitely proved that the previous  $\nu_3$  suboxide assignments were correct for  $\text{Al}_2\text{O}$ ,  $\text{Ga}_2\text{O}$ ,  $\text{In}_2\text{O}$ , and  $\text{InGaO}$ . However, the reported  $\nu_1$  and  $\nu_2$  modes for these same species were established to belong instead to the  $\text{M}_4\text{O}_2$  dimer. Force constants were calculated from a model based upon a slightly skewed octahedral complex with  $\text{C}_{2h}$  symmetry.

## ACKNOWLEDGEMENTS

The author wishes to express his appreciation for the assistance and guidance of Professor K. Douglas Carlson during the course of this research. His interest, insight, and support were invaluable towards the completion of this work.

The author thanks both the National Aeronautics and Space Administration and the National Science Foundation for support through a NASA Predoctoral Traineeship (1967-1969) and a NSF Predoctoral Fellowship (1969-1971).

The author is grateful to Dr. Fred J. Kohl for many interesting discussions and his aid with the mass spectrometric experiments. He wishes to thank Mr. Carl A. Stearns for his assistance in performing the mass spectrometer experiments.

Appreciation is extended to the author's associates in the High Temperature Chemistry Laboratory for their friendship and help. The author is especially grateful to Mr. Michael Zehe who assisted in several phases of this research, and to Mr. Reed Corderman who helped perform some of the experiments. He also wishes to sincerely thank Drs. Daniel Makowiecki and Michael Sink for many helpful suggestions and words of wisdom.

A special note of thanks and appreciation is extended to the author's wife, Annette, for her patience, understanding, and encouragement during the course of this investigation. It is to her that this dissertation is dedicated.

The careful typing of this thesis by Mrs. Marlene Carlson is

greatly appreciated.

This research was supported by a grant from the National  
Science Foundation.

## TABLE OF CONTENTS

	Page
ABSTRACT.....	ii
ACKNOWLEDGEMENTS.....	iv
LIST OF TABLES.....	ix
LIST OF FIGURES.....	xi
Chapter 1. INTRODUCTION.....	1
Chapter 2. BACKGROUND INFORMATION.....	4
2.1 Geometry and Spectroscopic Data of the Suboxides.....	4
2.2 Other Vapor Species.....	11
Chapter 3. MASS SPECTROMETRIC INVESTIGATIONS.....	14
3.1 Experimental Apparatus and Technique.....	14
3.2 Identification of Vapor Species.....	15
a) Aluminum-Oxygen System.....	15
b) Gallium-Oxygen System.....	18
c) Indium-Oxygen System.....	18
Chapter 4. MATRIX ISOLATION TECHNIQUE AND APPARATUS.....	24
4.1 Matrix Isolation Technique.....	24
4.2 Experimental Equipment.....	25
a) The Cryostat and Condensation Target.....	25
b) Superstructure and Infrared Instrumentation.....	27
c) Matrix Gases and Chemicals.....	28
d) Knudsen Cell Assembly.....	28
e) Dry Box.....	31

	Page	
4.3	Experimental Procedures.....	34
	a) Matrix Isolation Ratio.....	34
	b) Vapor Pressures for Suboxides and Metals.....	35
	c) Procedure Additions.....	35
Chapter 5.	MATRIX ISOLATION EXPERIMENTS.....	39
5.1	Mixed Matrix Experiments.....	39
	a) Thallium and Thallium Suboxide.....	39
	b) Indium and Indium Suboxide.....	43
	c) Gallium and Gallium Suboxide.....	50
	d) Aluminum and Aluminum Suboxide.....	53
5.2	Isotopic Investigation of the Suboxides.....	62
	a) Aluminum Suboxide.....,.....	62
	b) Gallium Suboxide.....	68
	c) Indium Gallium Suboxide.....	80
5.3	Additional Experiments and Review of Earlier Research.....	83
	a) Aluminum Suboxide Diffusion Study.....	83
	b) A New Look at the InGaO System.....	83
Chapter 6.	VIBRATIONAL ASSIGNMENTS AND STRUCTURAL ANALYSIS.....	92
6.1	Assignment of M + O <sub>2</sub> Frequencies.....	92
	a) Tl + O <sub>2</sub> .....	93
	b) In + O <sub>2</sub> .....	94
	c) Ga + O <sub>2</sub> .....	94
	d) Al + O <sub>2</sub> .....	95

	Page
6.2 Force Constants and Bond Angles for the Superoxides.....	96
6.3 Analysis for $M_2O$ in Ar + $O_2$ .....	103
6.4 Assignment of $^{18}O$ Suboxide Frequencies.....	104
6.5 Structural Analysis of $M_4O_2$ .....	107
Chapter 7. DISCUSSION OF THE RESULTS.....	115
APPENDIX 1. EQUATIONS FOR $M_4O_2$ VIBRATIONS.....	118
APPENDIX 2. THERMODYNAMIC FUNCTIONS FOR TWO GROUP III A METAL SUPEROXIDES.....	122
BIBLIOGRAPHY.....	124

LIST OF TABLES

	Page	
2.1-1	Vibrational Frequencies ( $\text{cm}^{-1}$ ) for the Group III A Suboxides Reported Prior to this Work.....	8
3.2-1	Mass Spectrum of the Vapor over Al(l) + $\text{Al}_2\text{O}_3(\text{s})$ (30 eV electrons).....	17
3.2-2	Mass Spectrum of the Vapor over Ga(l) + $\text{Ga}_2\text{O}_3(\text{s})$ (30 eV electrons).....	19
3.2-3	Mass Spectrum of the Vapor over In(l) + $\text{In}_2\text{O}_3(\text{s})$ (30 eV electrons).....	20
4.2-1	Research Chemicals.....	29
4.3-1	Summary of Vapor Pressure Equations.....	36
5.1-1	Infrared Frequencies ( $\text{cm}^{-1}$ ) of Tl and $\text{Tl}_2\text{O}$ Matrix Reactions with $\text{O}_2$ in Ar.....	46
5.1-2	Infrared Frequencies ( $\text{cm}^{-1}$ ) of In and $\text{In}_2\text{O}$ Matrix Reactions with $\text{O}_2$ in Ar.....	51
5.1-3	Infrared Frequencies ( $\text{cm}^{-1}$ ) of Ga and $\text{Ga}_2\text{O}$ Matrix Reactions with $\text{O}_2$ in Ar.....	55
5.1-4	Infrared Frequencies ( $\text{cm}^{-1}$ ) of Al and $\text{Al}_2\text{O}$ Matrix Reactions with $\text{O}_2$ in Ar ( $\text{N}_2$ ).....	60
5.2-1	Infrared Frequencies ( $\text{cm}^{-1}$ ) of Oxygen-18 Enriched $\text{Al}_2\text{O}$ in Ar (Exp. 3.).....	69
5.2-2	Infrared Frequencies of Oxygen-18 Enriched $\text{Ga}_2\text{O}$ .....	78
5.2-3	Infrared Frequencies ( $\text{cm}^{-1}$ ) of Oxygen-18 Enriched $\text{Ga}_2\text{O}$ , $\text{InGaO}$ , and $\text{In}_2\text{O}$ in Ar.....	82
5.3-1	Infrared Frequencies ( $\text{cm}^{-1}$ ) of $\text{Al}_2\text{O}$ in Ar.....	88
5.3-2	Infrared Frequencies ( $\text{cm}^{-1}$ ) of the $\text{InGaO}$ System From 500-640 $\text{cm}^{-1}$ .....	91
6.1-1	Vibrational Assignments for the $\text{MO}_2$ Molecules.....	97

	Page	
6.2-1	Potential Functions Applied to the Group III A Superoxides.....	97
6.2-2	Force Constants of In and Tl Superoxides Under the Assumption of a Central Force Field and Modified Central Force Field.....	98
6.2-3	Metal-Oxygen and Oxygen Stretching Force Constants and Bond Lengths.....	101
6.2-4	Corrected Superoxide Force Constants and Bond Lengths.....	102
6.4-1	Bond Angles Calculated from Isotopic Data.....	105
6.4-2	Estimated Vibrational Frequencies for the Group III A Suboxides.....	108
6.5-1	Calculations for Group III A Metal Suboxide Dimers.....	112
A.2-1	Thermodynamic Functions for $\text{InO}_2$ .....	122
A.2-2	Thermodynamic Functions for $\text{TlO}_2$ .....	123

LIST OF FIGURES

	Page
4.2-1	Cross Section of the Cryostat..... 26
4.2-2	Knudsen Cells..... 32
5.1-1	Infrared Spectrum of Tl in Ar + O <sub>2</sub> ..... 40
5.1-2	Infrared Spectrum of Tl <sub>2</sub> O in Ar + O <sub>2</sub> ..... 42
5.1-3a	Infrared Spectrum of Tl and Tl <sub>2</sub> O in Ar + O <sub>2</sub> (IR-11)..... 44
5.1-3b	Infrared Spectrum of Tl and Tl <sub>2</sub> O in Ar + O <sub>2</sub> (IR-7)..... 45
5.1-4	Infrared Spectrum of In in Ar + O <sub>2</sub> (a. IR-7, b. IR-11)..... 48
5.1-5	Infrared Spectrum of In <sub>2</sub> O in Ar + O <sub>2</sub> ..... 49
5.1-6	Infrared Spectrum of Ga + Ga <sub>2</sub> O in Ar + O <sub>2</sub> (a. IR-7, b. IR-11)..... 52
5.1-7	Infrared Spectrum of Ga + Ga <sub>2</sub> O in Ar + O <sub>2</sub> ..... 54
5.1-8	Infrared Spectrum of Al in Ar + O <sub>2</sub> (a. Before Diffusion, b. After Diffusion)..... 56
5.1-9	Infrared Spectrum of Al in Ar + O <sub>2</sub> (a. After 1 Diffusion, b. After Several Diffusions)..... 57
5.1-10	Infrared Spectrum of Al + Al <sub>2</sub> O in Ar + O <sub>2</sub> ..... 59
5.2-1	Infrared Spectrum of <sup>18</sup> O Enriched Al <sub>2</sub> O in Ar..... 63
5.2-2	Infrared Spectrum of <sup>18</sup> O Enriched Al <sub>2</sub> O in Ar (a. Before Diffusion, b. After Diffusion)..... 65
5.2-3	Infrared Spectrum of <sup>18</sup> O Enriched Al <sub>2</sub> O in Ar Before Diffusion..... 66
5.2-4	Infrared Spectrum of <sup>18</sup> O Enriched Al <sub>2</sub> O in Ar After Several Diffusions..... 67
5.2-5	Infrared Spectrum of <sup>18</sup> O Enriched Ga <sub>2</sub> O in Ar (Before Diffusion)..... 70

	Page	
5.2-6	Infrared Spectrum of $^{18}\text{O}$ Enriched $\text{Ga}_2\text{O}$ in Ar (After Diffusion).....	71
5.2-7	Partial Infrared Spectrum of $^{18}\text{O}$ Enriched $\text{Ga}_2\text{O}$ in Ar (a. Before Diffusion, b. After Diffusion).....	72
5.2-8	Infrared Spectrum of $^{18}\text{O}$ Enriched $\text{Ga}_2\text{O}$ in $\text{N}_2$ (Before Diffusion).....	74
5.2-9	Infrared Spectrum of $^{18}\text{O}$ Enriched $\text{Ga}_2\text{O}$ in $\text{N}_2$ (After Diffusion).....	75
5.2-10	Infrared Spectrum of $^{18}\text{O}$ Enriched $\text{Ga}_2\text{O}$ in Ar Before Diffusion.....	76
5.2-11	Infrared Spectrum of $^{18}\text{O}$ Enriched $\text{Ga}_2\text{O}$ in Ar After Diffusion.....	77
5.2-12	Infrared Spectrum of $^{18}\text{O}$ Enriched $\text{Ga}_2\text{O}$ , $\text{InGaO}$ , and $\text{In}_2\text{O}$ in Ar.....	81
5.3-1.	Infrared Spectrum of $\text{Al}_2\text{O}$ in Ar Before Diffusion.....	84
5.3-2	Infrared Spectrum of $\text{Al}_2\text{O}$ in Ar After Diffusion.....	85
5.3-3	Infrared Spectrum of $\text{Al}_2\text{O}$ in Ar After Four Diffusions.....	86
5.3-4	Partial Infrared Spectrum of $\text{InGaO}$ System in Ar (a. Before Diffusion, b. After Diffusion).....	87
5.3-5	Partial Infrared Spectrum of $\text{InGaO}$ System in $\text{N}_2$ .....	90
6.5-1	Possible $\text{M}_4\text{O}_2$ Structures.....	109
6.5-2	$\text{InGaO}$ System Dimers.....	114
A.1-1	$\text{M}_4\text{O}_2$ Dimer Structure.....	119

## CHAPTER 1

### INTRODUCTION

Many interesting molecules are formed in vaporization processes at high temperatures. The existence of such molecules has usually been confirmed by mass spectrometry, but this gives no structural information. Therefore, other types of studies are necessary to obtain these important data. Although there are several possibilities, most are limited by the severe thermal conditions required to obtain a sufficient concentration of molecules.

Infrared spectroscopy is one useful method which has been applied to high temperature investigations. Originally, measurements of the heated vapors were taken directly.<sup>1-3</sup> This had the advantage that both emission and absorption experiments could be performed on vapors at equilibrium. Unfortunately, there were often problems in the interpretation of the spectra. Absorptions were broadened by vibration-rotation interactions or even obscured by background radiation, and in some experiments molecular interactions were found. Molecules often condensed on parts of the optical system. Furthermore, only equilibrium systems could be studied. However, with the development of matrix isolation spectroscopy<sup>4-6</sup> most of these problems were circumvented, so that infrared studies of high temperature species became experimentally feasible. This dissertation is concerned with the application of infrared spectroscopy, using the matrix isolation technique, to the study of several oxides of the group III A metals: aluminum, gallium, indium, and thallium.

In previous investigations<sup>7-13</sup> reported for these molecules, it has been found that several oxide species exist in the vapors from a heated mixture of metal and metal sesquioxide. However, the suboxide molecule  $M_2O$  has been shown to be the major component of the vapor. Several attempts<sup>14-18</sup> have been made to determine the fundamental frequencies of these molecules. In a recent study<sup>13,19</sup> carried out in this laboratory, frequencies assigned to the  $\nu_2$  bending mode for all the suboxides were reported for the first time along with new data for the symmetric stretching frequencies  $\nu_1$ . The bending frequency was found to occur at a much higher energy than that predicted,<sup>15</sup> suggesting a possible ring structure with appreciable metal-metal bonding. Also a new molecule,  $InGaO$ , was found and studied.

The present study involves three types of experiments which were undertaken to provide additional and important information on these molecules. First, a careful mass spectrometric investigation was undertaken to determine all species which might exist in the vapor phase above a heated sample of metal and metal sesquioxide. This was carried out to check if any reported suboxide absorptions could possibly belong to other species. The previous experiments had not examined the possible existence of high molecular weight molecules such as dimer species. Several new molecules in extremely low concentrations are reported here. Secondly, experiments were carried out to produce molecules by direct reaction of species in the matrix. These experiments were based on methods recently described by Andrews<sup>20-23</sup> for producing unusual alkali metal oxides. The present reaction experiments were performed to check whether modes previously

assigned to those of the suboxides might instead be due to other kinds of molecules produced by diffusion and reaction. For the third set of experiments  $^{18}\text{O}$  enrichment studies were carried out to provide information for more conclusive assignments of frequencies. These various experiments provide the basis for a reassignment of previously reported frequencies and additional new information on the structures of the group III A metal oxides.

## CHAPTER 2

## BACKGROUND INFORMATION

2.1 Geometry and Spectroscopic Data of the Suboxides

The  $M_2O$  species, as triatomic molecules, must have  $C_{2v}$ ,  $D_{\infty h}$ ,  $C_s$ , or  $C_{\infty v}$  symmetry. Linevsky *et al.*<sup>15</sup> first demonstrated that the two antisymmetric configurations,  $C_s$  and  $C_{\infty v}$ , for  $Al_2O$  could be ruled out on thermochemical grounds. The dissociation energies indicated that an unsymmetrical Al-Al-O molecule would require a large distortion in the Al-O and Al-Al bond energies to account for the  $Al_2O$  experimental dissociation energy. Recently, Makowiecki<sup>13</sup> reported not only similar results for gallium and indium suboxides but also that the best agreement was obtained when a ring structure was postulated involving  $C_{2v}$  symmetry and metal-metal bonding.

An early electron diffraction study by Rambidi and Tolmachev<sup>24</sup> of gaseous  $Ga_2O$  and  $In_2O$  indicated that these molecules were of  $C_{2v}$  geometry with apex angles of 140 and  $150 \pm 10^\circ$ , respectively. However, in a later report Rambidi and Ezhov<sup>25</sup> reevaluated the previous data to investigate the possibility of the bending mode lying below  $200 \text{ cm}^{-1}$ , as had been indicated from the spectroscopic report of Linevsky *et al.*<sup>15</sup> They then concluded that the molecules had a linear structure because of a large effective contraction of the molecular core indicated by a low-lying deformation mode. An earlier electric deflection study by Büchler *et al.*<sup>26</sup> had indicated a linear structure for  $Al_2O$  since the molecule did not refocus in an inhomogeneous electric field. However, the sensitivity of this experiment is in doubt

because later experiments demonstrated that at the time the instrumentation could not distinguish weak dipole moments of molecules with bond angles above  $140^\circ$ .

An infrared analysis may be useful in determining structure. A symmetric triatomic molecule has three vibrational modes: symmetric stretching ( $\nu_1$ ), bending ( $\nu_2$ ), and asymmetric stretching ( $\nu_3$ ). Only  $\nu_2$  and  $\nu_3$ , with  $\nu_2$  being doubly degenerate, are allowed in the infrared for a linear  $D_{\infty h}$  geometry. For a  $C_{2v}$  structure, all three modes are infrared active and non-degenerate. The appearance of a  $\nu_1$  symmetric stretching mode would indicate  $C_{2v}$  symmetry, but its absence only shows that its relative intensity is at best quite weak. Another indication of structure is the bond angle which may be determined by isotopic substitution. The  $\nu_3$  splittings are calculated from the relationship,

$$\frac{(\nu_3^i)^2}{(\nu_3)^2} = \frac{M_o M_m^i (M_o^i + 2M_m^i \sin^2 \alpha)}{M_o^i M_m^i (M_o + 2M_m \sin^2 \alpha)}, \quad (2.1-1)$$

given by Herzberg<sup>27</sup> for symmetric triatomic molecules. In this expression  $M_m$  and  $M_o$  represent the masses of the metal and oxygen atoms, respectively,  $i$  an isotope,  $\alpha$  one-half the M-O-M bond angle, and  $\nu_3$  the antisymmetric stretching frequency. It is easily shown that a precision of better than  $0.1 \text{ cm}^{-1}$  is required for unequivocal geometric definition. This is difficult to achieve due to either instrumentation limitations or matrix perturbations causing shifts in the frequencies.

The first infrared investigation of these systems was performed by Mal'tsev and Shevel'kov.<sup>14</sup> Their experiments involved a direct gas

phase analysis of  $\text{Al}_2\text{O}$ ,  $\text{Ga}_2\text{O}$ , and  $\text{In}_2\text{O}$ . Both  $\nu_1$  and  $\nu_3$  were reported for the latter two and only  $\nu_3$  for  $\text{Al}_2\text{O}$ . Unfortunately, a lack of isotopic data and the rather broad absorptions leave the results in doubt.

The next investigation was reported by Linevsky, White, and Mann<sup>15</sup> on  $\text{Al}_2\text{O}$  in argon and krypton matrices. In this study both  $\nu_3$  and  $\nu_1$  were found. Isotopic data indicated a bent structure of  $C_{2v}$  symmetry with a bond angle of  $145 \pm 5^\circ$ . The  $\nu_1$  mode was quite weak and did not appear until a relatively heavy matrix was deposited. There was no hint of a  $\nu_2$  mode as low as  $250 \text{ cm}^{-1}$ , the limit of their instrument. An estimate of  $240 \text{ cm}^{-1}$  for this mode was made from an earlier ultraviolet study<sup>28</sup> of  $\text{Al}_2\text{O}$  gas.

In 1969, Hinchcliffe and Ogden<sup>16</sup> reported the asymmetric stretching frequencies for  $\text{Ga}_2\text{O}$ ,  $\text{In}_2\text{O}$ , and  $\text{Tl}_2\text{O}$  in nitrogen matrices. From <sup>18</sup>O data the bond angles were calculated to be  $143^\circ$ ,  $135^\circ$ , and  $131^\circ$  for the respective suboxides which indicated  $C_{2v}$  structure. This report gave no indication of either the  $\nu_1$  or  $\nu_2$  modes. Later Ogden et al.<sup>29</sup> published a short note on the non-dissociative reaction of oxygen with heated thallium metal. Experiments with <sup>16</sup>O-<sup>18</sup>O indicated a triplet structure near  $510 \text{ cm}^{-1}$  which was assigned to an  $\text{M}_x\text{O}_2$  molecule. A deposit of enriched  $\text{Tl}_2\text{O}$  gave a similar spectrum.

In a recent investigation at this laboratory, Makowiecki<sup>13,19</sup> reported all three modes for  $\text{Al}_2\text{O}$ ,  $\text{Ga}_2\text{O}$ ,  $\text{In}_2\text{O}$ ,  $\text{Tl}_2\text{O}$ , and a new molecule  $\text{InGaO}$ . The  $\nu_3$  and  $\nu_1$  data for  $\text{Al}_2\text{O}$  was in agreement with Linevsky, and the  $\nu_3$  values for  $\text{Ga}_2\text{O}$ ,  $\text{In}_2\text{O}$ , and  $\text{Tl}_2\text{O}$  corresponded to those in the Hinchcliffe and Ogden report. The  $\nu_1$  and  $\nu_2$  absorptions were

fairly intense except for  $\text{Al}_2\text{O}$  which required heavy deposits before they were observed. Simple frequency ratios of  $\nu_1/\nu_3$  and  $\nu_2/\nu_3$  determined that the three frequencies belonged to similar molecules in each system. The bending mode was found at relatively high values and was taken as an indication of a ring type structure involving metal-metal bonding. No absorptions were observed in the far infrared, and isotopic data was not available for positive identification or for force constant calculations.

Three other reports were published at this time. Shevel'kov, Klyuev, and Mal'tsev<sup>30</sup> obtained infrared data for the gas phase values of  $\text{Tl}_2\text{O}$ . All observed absorptions were comparable to those found above, although overtone assignments were slightly different. The major disparity was the absence of any  $\nu_2$  mode. A short note by Snelson<sup>17</sup> indicated that previously published  $\nu_1$  and  $\nu_3$  data for  $\text{Al}_2\text{O}$  were correct. The  $\nu_2$  mode was not observed above  $200\text{ cm}^{-1}$ , and the value of  $240\text{ cm}^{-1}$ , predicted by Linevsky, was shown to be an  $\text{AlO}$  absorption. A new prediction of  $120\text{ cm}^{-1}$  was made for the bending mode, which from mass considerations would place values for the other suboxide molecules below  $100\text{ cm}^{-1}$ . More recently, Brom, Devore, and Franzen<sup>18</sup> reported a matrix infrared investigation of  $\text{Tl}_2\text{O}$ . A new assignment for  $\nu_1$  was made with  $^{16}\text{O}$ - $^{18}\text{O}$  data. The  $\nu_1$  and  $\nu_2$  modes reported by Makowiecki were interpreted as probable dimer bands from  $\text{Tl}_4\text{O}_2$ . However, these experiments were difficult to interpret, for much of the  $^{18}\text{O}$  enrichment had been lost due to an atmospheric leak. The results of all these spectroscopic investigations are summarized in Table 2.1-1.

Table 2.1-1. Vibrational Frequencies ( $\text{cm}^{-1}$ ) for the Group III A Suboxides Reported Prior to this Work.

Species	$\nu_3(160)$	$\nu_3(180)$	$\nu_2$	$\nu_1(160)$	$\nu_1(180)$	Apex Angle	$r_{\text{m-o}}(\text{\AA})$	Method	Ref.
$\text{Al}_2\text{O}$	950							Gas Phase Spectra	a
$\text{Al}_2\text{O}$	994	951	[238]	715	700	$145 \pm 5$	1.66	Argon Matrix	b
$\text{Al}_2\text{O}$	988	946		709	694			Krypton Matrix	b
$\text{Al}_2\text{O}$	991.7		503	715.9				Argon Matrix	c
$\text{Al}_2\text{O}$	989.4		499	710				Krypton Matrix	c
$\text{Ga}_2\text{O}$	770			420				Gas Phase Spectra	a
$\text{Ga}_2\text{O}$	809.4	768.5				$143 \pm 5$	1.86	Nitrogen Matrix	d
$\text{Ga}_2\text{O}$	808.1		425.8	590.4				Nitrogen Matrix	c
$\text{Ga}_2\text{O}$	(822.6) (817.9)		416.5	595.6				Argon Matrix	c
$\text{In}_2\text{O}$	770			360				Gas Phase Spectra	a

Table 2.1-1. (Continued)

Species	$\nu_3(^{16}\text{O})$	$\nu_3(^{18}\text{O})$	$\nu_2$	$\nu_1(^{16}\text{O})$	$\nu_1(^{18}\text{O})$	Apex Angle	$r_{\text{m-o}}(\text{\AA})$	Method	Ref.
$\text{In}_2\text{O}$	722.4	684.3				135±7	2.04	Nitrogen Matrix	d
$\text{In}_2\text{O}$	721.8		412.6	595.6				Nitrogen Matrix	c
$\text{In}_2\text{O}$	(734.9) (741.3)		404.3	555.1				Argon Matrix	c
$\text{In}_2\text{O}$	745.4		404.8	560.3				Neon Matrix	c
$\text{In}_2\text{O}$	728.2		403.2	531.7				Krypton Matrix	c
$\text{Tl}_2\text{O}$	625.3	591.2				131±11	2.19	Nitrogen Matrix	d
$\text{Tl}_2\text{O}$	626.1		390.6	506.3				Nitrogen Matrix	c
$\text{Tl}_2\text{O}$	(646.6) (659.8)		381.5 <sup>f</sup>	510.1 <sup>f,8</sup>				Argon Matrix	c
$\text{Tl}_2\text{O}$	643.3	609.3	[130]	571	545	90	1.86	Argon Matrix	e
$\text{Tl}_2\text{O}$	634.6	600.3		560.4	535.7			Krypton Matrix	e

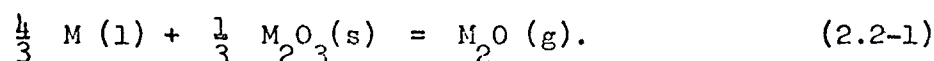
Table 2.1-1. (Continued)

Species	$\nu_3(^{16}\text{O})$	$\nu_3(^{18}\text{O})$	$\nu_2$	$\nu_1(^{16}\text{O})$	$\nu_1(^{18}\text{O})$	Apex Angle	$r_{\text{m-o}}(\text{\AA})$	Method	Ref.
InGaO	(788.9) (793.1)		431.4	550.5				Argon Matrix	c
InGaO	783.0			544.2				Nitrogen Matrix	c

- a. A. A. Mal'tsev and V. F. Shevel'kov, *Teplofiz, Vysok. Temp.* 2, 560 (1964).
- b. M. J. Linevsky, D. White, and D. E. Mann, *J. Chem. Phys.* 41, 542 (1964).
- c. D. M. Makowiecki, D. A. Lynch, Jr., and K. D. Carlson, *J. Phys. Chem.* 75, 1963 (1971).
- d. A. J. Hinchcliffe and J. S. Ogden, *Chem. Comm.* 18, 1053 (1969).
- e. J. M. Brom, Jr., T. Devore, and H. F. Franzen, *J. Chem. Phys.* 54, 2742 (1971).
- f. This was assigned to  $\text{Tl}_4\text{O}_2$  in ref. e.
- g. This was assigned to  $\text{M}_x\text{O}_2$  in ref. 29.

## 2.2 Other Vapor Species

It was demonstrated in this laboratory<sup>13</sup> and in others<sup>7-12</sup> that the suboxide molecule is the predominant vapor phase species formed in the equilibrium reaction



The metal is also present at equilibrium in the gas phase, but in all systems except aluminum it comprises only 5-10 per cent of the total vapor composition. For the Al-O system the metal amounts to about 30-40 per cent of the total. In these previous experiments, other detected species were found to have concentrations no larger than  $10^{-3}$  that of the suboxide molecule. However, the possible existence of heavy weight species, such as  $(M_2O)_2$ , was not directly investigated.

It was shown in several other investigations<sup>31-33</sup> that stable oxides, other than the suboxide, were present in the vapor phase. The predominant oxides of this group were MO and its dimer  $M_2O_2$  although their concentrations were normally very small compared to suboxide. An  $MO_2$  ion was detected mass spectrometrically,<sup>13</sup> but it was not confirmed as a stable molecule. Recently Farber, Srivastava, and Uy<sup>34</sup> reported the existence of  $AlO_2$  as a stable species in the vapor above a heated sample of  $Al_2O_3(s)$ . This molecule was predicted to have the linear symmetric structure O-Al-O as does  $BO_2$ <sup>35,36</sup> and in accord with Walsh's rule.<sup>37</sup> The only example of the suboxide dimer  $M_4O_2$  being present in a mass spectrometric investigation was in the thallium system<sup>12</sup> in which solid  $Tl_2O$  was vaporized. In this experiment no stable MO species were found in the vapor.

Gas phase vibrational frequencies for the MO monomers were tabulated by Brewer and Rosenblatt.<sup>38</sup> In the case of TlO only an estimate was given since the molecule was never observed. The first matrix vibrational investigation of AlO was published by Knight and Weltner.<sup>39</sup> The AlO dimer was originally assumed to have  $V_h$  symmetry (rhombic ring structure), but a vibrational investigation was never performed. More recently a linear M-O-O-M structure for the dimer was proposed by Uy and Drowart<sup>40</sup> on the basis of the linear structure of  $B_2O_2$ <sup>36</sup> and the fact that the dimerization energy of the MO molecules correlates better with the dissociation energy of  $O_2$  than with that of the  $M_2$  molecules.

Andrews<sup>20-23</sup> reported a series of experiments in which alkali metal atoms, (lithium, sodium, potassium, and rubidium), were reacted with oxygen molecules in inert matrices. The spectra indicated that  $MO_2$  and  $MO_2M$  were the two primary species observed for each metal reaction. From isotopic  $O_2$  data, the  $MO_2$  molecule was found to have two equivalent oxygen atoms and an isosceles triangular structure of  $C_{2v}$  symmetry. There are three infrared vibrations:  $\nu_1$  symmetric O-O stretch,  $\nu_2$  symmetric M-O stretch, and  $\nu_3$  antisymmetric M-O stretch. The data suggested that the molecule consisted of a metal cation bonded to a superoxide anion by Coulombic forces. The  $MO_2M$  species were determined to be a planar rhombus of  $D_{2h}$  symmetry. It was the structure for a molecule formed by diffusion of a metal atom into an  $MO_2$  molecule with an orientation which minimized the repulsion between the two cations. The difference between this molecule and an  $(MO)_2$  dimer may be slight. This new type of reaction provides a

possible method in these experiments for forming  $\text{MO}_2$  or  $\text{MO}_2\text{M}$  species of the group III A metals.

## CHAPTER 3

## MASS SPECTROMETRIC INVESTIGATIONS

The investigations reported in this chapter were carried out to determine all species which might exist in the vapor phase above a heated sample of metal and metal sesquioxide. Of principle interest were those molecules which might also be observed in the infrared experiments. These investigations were carried out in collaboration with F. J. Kohl and C. A. Stearns of the NASA Lewis Research Center.

Mass spectrometric investigations have proven useful for high temperature vaporization studies<sup>41-43</sup> in which molecular identifications or thermodynamic determinations have been made. The vaporization of solid sesquioxides of the group III A metals has been the subject of several previous studies.<sup>9,11,31-33</sup> In general, the predominant species are found to be M, MO, M<sub>2</sub>O, O and O<sub>2</sub>. Under reducing conditions, such as the vaporization of mixtures of metal and metal sesquioxide, the major components are M<sub>2</sub>O and M. Unfortunately, very little information has been available for this type of system with regard to higher molecular weight species.

### 3.1 Experimental Apparatus and Technique

The Knudsen cell double-focusing mass spectrometric system employed in these experiments has been described previously.<sup>13,44,45</sup> The mass spectrometer was a modified consolidated Electroynamics Corp., Mattuch-Herzog unit, model 21-110, with a Knudsen cell assembly designed and built at NASA Lewis Research Center. As in a previous investigation,<sup>13</sup> yttria-stabilized zirconia liners were fitted

inside tantalum or tungsten Knudsen cells.

Identification of ions was made by their mass-to-charge (M/e) ratio and isotopic weight distribution. Relative peak intensities were correlated with the normal isotopic abundances of  $^{69}\text{Ga}$ ,  $^{71}\text{Ga}$ ,  $^{113}\text{In}$ , and  $^{115}\text{In}$ . The resolution of the mass spectrometer was approximately 1500 based upon the 10 per cent valley definition.<sup>46</sup> This resolution was sufficient to separate organic background peaks from metal or metal-oxide peaks at the same nominal (M/e) ratio.

Shuttering profile measurements provided proof that the detected species were effused from the Knudsen cell. A moveable slit between the ion source and the Knudsen cell was used as the shutter. The measured ion currents for each species originating from the cell corresponded to the difference between the output signal measured with the shutter in the open and closed positions, respectively. All ions from Al, Ga, and In containing species exhibited a shutter effect of 100 per cent.

The multiplier gains for the various ions and the appearance potentials were determined by the use of previously described techniques.<sup>45</sup> Appearance potentials were measured by recording ion intensities against electron energy (ionization efficiency curves) and applying the linear extrapolation method.<sup>46</sup>

### 3.2 Identification of Vapor Species

#### a) Aluminum-Oxygen System

A sample of aluminum metal and  $\alpha$  -  $\text{Al}_2\text{O}_3$  in a mole ratio of 4:1 was loaded into a tantalum Knudsen cell with a zirconia liner

and degassed for several hours. Then the sample temperature was slowly increased to 1531 K and the mass spectrum recorded. In a second experiment a tungsten Knudsen cell was employed and the mass spectrum was recorded at two temperatures. The relative ion intensities and the measured appearance potentials are listed in Table 3.2-1. The appearance potentials were in good agreement with those reported by Drowart *et al.*<sup>47</sup> and indicated by their relatively small values that Al and  $\text{Al}_2\text{O}$  were parent species as previously determined. Both  $\text{AlO}_2^+$  and  $\text{Al}_2\text{O}_2^+$  have been classified as parent species in earlier investigations, although some of the  $\text{AlO}_2^+$  intensity in these experiments may be from fragmentation of  $\text{Al}_2\text{O}_2$ . The only ion previously unreported for this system was  $\text{Al}_3\text{O}_2^+$ . Its intensity was quite low, as was also the case for  $\text{AlO}_2^+$  and  $\text{Al}_2\text{O}_2^+$ , and prevented the measurement of an appearance potential. It was assumed that a parent  $\text{Al}_3\text{O}_2$  molecule did exist.

Ionization efficiency curves are characterized by three distinct segments: a linear threshold region, a region of maximum intensity between 20 and 40 eV, and a region of slowly decreasing intensity with increasing electron energy. All such curves were normal in appearance except for  $\text{AlO}^+$  which showed a distinct break in the linear region at  $16.1 \pm 0.5$  eV. This break indicated the onset of  $\text{AlO}^+$  formation from the fragmentation of  $\text{Al}_2\text{O}$ . The parent AlO with an appearance potential of  $10.0 \pm 0.5$  eV was responsible for less than two per cent of the total  $\text{AlO}^+$  intensity. The  $\text{Al}_2^+$  intensity was slightly smaller than that of  $\text{AlO}^+$ . However, the high appearance potential ( $16.5 \pm 0.5$  eV) of this ion indicated it was formed entirely by frag-

Table 3.2-1. Mass Spectrum of the Vapor over Al(l) + Al<sub>2</sub>O<sub>3</sub>(s)  
(30 eV electrons).

Ion <sup>a</sup>	Relative Intensity			Appearance Potential (eV)	Probable Parent Species
	Temp. (K) 1531	Temp. 1611	Temp. 1708		
Al <sup>+</sup>	7.3 x 10 <sup>-1</sup>	~1.0	d	5.98 <sup>b</sup>	Al, Al <sub>2</sub> O
AlO <sup>+</sup>	1.2 x 10 <sup>-2</sup>	d	d	10.0±0.5	AlO <sup>c</sup>
				16.1±0.5	Al <sub>2</sub> O
Al <sub>2</sub> <sup>+</sup>	7.3 x 10 <sup>-3</sup>	d	d	16.5±0.5	Al <sub>2</sub> O <sup>f</sup>
AlO <sub>2</sub> <sup>+</sup>	7.0 x 10 <sup>-6</sup>	d	d	e	Al <sub>2</sub> O <sub>2</sub> , AlO <sub>2</sub>
Al <sub>2</sub> O <sup>+</sup>	1.0	1.0	1.0	8.0±0.1	Al <sub>2</sub> O
Al <sub>2</sub> O <sub>2</sub> <sup>+</sup>	2.8 x 10 <sup>-4</sup>	1.1 x 10 <sup>-4</sup>	d	e	Al <sub>2</sub> O <sub>2</sub>
Al <sub>3</sub> O <sub>2</sub> <sup>+</sup>	- - -	5.5 x 10 <sup>-6</sup>	4.9x10 <sup>-6</sup>	e	Al <sub>3</sub> O <sub>2</sub>

a No other Al-containing ions were detected up to M/e =175.

b Standard for calibration of electron energy scale. Taken from ref. 46.

c The AlO<sup>+</sup> ion fraction which had an appearance potential of 10.0±0.5 eV was less than 2% of the total AlO<sup>+</sup> ion current.

d Detected but not measured.

e Intensity was too low for reliable measurement.

f The relative intensity of parent Al<sub>2</sub><sup>+</sup> is estimated to be about 4 x 10<sup>-5</sup>.

mentation of the parent  $\text{Al}_2\text{O}$ .

There was no evidence for the presence of any other species. The suboxide molecule intensity is predominant by approximately  $10^4$  over any other aluminum oxide.

b) Gallium-Oxygen System

A sample of gallium metal and  $\beta\text{-Ga}_2\text{O}_3$  was loaded into a tungsten Knudsen cell and degassed for several hours. The sample temperature was increased and a mass spectrum was recorded at 1286 and 1320 K. The same ions were detected at each temperature. A list of ions and their relative intensities is given in Table 3.2-2. The appearance potentials for  $\text{Ga}^+$  and  $\text{Ga}_2\text{O}^+$  agreed with those of Burns,<sup>31</sup> and indicated both ions were parent species. The high values of the  $\text{GaO}^+$  and  $\text{Ga}_2^+$  appearance potentials showed that these ions were fragments of the  $\text{Ga}_2\text{O}$  parent. No  $\text{GaO}$  molecule was detected. The  $\text{Ga}_2\text{O}_2^+$  and  $\text{GaO}_2^+$  species were of very low concentration. The former was probably a parent molecule while the latter may be either fragment or parent. A new ion was found which corresponded to  $\text{Ga}_3\text{O}^+$ . Its relative intensity was too small for an appearance potential measurement and therefore could only be tentatively assigned as a parent.

c) Indium-Oxygen System

Four separate experiments were performed for the indium-oxygen system. In each case a sample of indium metal and  $\text{In}_2\text{O}_3$  powder in a 4:1 mole ratio was loaded into a tantalum Knudsen cell. The sample was degassed for several hours before a mass spectrum was recorded. The ions and their relative intensities are listed in Table 3.2-3.

Table 3.2-2. Mass Spectrum of the Vapor over Ga(l) + Ga<sub>2</sub>O<sub>3</sub>(s)  
(30 eV electrons).

Ion <sup>a</sup>	Relative Intensity		Appearance Potential (eV)	Probable Parent Species
	Temp. (K) 1286	Temp. 1320		
Ga <sup>+</sup>	1.1 x 10 <sup>-1</sup>	c	6.00 <sup>b</sup>	Ga, Ga <sub>2</sub> O
GaO <sup>+</sup>	1.4 x 10 <sup>-3</sup>	c	15.0±0.4	Ga <sub>2</sub> O
GaO <sub>2</sub> <sup>+</sup>	~10 <sup>-5</sup>	c	d	Ga <sub>2</sub> O <sub>2</sub> , (GaO <sub>2</sub> )
Ga <sub>2</sub> <sup>+</sup>	4.4 x 10 <sup>-2</sup>	c	14.5±0.4	Ga <sub>2</sub> O
Ga <sub>2</sub> O <sup>+</sup>	1.0	1.0	9.1±0.2	Ga <sub>2</sub> O
Ga <sub>2</sub> O <sub>2</sub> <sup>+</sup>	2.4 x 10 <sup>-5</sup>	1.5 x 10 <sup>-5</sup>	d	Ga <sub>2</sub> O <sub>2</sub>
Ga <sub>3</sub> O <sup>+</sup>	3.0 x 10 <sup>-6</sup>	3.1 x 10 <sup>-6</sup>	d	Ga <sub>3</sub> O

a No other Ga-containing ions were detected up to M/e ≈350.

b Standard for calibration of electron energy scale. Taken from ref. 46.

c Detected but not measured.

d Intensity was too low for reliable measurement.

Table 3.2-3. Mass Spectrum of the Vapor over (In(l) + In<sub>2</sub>O<sub>3</sub>(s) (30 eV electrons).

Ion <sup>a,b</sup>	Relative Intensity				Appearance Potential (eV)	Probable Parent Species
	Temp. (K) 1173	Temp. 1191	Temp. 1190	Temp. 1239		
In <sup>+</sup>	7.5x10 <sup>-1</sup>	d	d	d	5.79 <sup>c</sup>	In, In <sub>2</sub> O
InO <sup>+</sup>	1.6x10 <sup>-3</sup>	d	d	d	14.8±0.5	In <sub>2</sub> O
InO <sub>2</sub> <sup>+</sup>	1.4x10 <sup>-5</sup>	d	d	d	e	In <sub>2</sub> O <sub>2</sub> , (InO <sub>2</sub> )
In <sub>2</sub> <sup>+</sup>	9.2x10 <sup>-2</sup>	d	d	d	12.9±0.5	In <sub>2</sub> O
In <sub>2</sub> O <sup>+</sup>	1.0	1.0	1.0	1.0	8.3±0.5	In <sub>2</sub> O
In <sub>2</sub> O <sub>2</sub> <sup>+</sup>	3.2x10 <sup>-4</sup>	2.2x10 <sup>-4</sup>	2.6x10 <sup>-5</sup>	d	e	In <sub>2</sub> O <sub>2</sub>
In <sub>3</sub> O <sup>+</sup>	---	1.6x10 <sup>-5</sup>	1.4x10 <sup>-5</sup>	d	e	In <sub>3</sub> O
In <sub>2</sub> WO <sub>4</sub> <sup>+</sup>	---	1.4x10 <sup>-5</sup>	---	d	e	In <sub>2</sub> WO <sub>4</sub>
In <sub>4</sub> O <sub>2</sub> <sup>+</sup>	---	4.0x10 <sup>-6</sup>	6.3x10 <sup>-6</sup>	d	e	In <sub>4</sub> O <sub>2</sub>
InTaO	---	---	---	2.8x10 <sup>-5</sup>	e	InTaO
InTaO <sub>2</sub> <sup>+</sup>	---	---	---	4.3x10 <sup>-6</sup>	e	InTaO <sub>2</sub>

a No other In-containing ions were detected up to M/e ≈ 830.

Table 3.2-3. (Continued)

---

---

- b At 1191 K, shutterable peaks at  $M/e = 553 \pm 2$  and  $591 \pm 2$  were observed. These could not be assigned definitely to In-containing species (intensities  $10^{-5}$ - $10^{-6}$ ).
- c Standard for calibration of electron energy scale. Taken from ref. 46.
- d Detected but not measured.
- e Intensity was too low for reliable measurement.

The appearance potentials for  $\text{In}^+$  and  $\text{In}_2\text{O}^+$  agreed with those reported by Burns *et al.*,<sup>32</sup> and the relative ion intensities were comparable to those recorded by Shchukarev and associates<sup>9</sup> for  $\text{In}^+$ ,  $\text{InO}^+$ ,  $\text{InO}_2^+$ ,  $\text{In}_2^+$ ,  $\text{In}_2\text{O}^+$ , and  $\text{In}_2\text{O}_2^+$ . Of these,  $\text{In}$ ,  $\text{In}_2\text{O}$ , and  $\text{In}_2\text{O}_2$  were definitely parent species with the suboxide intensity  $10^4$  greater than any other indium oxide molecule. The  $\text{In}_2^+$  and  $\text{InO}^+$  appearance potentials indicated that they were fragments from  $\text{In}_2\text{O}$ . It was noted that, as was found for the gallium system, the  $\text{M}_2^+$  intensity was greater than that of  $\text{MO}^+$ . The same kind of intensity distribution was also found in the thallium suboxide studies<sup>11,12</sup> and was considered to have possible structural significance. The  $\text{InO}_2^+$  peak was too small for measuring its appearance potential.

At slightly higher temperatures several previously unreported ions were detected. These included  $\text{In}_3\text{O}^+$ ,  $\text{In}_4\text{O}_2^+$ ,  $\text{InTaO}^+$ ,  $\text{InTaO}_2^+$ , and  $\text{In}_2\text{Wo}_4^+$ , all of which were considered to be parent molecular species. The  $\text{In}_3\text{O}$  molecule is apparently similar to  $\text{Ga}_3\text{O}$ , mentioned in the previous section. The  $\text{In}_4\text{O}_2$  molecule is apparently the dimer of indium suboxide. A suboxide dimer is known to exist in the thallium-oxygen system, but no other dimers for the group III A metal oxides have been previously detected through mass spectrometric experiments.

The remaining three molecules were mixed metal species. The indium tantalum oxides were probably formed at the orifice since the orifice of the tantalum cell was smaller than that of the inner zirconia liner. This allows some species to come into direct contact with the tantalum walls. After completion of the experiment there was evidence of an indium residue near the orifice between the liner

and the cell. The indium tungsten oxide was more difficult to explain. Two tungsten filaments surrounded the cell and were the most probable source of reaction with the  $\text{In}_2\text{O}_3$ . No other ions were found which could be attributed to an indium-containing species.

## CHAPTER 4

### MATRIX ISOLATION TECHNIQUE AND APPARATUS

#### 4.1 Matrix Isolation Technique

Dewar<sup>48</sup> first used some semblance of the matrix isolation technique in 1901. Later in 1954, Pimentel *et al.*<sup>49</sup> began isolating materials in matrices at low temperatures for spectroscopic studies. However, it was not until 1961 that Linevsky<sup>50</sup> first applied the technique to the investigation of vapors formed at elevated temperatures. Since that time it has become an important tool for the chemist.

The method is basically a molecular beam sampling technique in which the molecules of the beam are collected, along with a large excess of a chemically inert substance such as one of the rare gases, and cooled to approximately 4 K. The rare gas then forms the matrix. Since the molecules are highly diluted and the matrix is inert, ideally there are no forces acting upon the molecules other than very weak electrostatic forces which provide only slight perturbations of the energy levels from the gas phase values.

Some of the advantages of this method are the ability to investigate very reactive molecules, such as radicals and those stable only at high temperatures, or molecules which are normally in very low concentrations. High temperature vibrational studies can be performed without having rotational or hot bands to obscure the background. Monomers can usually be distinguished from polymers by either varying the dilution or diffusing a matrix. In the latter method the matrix is warmed 10-15° and then quenched by recooling. A monomer ab-

sorption tends to sharpen and decrease in intensity while a dimer band usually broadens and either stays the same size or increases in intensity.

However, there are some disadvantages. Polymers may be formed thus making it difficult to interpret some spectra. The matrices tend to scatter light (Rayleigh scattering), especially during diffusion studies. Multiple trapping sites may exist and cause vibrational splittings, and selection rules may be broken and degeneracies split.

#### 4.2 Experimental Equipment

##### a) The Cryostat and Condensation Target

A modified Sulfrian "Select-a-Stat  $\infty$ " liquid helium cryostat, described by Thompson<sup>51</sup> and Makowiecki<sup>13</sup>, was employed to cool the condensation target. This cryostat, illustrated in Fig. 4.2-1, consists of a double dewar assembly surrounded by a stainless steel vacuum jacket connected to a rotatable brass tail section. The inner dewar, containing liquid helium, is attached by a stainless steel rod to the copper block which holds the condensation target. A spiraled copper tube is soldered to the rod and allows liquid helium to be passed from the dewar to the block for effective cooling. The copper tubing vents at a micrometer valve located at the top of the cryostat. Temperature control is maintained by adjusting either the micrometer valve or the backing pressure above the liquid helium.

Two heat shields surround the condensation target. The first is attached to the copper block and is maintained at liquid helium

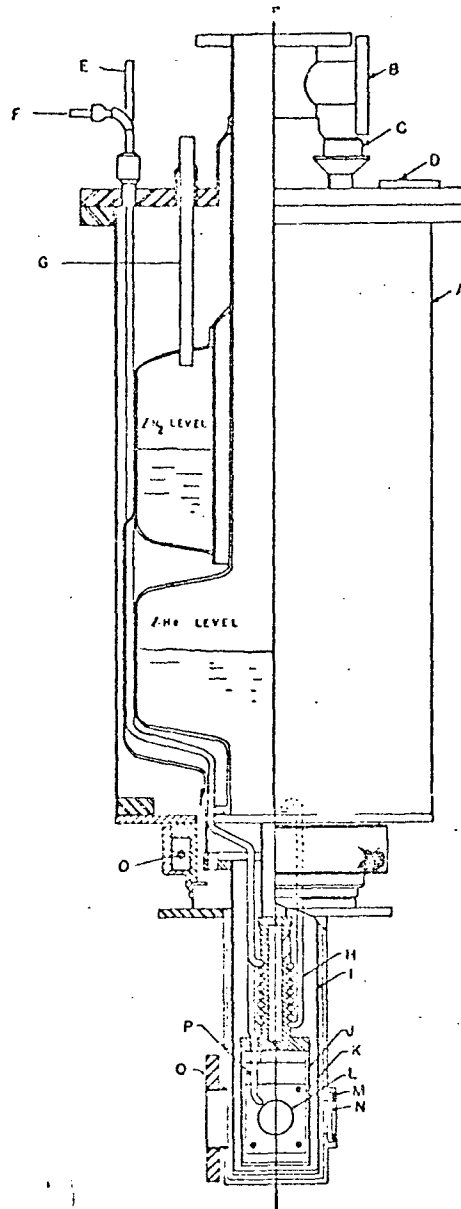


Fig. 4.2-1

Cross section of the cryostat: Body section (A);  $\lambda$ -He pump-out port (B); Richard's valve (C); thermocouple feedthrough (D); spray-on tube entrance (E); micrometer valve outlet (F);  $\lambda$ -N<sub>2</sub> fill/vent tube (G);  $\lambda$ -He cooling coil (H);  $\lambda$ -N<sub>2</sub> cold shield (I);  $\lambda$ -He cold shield (J); cold block and plate (K); deposition target (L); optical window sealing ring (M); outer optical window (N); ball bearing race (O); spray-on tube (P); molecular beam source flange (Q). Drawing courtesy of Sulfrin Cryogenics, Inc., reproduced by permission.

temperatures. The second is directly attached to the outer dewar containing liquid nitrogen.

The condensation target for these experiments consisted either of CsBr or CsI polished windows. The former has a usable range of 4000-250  $\text{cm}^{-1}$ . The latter extends the range to 200  $\text{cm}^{-1}$ . These windows are held onto the copper block by a copper front plate which is secured by four brass screws. An indium gasket is employed to maintain good thermal conductivity between block and window. The open sight diameter of the target is 3.18 cm. Two copper-Constantan thermocouples, which are soldered to the block and plate respectively, measure the temperatures.

The vacuum system consists of a two-inch oil diffusion pump, backed by a small Precision Scientific mechanical pump. Under normal conditions a vacuum of  $2 \times 10^{-4}$  torr was maintained; with liq.  $\text{N}_2$  in the dewar the vacuum was  $9 \times 10^{-6}$  torr, and with liq. He the vacuum was  $2 \times 10^{-6}$  torr. It was experimentally determined that as long as the pressure did not rise above  $1 \times 10^{-5}$  torr with liq. He, successful experiments could be performed with no appreciable change in helium holding time. Above this pressure the thermal conduction was appreciable, and the matrices tended to flow and were lost.

#### b) Superstructure and Infrared Instrumentation

The entire isolation apparatus was supported on a moveable unistrut framework which could fit around either of the two infrared instruments. Approximately five minutes were required to complete a move. The instruments were the Beckman IR-7, which has the range of

4000-650  $\text{cm}^{-1}$ , and the Beckman IR-11, which has the range of 800-33  $\text{cm}^{-1}$ . However, during the course of this research the latter instrument had a useful range of 800-250  $\text{cm}^{-1}$  and even here the energy was quite low. The two instruments were calibrated with atmospheric water bands,  $\text{CO}_2$ , and a 10 cm gas cell of  $\text{NH}_3$ . The absolute wavenumber accuracy was better than  $\pm 1.0 \text{ cm}^{-1}$  for all experiments.

The matrix gas was contained in a small glass vacuum system attached to the unistrut framework. A small manometer allowed measurement of pressures up to 300 mm. The glass system was connected by a manifold to two stainless steel tubes of 0.24 cm diameter which carried the gas to the target. The tube openings were positioned approximately 1.27 cm from the window at a  $45^\circ$  angle. The rate of deposition could be varied by means of a needle valve on the manifold.

c) Matrix Gases and Chemicals

Argon, which was the primary matrix gas, was Matheson's "Gold Label" grade with a stated purity of 99.9995 per cent. This gas was used without further purification although earlier tests<sup>13</sup> had shown neon to be an impurity. Experiments verified that this produced no noticeable effect on the spectra. Research grade  $\text{N}_2$  was used for several experiments. Oxygen for the mixed matrix experiments was Linde's 99 per cent pure grade. Further purification was not required for either of these gases. A list of other chemicals employed in this study is given in Table 4.2-1.

d) Knudsen Cell Assembly

A water-cooled condenser, described previously,<sup>13</sup> was at-

Table 4.2-1. Research Chemicals.

Material	Stated Purity	Source	$^{18}\text{O}$ %	Minor Impurities <sup>a</sup>
Al	-----	Fischer	---	Fe
Ga	99.999%	Alfa Inorganics	---	In
In	-----	Sulfrian	---	Cr
Tl	99.9999%	Alfa Inorganics	---	None
$\text{Al}_2\text{O}_3$	Ultra Pure	Linde	---	None
$\text{Ga}_2\text{O}_3$	99.99%	ROC/RIC	---	None
$\text{In}_2\text{O}_3$	99.999%	ROC/RIC	---	None
$\text{Tl}_2\text{O}_3$	Optronic Grade	Alfa Inorganics	---	Si
$\text{Al}_2\text{O}_3$	-----	Miles Labs.	72	--
$\text{Ga}_2\text{O}_3$	-----	Miles Labs.	77	--
$\text{Ga}_2\text{O}_3$	-----	Miles Labs.	86.5	--

a Detected by emission spectroscopy. Private communication, Fred J. Kohl, NASA Lewis Research Center, Cleveland, Ohio.

tached to the large port of the cryostat's rotatable tail section. Either of two Knudsen cell assemblies<sup>13</sup> was attachable to the condenser. Both assemblies consisted of a brass flange, Ceramaseal high current feedthroughs, and 0.635 cm copper tubing as water-cooled electrical conductors.

The low temperature assembly was usable for temperatures up to 1600 K. The Knudsen cell was held in place by two 0.318 cm zirconia rods. The heating was maintained by radiation from a 5 mil circular strip of tantalum sheet surrounding the crucible. The sheet was spot-welded to two 0.635 cm tantalum tubes of 15 mil thickness which were secured to the feedthroughs by set screws. A 20 mil Chromel-Alumel thermocouple, for temperature measurement, was positioned in a black-body hole of the Knudsen cell.

The high temperature assembly was usable for temperatures above 1200 K. In this case the Knudsen cell was heated resistively. The tantalum leads of the cell were fitted into slots in two 0.635 cm molybdenum rods, with the cell placed between them. The rods were locked in place to the feedthroughs by set screws. The cell skin temperature was measured by pyrometer through the rear window. Appropriate corrections were made to obtain the true orifice temperature.

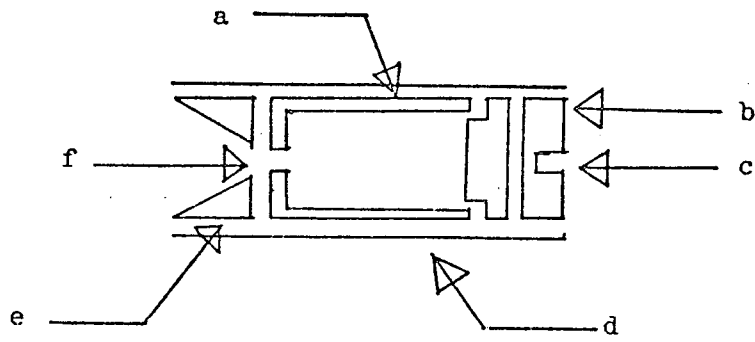
Both heating assemblies appeared to be quite reliable. At no time were any temperature gradients of any consequence seen. The source of power for both assemblies was a double variac arrangement. Line voltage, 125 V at up to 30 amps, was fed into a 6.1 KVA variac. The output was fed into a second 6.1 KVA variac which was stripped of its outer casing. A secondary wiring was formed by wrapping number

zero fine strand welding cable six times around the core. The leads from this cable were bolted to the water-cooled copper conductors of either of the two assemblies. The maximum output was 600 amps at 3 volts. This type of heating arrangement was quite steady, requiring no controls other than the manual positioning of the first variac.

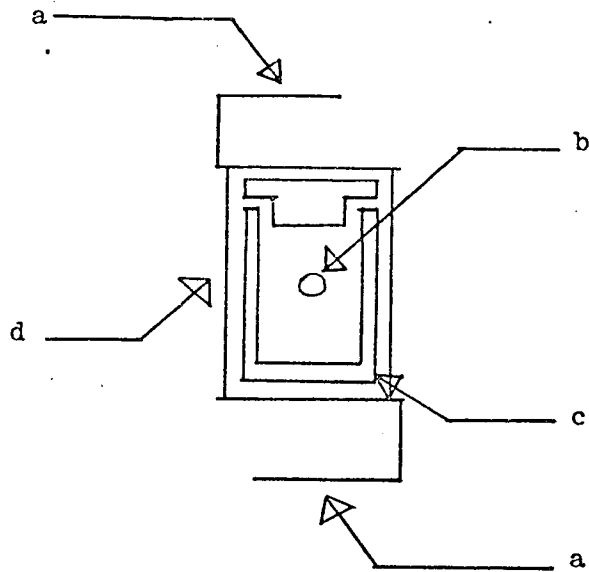
Two types of Knudsen cells were employed as shown in Fig. 4.2-2. The first consisted of either a zirconia or thoria inner crucible and fitted top with an orifice in its bottom, 1.27 cm tall by 1.27 cm diameter. The outer covering was a 15 mil tantalum tube of 1.59 cm diameter with press-fit graphite plugs at each end. The plug over the orifice end was drilled out 0.953 cm in diameter. The other plug had a black-body hole for a thermocouple. The other cell, again had either a zirconia or thoria inner crucible of the same dimensions. In this case the orifice was in the side. The outer walls consisted of 15 mil tantalum tube of 1.59 cm diameter. The ends were 20 mil tantalum sheet bent to a block C shape and spot-welded into position.

e) Dry Box

For the oxygen-18 experiments a dry box from Kewaunee Scientific was used for crucible loading under a dry nitrogen atmosphere. The small purging system, in continuous operation, consisted of a small pump forcing the nitrogen through a vycor tube containing heated copper turnings for oxygen removal and then through two Drierite traps to purge any residual water vapors. The copper turnings could be regenerated by passing hydrogen gas over them to produce water which was extracted by the Drierite.



I. Low Temperature Cell



II. High Temperature Cell

Fig. 4.2-2. Knudsen Cells

Legend for Fig. 4.2-2:

Low Temperature Knudsen Cell

- a. zirconia or thoria liner
- b. graphite end plug
- c. black-body thermocouple hole
- d. tantalum sheath
- e. graphite plug
- f. orifice

High Temperature Knudsen Cell

- a. tantalum end plates and electrical leads
- b. orifice
- c. zirconia or thoria liner
- d. tantalum sheath

### 4.3 Experimental Procedures

#### a) Matrix Isolation Ratio

In order to perform a successful matrix experiment, it is necessary to have a good isolation ratio of moles of matrix gas to moles of reactive species (M/R). Therefore, the number of moles of both species must be reasonably well measured. It has been found that M/R ratios of 300-20,000 are acceptable depending upon the particular goal of an experiment. There is obviously more chance for association or reaction with a lower ratio. Below 300 there is usually too much scattering and above 20,000 there are not enough reactive species. During these experiments a typical run would involve 10-20,000  $\mu$  moles of matrix gas and 2-20  $\mu$  moles of reactive molecules. However, some absorptions could be seen at approximately 0.1  $\mu$  moles.

The ideal gas law is used to calculate the moles of matrix gas. The gas is maintained in a fixed volume at room temperature with the change in pressure measured with a manometer. Unfortunately, not all of the matrix gas condenses when it hits the target. The correction for this is the condensation coefficient which is 0.6 for argon and neon and unity for nitrogen, oxygen, carbon dioxide, krypton, and xenon due to their higher sublimation temperatures.

Likewise the moles (Z) of the reactive species can be determined from a modified Knudsen effusion equation<sup>52</sup>

$$Z = 2.66 \times 10^{-3} Q_a G P t (2 \Pi M R T)^{-1/2} \quad (4.3-1)$$

provided the vapor pressure is known. The constant  $2.66 \times 10^{-3}$  allows Z to be expressed in  $\mu$  moles ( $10^{-6}$  moles), with P being the vapor pres-

sure in atmospheres,  $t$  the time of the steady-state deposition in minutes,  $M$  the molecular weight of the species,  $R$  the gas constant, and  $T$  the absolute temperature. The product  $Qa$  is the effective orifice area expressed in  $\text{cm}^2$  where  $a$  is the cross-sectional area and  $Q$  is the Clausing factor (a function of the diameter and depth of the orifice). The geometry factor  $G$  is a dimensionless quantity which gives the fraction of effusing molecules that hit the target. From the Cosine Law of molecular effusion<sup>53</sup>, we have the approximation that

$$G = \frac{r^2}{L^2 + r^2} \quad (4.3-2)$$

where  $r$  is the radius of the condensation target (1.59 cm) and  $L$  is the perpendicular distance from the orifice to the target (7.62 cm).  $G$  has the value 0.0416 for the present experiments. It is assumed that all molecules hitting the target are condensed.

#### b) Vapor Pressures for Suboxides and Metals

The pressures for these experiments were those determined by Makowiecki<sup>13</sup> for all the suboxides except aluminum which was taken from the literature.<sup>7,54</sup> The metal pressures for the matrix reaction experiments were taken from established values.<sup>55</sup> A list of all pressure equations is given in Table 4.3-1.

#### c) Procedure Additions

The procedure normally followed during an experiment is described in detail by Makowiecki.<sup>13</sup> However, two additional steps were necessary for this research. In those experiments involving a

Table 4.3-1. Summary of Vapor Pressure Equations.<sup>a</sup>

Species	A	B	Temp. Range (K)	Ref.
Al	15812	5.87	1200-2000	b
Ga	13800	5.52	1200-1600	b
In	12294	5.27	1100-1400	b
Tl	9022	5.22	800-1000	b
Al <sub>2</sub> O	24200	8.9	1400-1400	c
Ga <sub>2</sub> O	11700	5.42	1000-1300	d
In <sub>2</sub> O	13180	7.43	900-1200	d
Tl <sub>2</sub> O	9090	7.62	700-900	d
Mixed System <sup>e</sup>				
Ga <sub>2</sub> O	12720	4.76	1000-1300	f
In <sub>2</sub> O	15710	8.06	1000-1300	f
InGaO	13640	6.24	1000-1300	f

a Parameters A and B apply to the equation

$$\log P \text{ (atm)} = -A/T + B .$$

b R. Hultgren, R. L. Orr, P. D. Anderson, and K. K. Kelley, Selected Values of Thermodynamic Properties of Metals and Alloys, Wiley and Sons, Inc. (1963).

c L. Brewer and A. W. Searey, *J. Am. Chem. Soc.* **73**, 5308 (1951).

d D. M. Makowiecki, "Infrared Spectra of the Group III A Metal Suboxides," Ph.D. Thesis, Case Western Reserve University, January, 1971.

e Pressures over In(l) + Ga<sub>2</sub>O<sub>3</sub>(s).

f Private Communication, Fred J. Kohl, NASA Lewis Research Center, Cleveland, Ohio.

mixed matrix, the oxygen was bled into the evacuated storage bulb first and then either argon or nitrogen was added. Teflon chips inside the bulb allowed for proper mixing of the two gases. Also, in most cases the bulbs were filled 24 hours in advance of an experiment and allowed to equilibrate before use. During the experiment it was noted that the micrometer valve for the matrix gas had to be opened further to maintain a steady deposition flow. This was due to a slight condensation of oxygen in the spray-on lines. This same effect had previously been noted in pure nitrogen experiments.

The second procedural change dealt with the handling of the oxygen-18 enriched sesquioxides of aluminum and gallium. These were maintained inside sealed casings and left in a freezer until needed. They were then transferred to the dry box for loading the sample into the crucible. This was necessary because of the rapid oxygen isotopic exchange which proceeded even at room temperature.<sup>56</sup> Although the samples were nominally 70 per cent enriched, the experimental results indicated no more than 40 per cent enrichment after heating. Apparently much of this loss was from oxygen exchange in the thoria and zirconia crucibles at high temperatures. After several heatings of each cell, the isotopic exchange appeared to equilibrate. Further evidence for this exchange process was that in later experiments employing unenriched sesquioxide material, small absorptions from  $^{18}\text{O}$  were found.

It should be noted that Makowiecki<sup>13</sup> used relatively short deposition times at fairly high deposition rates. Although the isolation ratios were adequate, there is an increased chance of molecular inter-

actions as the vapor pressure approaches the upper limits of Knudsen conditions. The experiments in this study were performed under conditions as closely as possible duplicating those employed by the above mentioned author.

## CHAPTER 5

## MATRIX ISOLATION EXPERIMENTS

5.1 Mixed Matrix Experiments

It was decided that the study of the effect of isolating suboxide molecules in matrices containing approximately 20 per cent oxygen would be interesting because the possibility existed that previously observed absorptions were from reactions of free oxygen with suboxide molecules. Also, the recent investigations by Andrews<sup>20-23</sup> on alkali metals reacting with oxygen in mixed matrices provided the impetus to begin a similar search with the group III A metals to obtain an additional check that the suboxide absorptions were not due to reactions between free metal and oxygen.

These experiments were performed in reverse order beginning with thallium and ending with aluminum. The reason for this is the apparent better diffusion of heavier molecules in a matrix over lighter ones.<sup>57</sup> Although it is possible that absorptions lie below  $250\text{ cm}^{-1}$ , the condition of the IR-11 did not allow any measurements in this region. In the case of aluminum the instrument did not have enough energy to allow any spectra.

a) Thallium and Thallium Suboxide

Approximately  $10\mu$  moles of thallium metal were deposited from a previously outgassed Knudsen cell in an Ar + O<sub>2</sub> matrix with an Ar/Tl ratio of 800 and an O<sub>2</sub>/Tl ratio of 100. No evidence for any previously assigned Tl<sub>2</sub>O absorptions was seen. However, two new absorptions were observed as shown in Fig. 5.1-1. The first appeared to be a

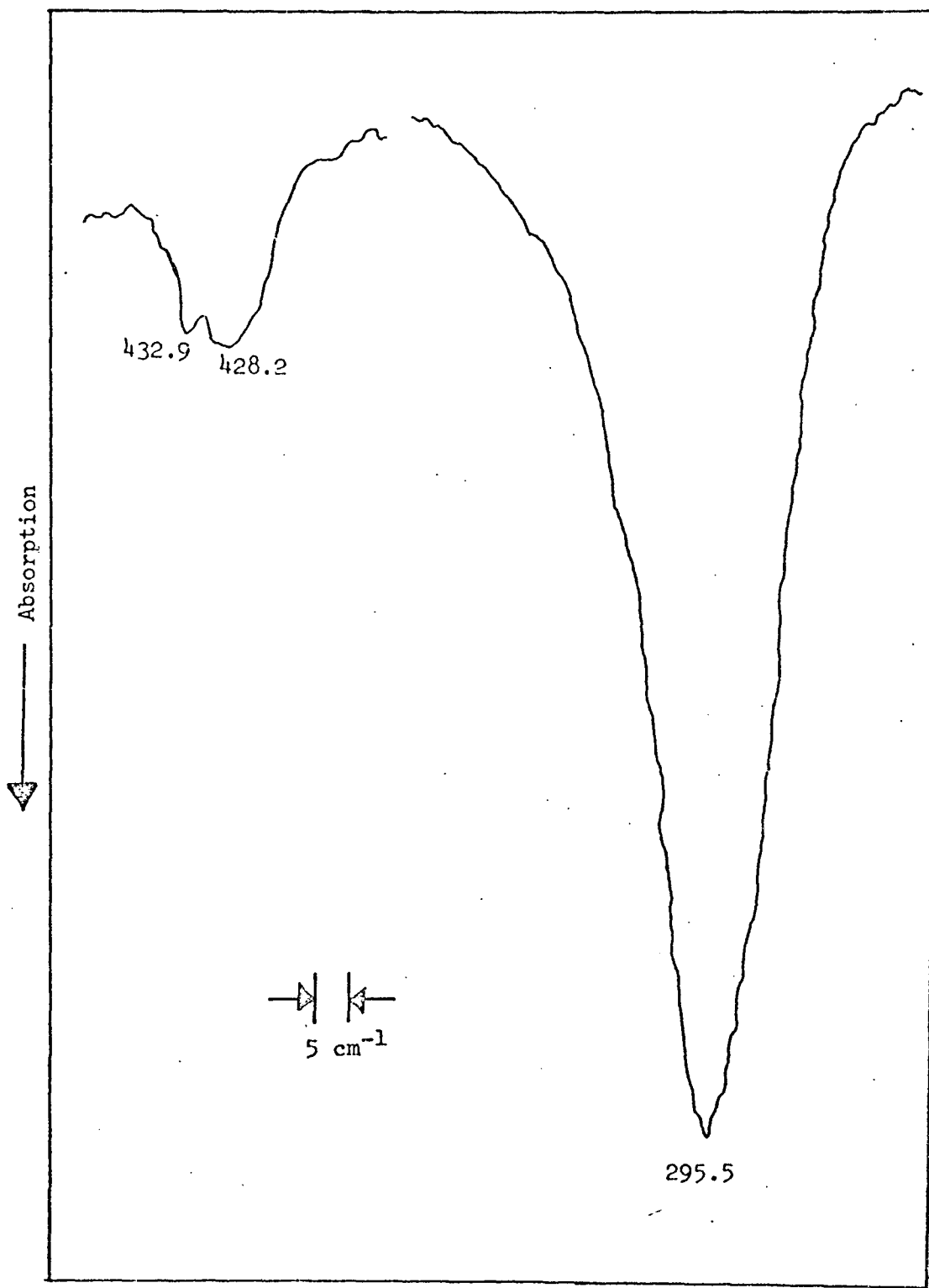


Fig. 5.1-1. Infrared Spectrum of Tl in Ar + O<sub>2</sub>.

possible doublet at 428.2 and 432.9  $\text{cm}^{-1}$ . The second, at 295.5  $\text{cm}^{-1}$ , was quite intense and broad. Both disappeared rapidly upon diffusion leading to the possibility that they belong to the same molecule. The slightest attempt at a simple annealing caused great losses in intensity. There were no indications of additional absorptions being formed at this time. Unfortunately, the matrix diffused completely before a spectrum could be taken on the IR-7.

In order to verify that the above absorptions were new, it was necessary to isolate  $\text{Tl}_2\text{O}$  in an  $\text{Ar} + \text{O}_2$  matrix. The cell was reloaded, and the sample of  $\text{Tl} + \text{Tl}_2\text{O}_3$  was heated to 780 K for nine minutes. A deposit of 7  $\mu$  moles of  $\text{Tl}_2\text{O}$  and less than 1  $\mu$  mole of  $\text{Tl}$  was isolated with the ratios  $\text{Ar}/\text{Tl}_2\text{O}$  of 1500 and  $\text{O}_2/\text{Tl}_2\text{O}$  of 300. The thallium was isolated at M/R of 10,000, which indicated very little chance for a matrix reaction. The spectrum, represented in Fig. 5.1-2, shows absorptions at 384.5, 473.2, 509.5, 532.5 and a doublet at 640.7 and 661.4  $\text{cm}^{-1}$ . The 532.5 and 473.2  $\text{cm}^{-1}$  absorptions have been observed previously<sup>13,18</sup> but do not appear with any regularity and are unassignable. The remaining absorptions are those found in the  $\text{Tl}_2\text{O}$  experiments.<sup>13</sup> There appears to be a frequency shift of about 3  $\text{cm}^{-1}$  by diluting the Ar matrix with  $\text{O}_2$ .

In the next experiment, an attempt was made to isolate both the " $\text{Tl}_2\text{O}$ " molecules and a high concentration of  $\text{Tl}$  metal in order to investigate whether any additional absorptions would be detected. To do this it was necessary to load the Knudsen cell with a very small sample of  $\text{Tl}_2\text{O}_3$  and a large excess of  $\text{Tl}$  metal. A higher deposition temperature was employed so that all the  $\text{Tl}_2\text{O}_3$  was depleted

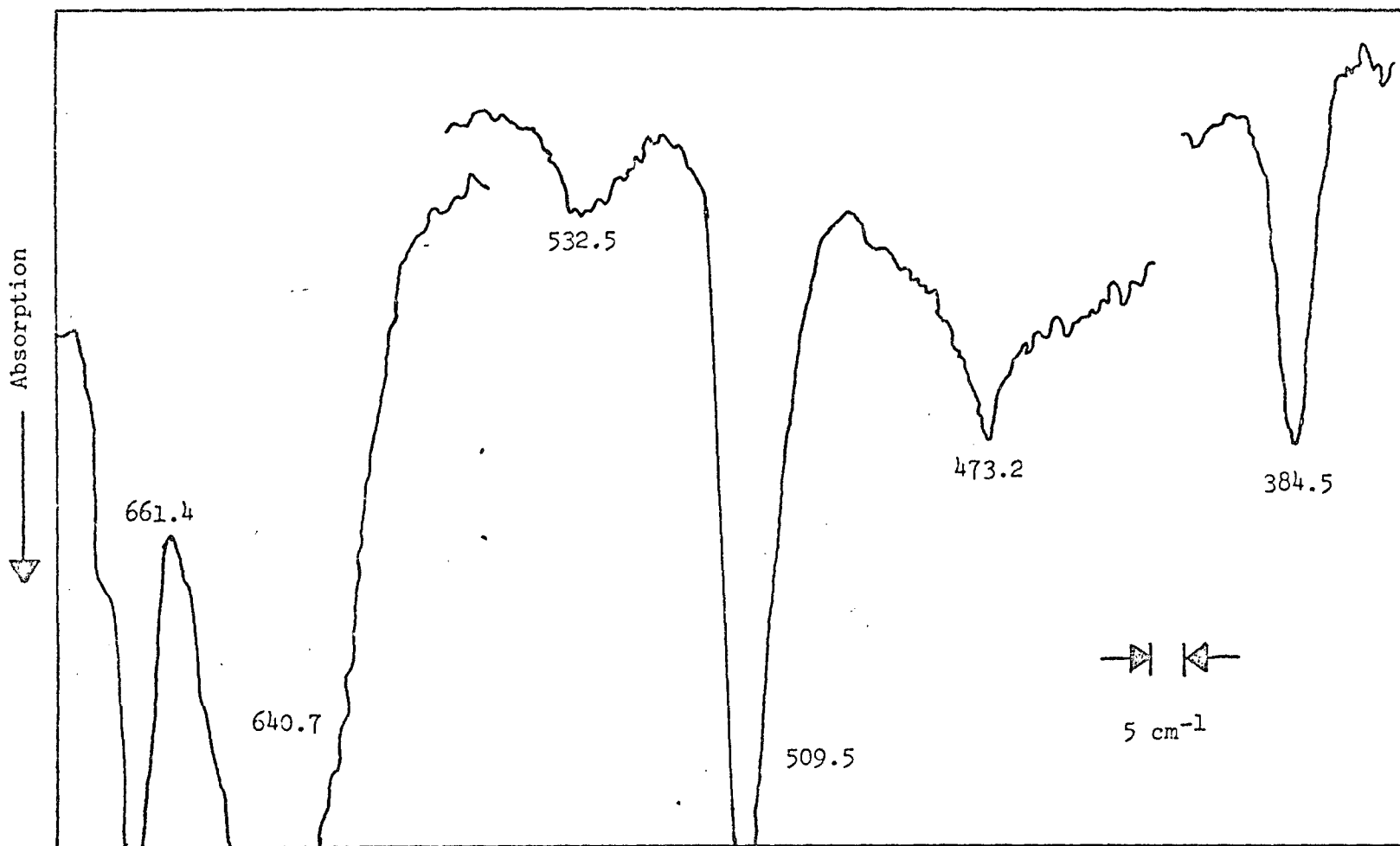


Fig. 5.1-2. Infrared Spectrum of Tl<sub>2</sub>O in Ar + O<sub>2</sub>.

in the  $Tl_2O$  reaction and a high concentration of Tl was produced. The cell was heated to 1000 K for a 7.5 minute deposition. The isolation ratio was not calculated because of the unknown quantities. The matrix contained 17 per cent oxygen in argon. The weak absorption at 384.3, 509.7, 640.3 and 661.5  $cm^{-1}$ , shown in Fig. 5.1-3a, is from the  $Tl_2O$  system. It appears that the last absorption may be due to solid  $CO_2$  in this experiment as it is quite sharp and intense whereas the others are weaker and broadened. The remaining bands at 295.9  $cm^{-1}$  and the doublet at 432 and 428  $cm^{-1}$  were observed in the "Tl +  $O_2$ " matrix reaction. In diffusion experiments the " $Tl_2O$ " absorptions tended to remain longer than those from the Tl experiment. The spectrum from the IR-7, shown in Fig. 5.1-3b, indicates several weak absorptions between 650 and 1500  $cm^{-1}$ . The first at 721  $cm^{-1}$  has been reported<sup>19</sup> previously as an overtone for the " $Tl_2O$ " system. The doublet at 1035.7 and 1022.0  $cm^{-1}$  is apparently related to the "Tl +  $O_2$ " system although a weak " $Tl_2O$ " overtone is reported at 1006  $cm^{-1}$ . The last absorption at 1082.1  $cm^{-1}$  is very weak and may be only a ghost since the instrument has a strong single beam background band between 1075 and 1100  $cm^{-1}$ . However, upon diffusion this absorption disappears very quickly, even faster than the doublet, and is tentatively assigned as being from the "Tl +  $O_2$ " reaction.

A list of the absorptions from these experiments is given in Table 5.1-1 with their relative intensities and probable precursor system.

b) Indium and Indium Suboxide

A cell previously employed for an  $In_2O$  study was degassed

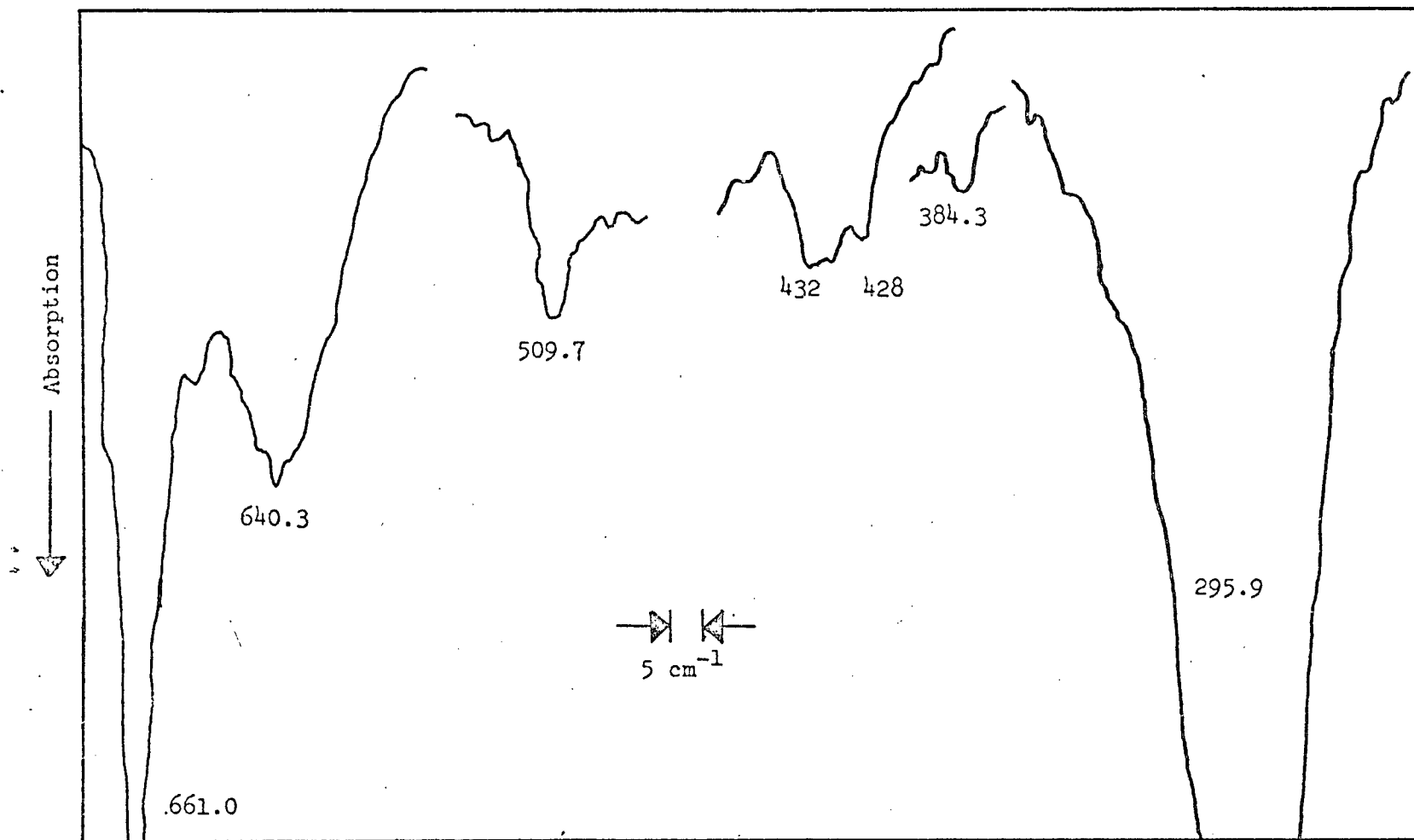


Fig. 5.1-3a. Infrared Spectrum of Tl and Tl<sub>2</sub>O in Ar + O<sub>2</sub>. (IR-11).

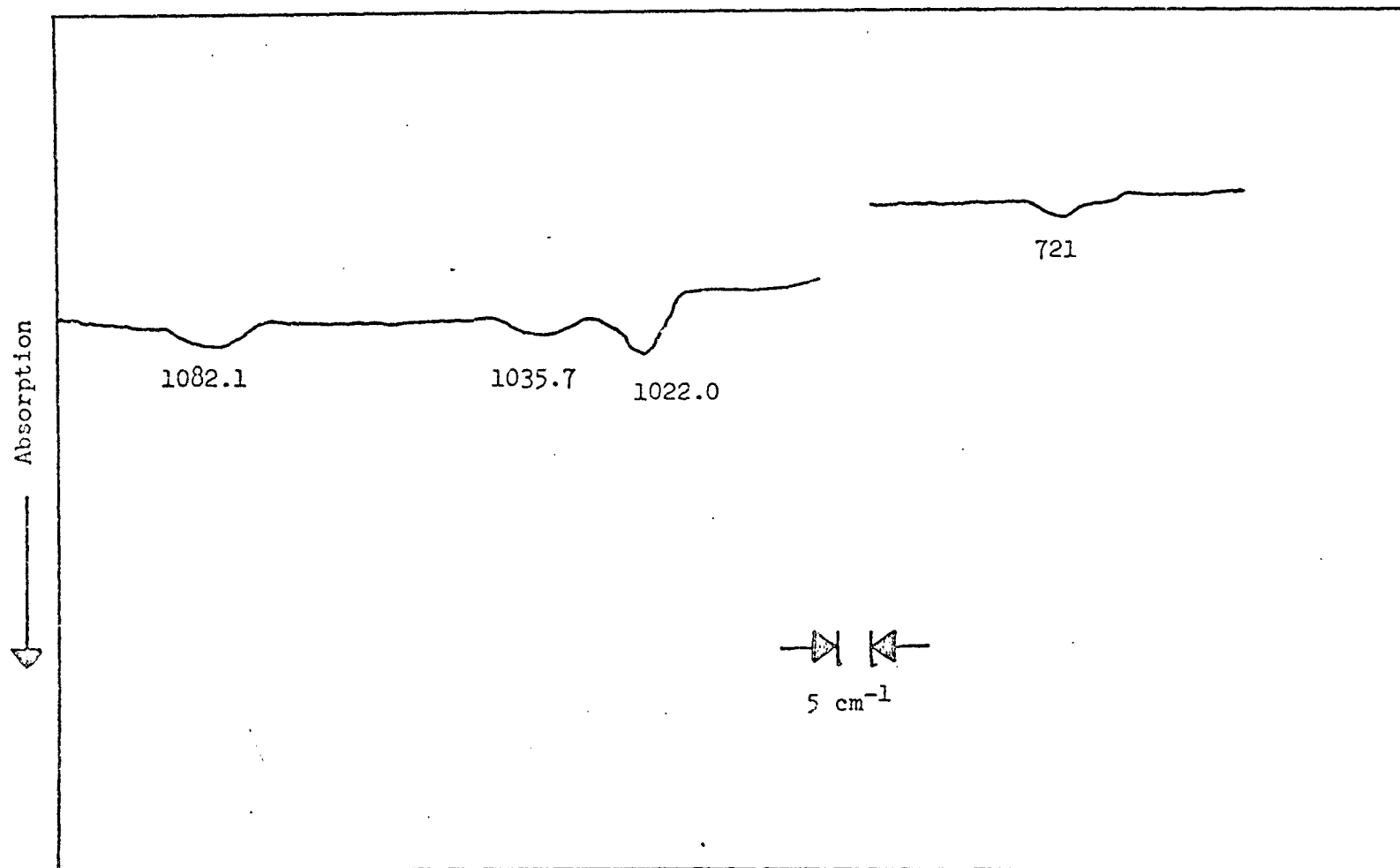


Fig. 5.1-3b. Infrared Spectrum of Tl and Tl<sub>2</sub>O in Ar + O<sub>2</sub> (IR-7).

Table 5.1-1. Infrared Frequencies ( $\text{cm}^{-1}$ ) of Tl and  $\text{Tl}_2\text{O}$  Matrix Reactions with  $\text{O}_2$  in Ar.

Absorptions <sup>a</sup>	Intensities <sup>b</sup>	Precursor System
295.9	100	$\text{Tl} + \text{O}_2$
384.3	8	$\text{Tl}_2\text{O}$
428.2	13	$\text{Tl} + \text{O}_2$
432.9	12	$\text{Tl} + \text{O}_2$
473.2	2	$\text{Tl}_2\text{O}$
509.5	11	$\text{Tl}_2\text{O}$
532.5	3	$\text{Tl}_2\text{O}$
640.5	31	$\text{Tl}_2\text{O}$
661.2	50	$\text{Tl}_2\text{O} (\text{CO}_2)$
721	2	$\text{Tl}_2\text{O}$
1022.0	5	$\text{Tl} + \text{O}_2$
1035.7	3	$\text{Tl} + \text{O}_2$
1082.1	4	$\text{Tl} + \text{O}_2$

a Accuracy considered better than  $\pm 1.0 \text{ cm}^{-1}$ .

b Relative intensities all normalized to the most intense peak.

and loaded with In metal. The cell was heated for 8 minutes at a temperature in excess of 1020 K. The exact temperature was not determined as the thermocouple became dislodged during the heating. A large sample of In was known to have been deposited as the heat shields were coated with a metallic cover. The matrix contained 23 per cent oxygen in argon. Two bands were observed, as shown in Fig. 5.1-4b, at 456.4 and 332.2  $\text{cm}^{-1}$ . Both intensities decreased rapidly during a He fill with the former disappearing completely. The spectrum from the IR-7, Fig. 5.1-4a, shows a very small rounded absorption at 735.0  $\text{cm}^{-1}$  which is the  $\nu_3$  for  $\text{In}_2\text{O}$ . Apparently a small amount of  $\text{In}_2\text{O}_3$  powder remained in the cell and reacted forming  $\text{In}_2\text{O}$  during this experiment. It is interesting to note that this band corresponds to the value assigned as the true  $\nu_3$  in the doublet reported by Makowiecki.<sup>13</sup> Two other absorptions were observed at 1012.8 and 1082.3  $\text{cm}^{-1}$ . The latter disappeared faster upon diffusion but again may be no more than background. The former diffuses slower than the  $\text{In}_2\text{O}$   $\nu_3$ , but does eventually disappear before the matrix is lost. A later experiment showed essentially no  $\text{In}_2\text{O}$   $\nu_3$  and a sharp 2 per cent absorption at 1012.6  $\text{cm}^{-1}$ . However, the only other hint of a peak was a very weak and broad band at 332  $\text{cm}^{-1}$ .

The cell was reloaded with In and  $\text{In}_2\text{O}_3$ . After it was outgassed, the sample was heated for 8 minutes at 1163 K to deposit 3-4  $\mu$  moles  $\text{In}_2\text{O}$  and 0.3  $\mu$  moles In with isolation ratios of 4500 for Ar/ $\text{In}_2\text{O}$  and 1000 for  $\text{O}_2$ / $\text{In}_2\text{O}$ . Absorptions, illustrated in Fig. 5.1-5, at 406.8, 553.8, and 733.1  $\text{cm}^{-1}$  are within 2  $\text{cm}^{-1}$  of those observed in

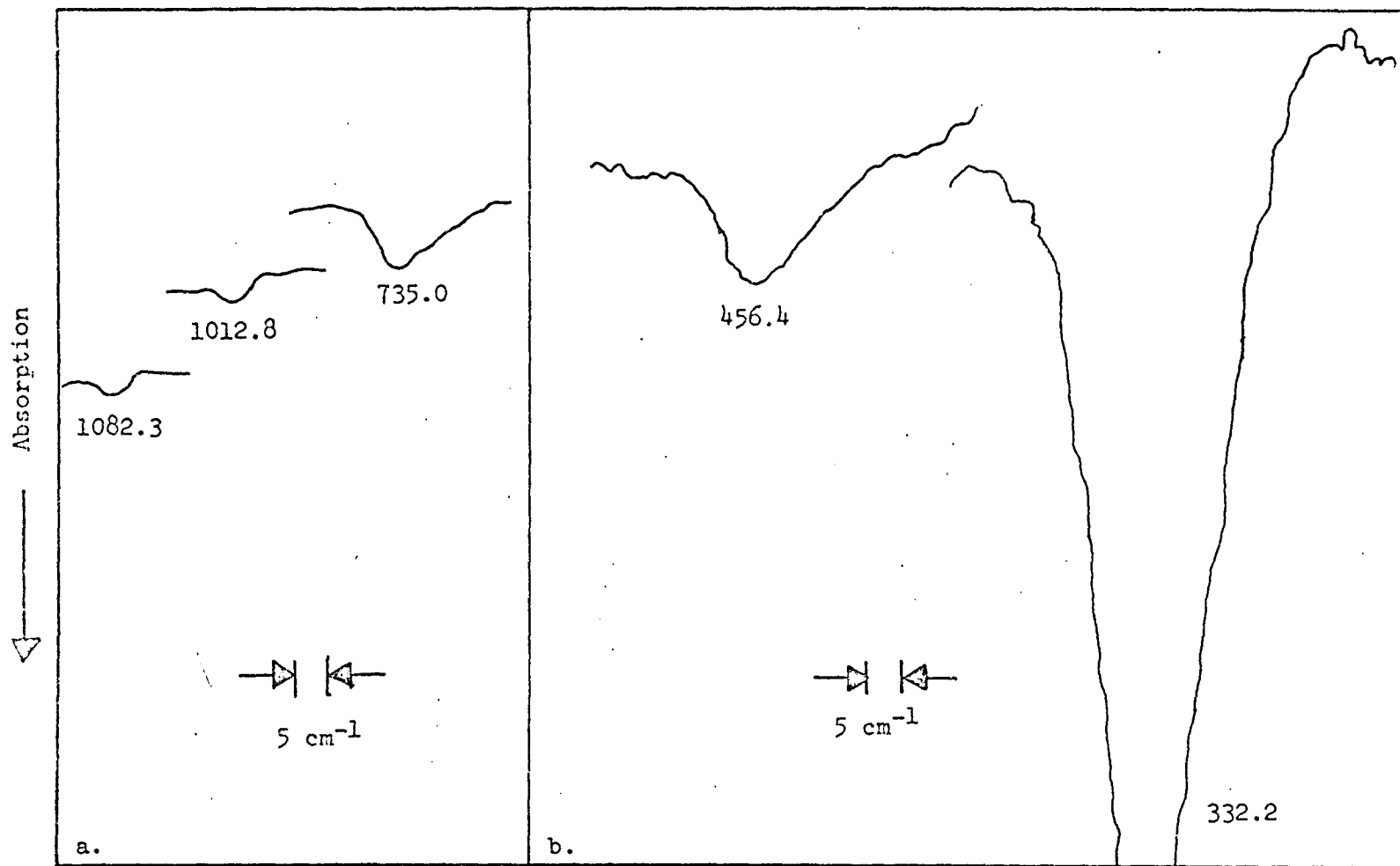


Fig. 5.1-4. Infrared Spectrum of In in Ar + O<sub>2</sub> (a. IR-7, b. IR-11).

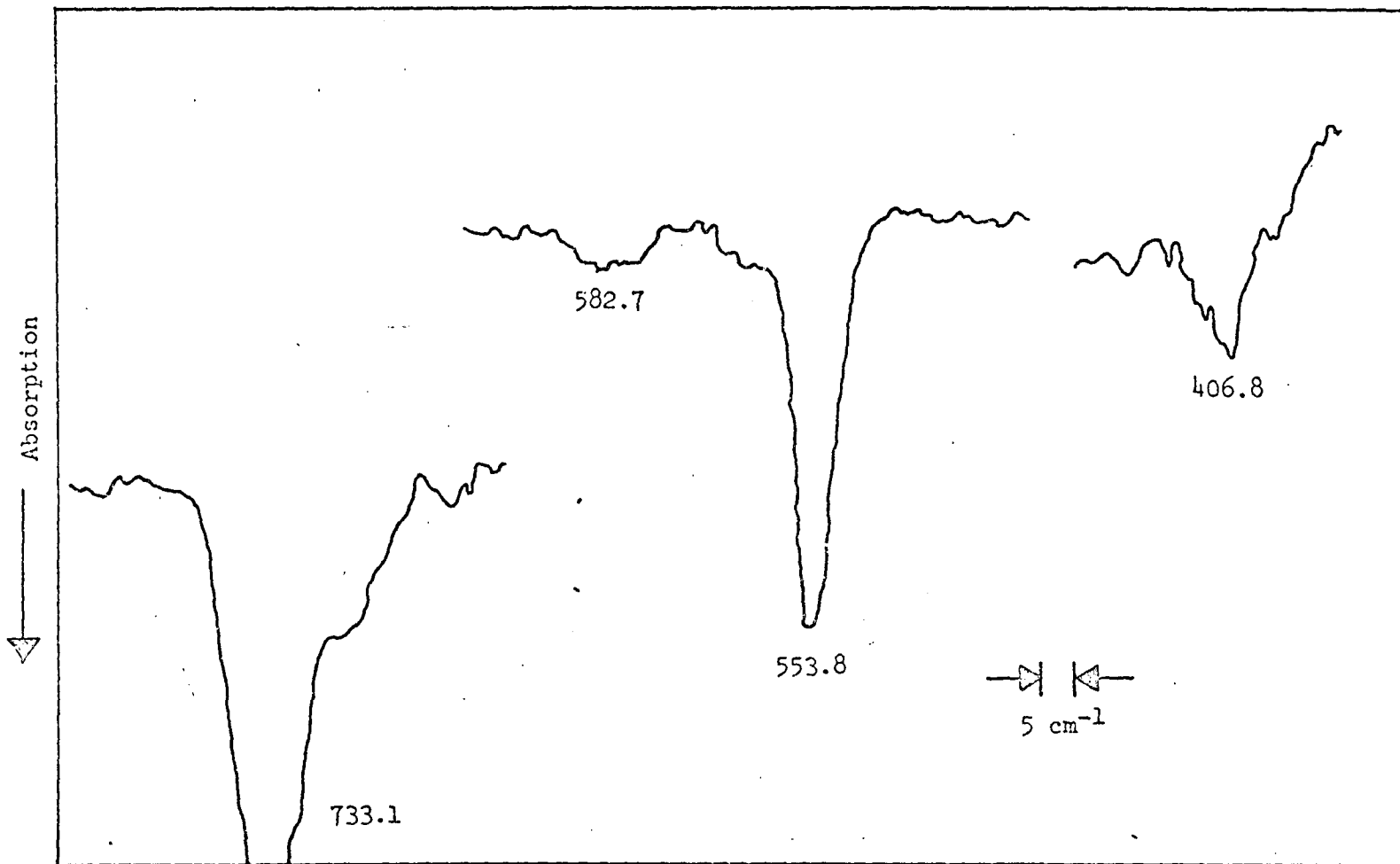


Fig. 5.1-5. Infrared Spectrum of In<sub>2</sub>O in Ar + O<sub>2</sub>.

the "In<sub>2</sub>O" system. The shift was positive for the low absorption and negative for the last two. The  $\nu_3$  was broadened, but apparently was not split. The small rounded peak at  $582.7 \text{ cm}^{-1}$  was also seen in previous In<sub>2</sub>O experiments, but only with a neon matrix. Table 5.1-2 lists the observed frequencies for these experiments. Further experiments showed no other absorptions and no new details.

c) Gallium and Gallium Suboxide

The same Knudsen cell used in earlier Ga<sub>2</sub>O experiments was loaded with a small amount of Ga<sub>2</sub>O<sub>3</sub> powder and a large excess of Ga metal. The sample was degassed and then heated for 7 minutes at 1400 K. Again the exact isolation ratio was not known because of the composition of deposition material. The Ar matrix was composed of 19 per cent O<sub>2</sub>. The spectrum in Fig. 5.1-6a depicts the Ga<sub>2</sub>O  $\nu_3$  at  $816.7 \text{ cm}^{-1}$  which is a shift down of  $5 \text{ cm}^{-1}$ . The doublet from multiple trapping sites (site splitting) seen in an earlier investigation<sup>13</sup> had been reduced into one broadened absorption. There was a weak band at  $1088.4 \text{ cm}^{-1}$  which again disappeared rapidly upon diffusion. There was a strong absorption, shown in Fig. 5.1-6b, at  $383.3 \text{ cm}^{-1}$  apparently corresponding to those at  $332.2$  and  $295.9 \text{ cm}^{-1}$  in the "In- and Tl- oxygen" systems. The broad weak peak at  $589.2 \text{ cm}^{-1}$  was from the "Ga<sub>2</sub>O" system and was also shifted lower  $5 \text{ cm}^{-1}$ .

During a later experiment in which effectively no Ga<sub>2</sub>O<sub>3</sub> was present in the cell, the Ga<sub>2</sub>O  $\nu_3$  was extremely weak. The one per cent absorption at  $818.1 \text{ cm}^{-1}$  appeared to have shifted less than in the above experiment. It seemed that in a mixed matrix the degree of fre-

Table 5.1-2. Infrared Frequencies ( $\text{cm}^{-1}$ ) of In and  $\text{In}_2\text{O}$  Matrix Reactions with  $\text{O}_2$  in Ar.

Absorptions <sup>a</sup>	Intensities <sup>b</sup>	Precursor System
332.2	100	In + $\text{O}_2$
406.8	5	$\text{In}_2\text{O}$
456.4	16	In + $\text{O}_2$
553.8	15	$\text{In}_2\text{O}$
582.7	4	$\text{In}_2\text{O}$
733.1 (735.0)	35	$\text{In}_2\text{O}$
1012.8	3	In + $\text{O}_2$
1082.3	2	In + $\text{O}_2$

a Accuracy considered better than  $\pm 1.0 \text{ cm}^{-1}$ .

b Relative intensities all normalized to the most intense peak.

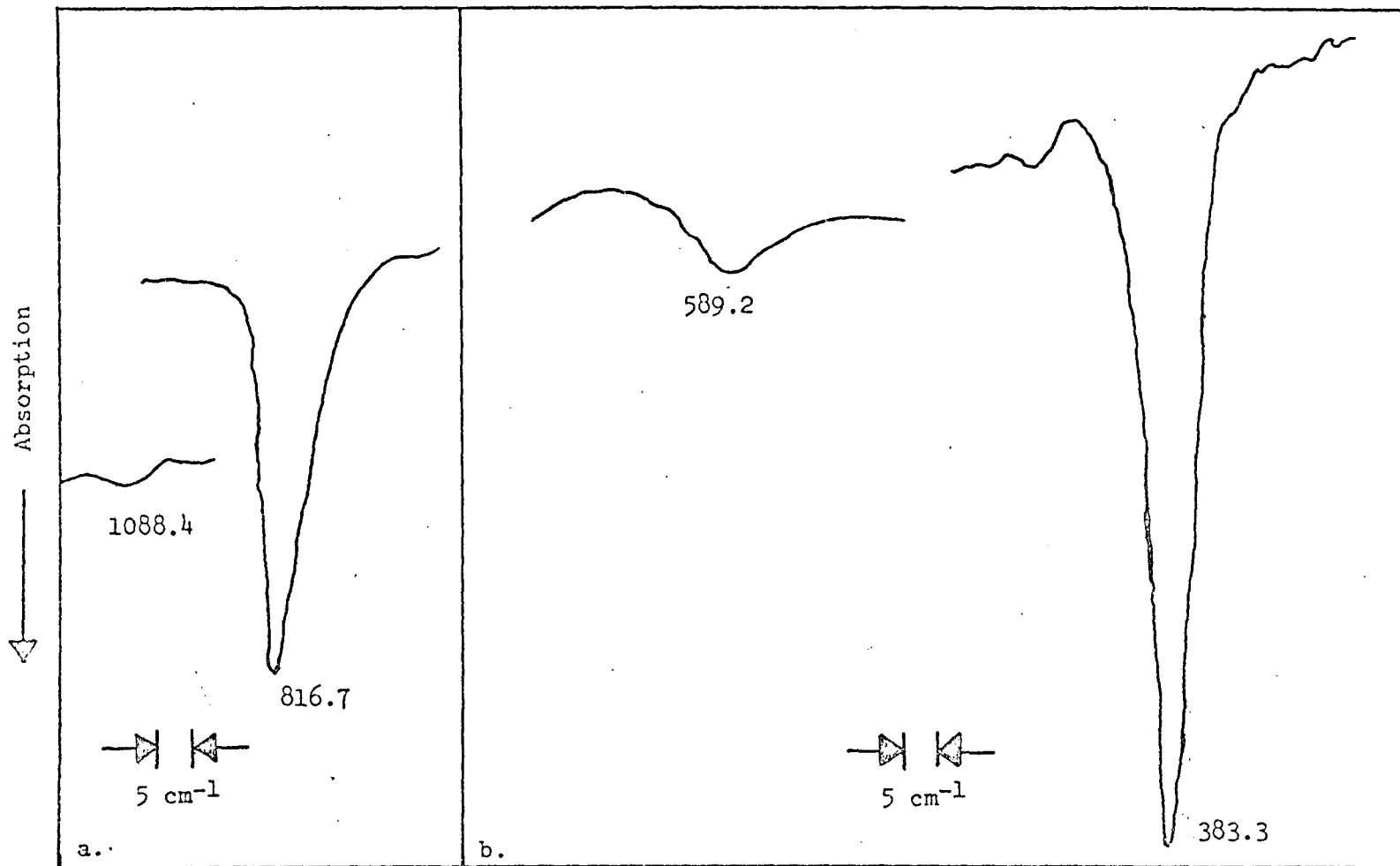


Fig. 5.1-6. Infrared Spectrum of Ga + Ga<sub>2</sub>O in Ar + O<sub>2</sub> (a. IR-7, b. IR-11).

quency shift was possibly related to the  $M_2O$  rather than the  $O_2$  concentration. This same phenomenon was noticed in the  $In_2O$  mixed matrix experiments.

The sample, replenished with  $Ga_2O_3$ , was deposited for 8 minutes at 1350 K in an argon matrix with 18 per cent  $O_2$ . The spectrum, Fig. 5.1-7, contained only four absorptions between 250 and 1500  $cm^{-1}$ . The three at 816.7, 594.3, and 416.6  $cm^{-1}$  were from the " $Ga_2O$ " system while the fourth at 382.9  $cm^{-1}$  corresponded to the " $Ga + O_2$ " reaction product.

Further experiments produced no other bands. A list of absorptions along with their probable origins is given in Table 5.1-3.

d) Aluminum and Aluminum Suboxide

A new zirconia cell was loaded with powdered Al metal, spot-welded into the high temperature heating assembly, and degassed. The sample was deposited for 8 minutes at 1683 K in an Ar matrix with 21 per cent  $O_2$  and an Ar/Al ratio of 410 and  $O_2$ /Al of 185. Before diffusion, Fig. 5.1-8a, absorptions were observed at 686.1, several between 782 and 878, 991.4, 1071.6, 1039.6, and 1116.0  $cm^{-1}$ . After diffusion, Fig. 5.1-8b, the region between 800 and 880  $cm^{-1}$  had cleared considerably and definite peaks were seen. The  $Al_2O_3$ , at 991.4  $cm^{-1}$ , had decreased drastically in intensity.

A further example of this is shown in Fig. 5.1-9 from the same Al sample heated for nine minutes at 1673 K in an argon matrix with 21 per cent oxygen. Spectrum (a) shows the absorptions after one diffusion; spectrum (b) shows the absorptions immediately before the ma-

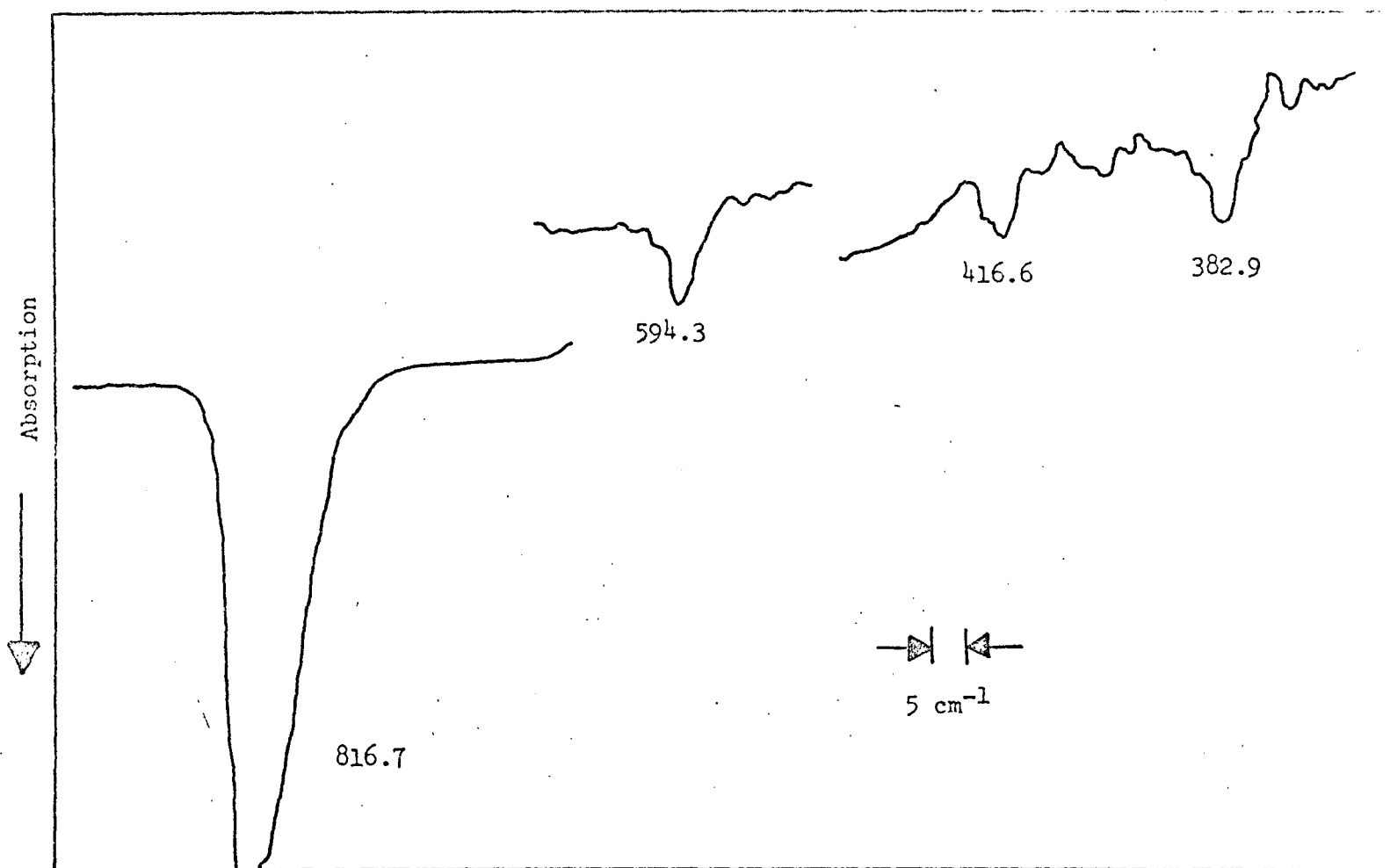


Fig. 5.1-7. Infrared Spectrum of Ga + Ga<sub>2</sub>O in Ar + O<sub>2</sub>.

Table 5.1-3. Infrared Frequencies ( $\text{cm}^{-1}$ ) of Ga and  $\text{Ga}_2\text{O}$  Matrix Reactions with  $\text{O}_2$  in Ar.

Absorptions <sup>a</sup>	Intensities <sup>b</sup>	Precursor System
383.3	100	$\text{Ga} + \text{O}_2$
416.6	1	$\text{Ga}_2\text{O}$
594.3 (589.2)	12	$\text{Ga}_2\text{O}$
816.7 (818.1)	52	$\text{Ga}_2\text{O}$
1088.4	3	$\text{Ga} + \text{O}_2$

a Accuracy considered better than  $\pm 1.0 \text{ cm}^{-1}$ .

b Relative intensities all normalized to the most intense peak.

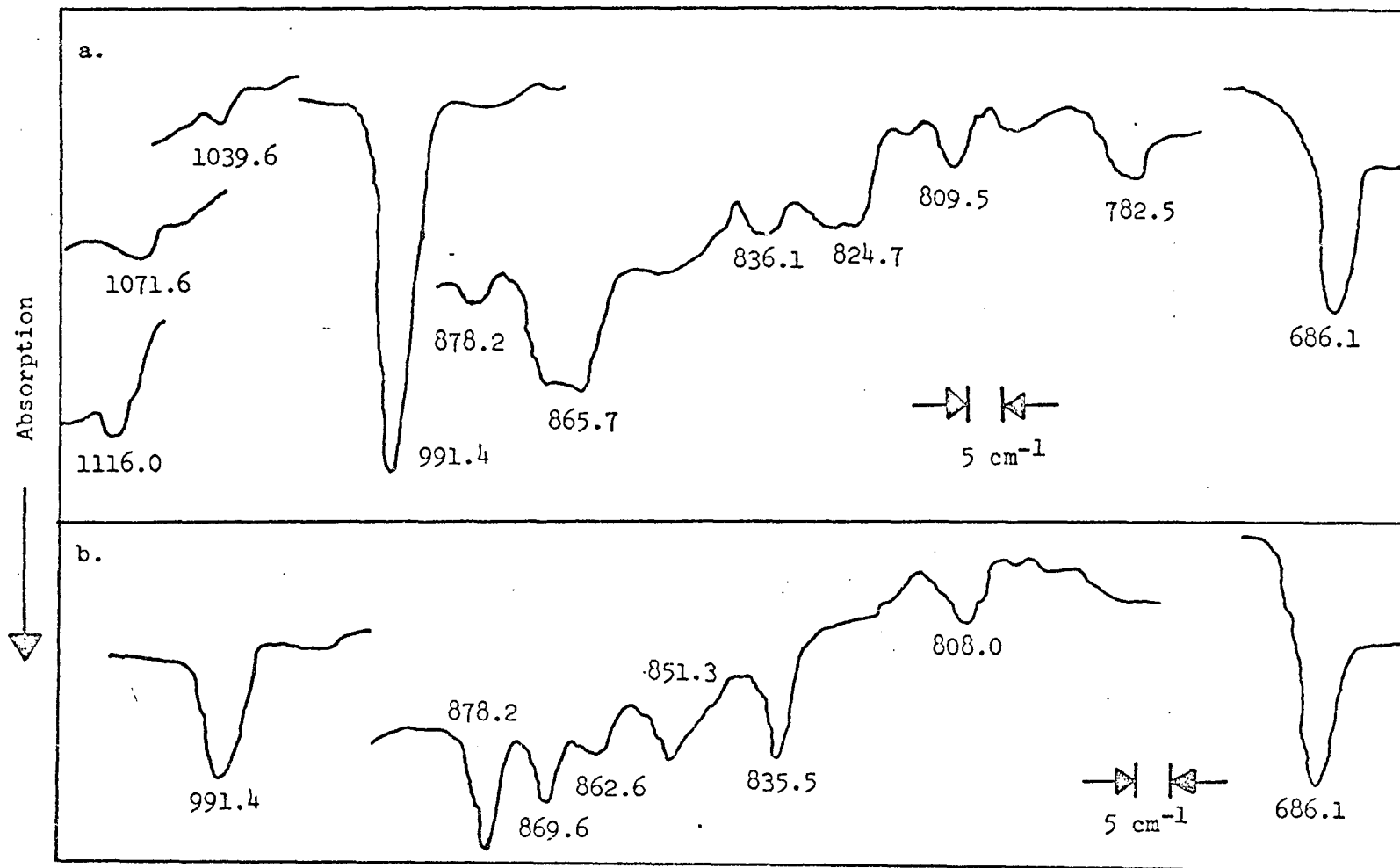


Fig. 5.1-8. Infrared Spectrum of Al in Ar + O<sub>2</sub> (a. Before Diffusion, b. After Diffusion).

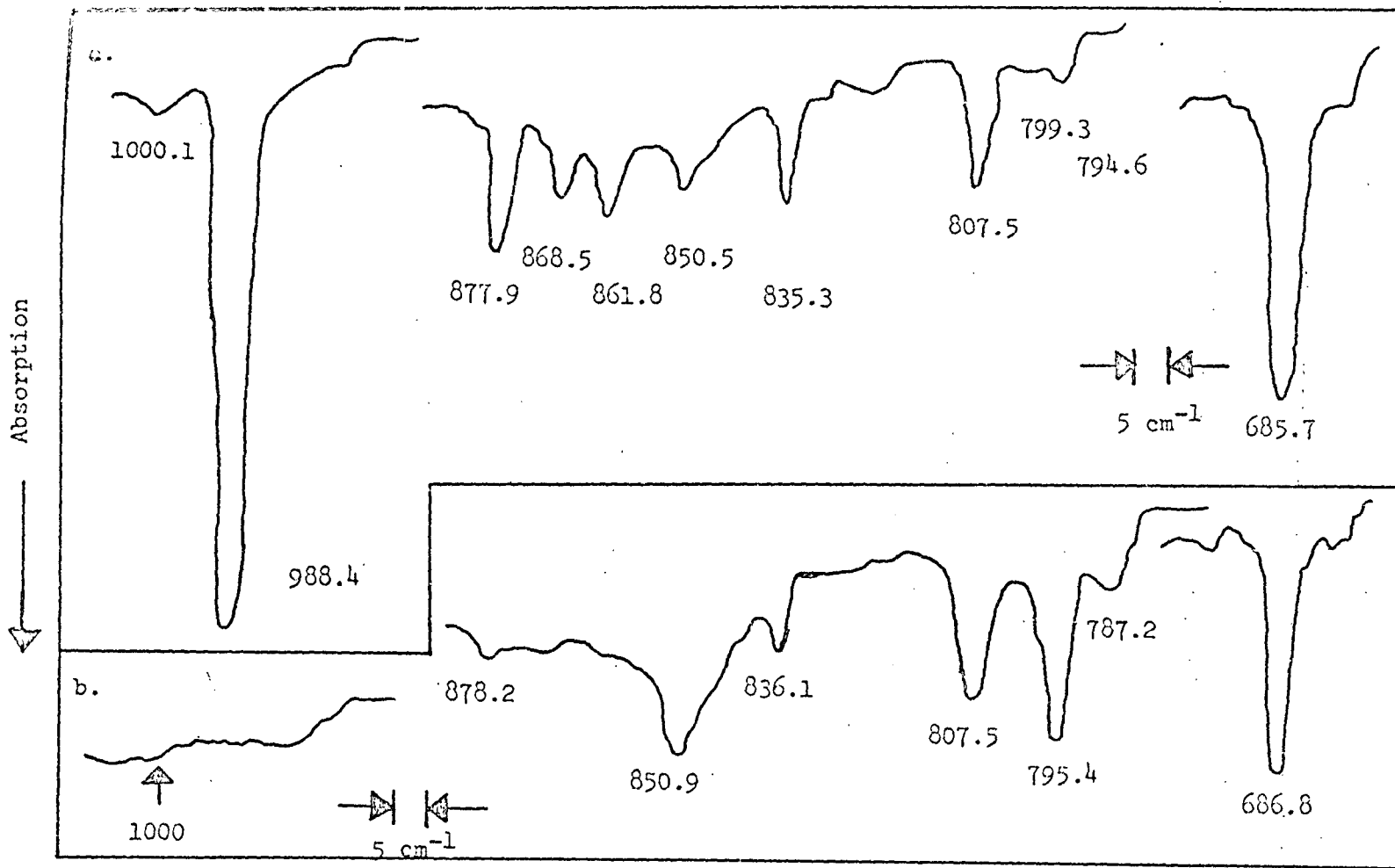


Fig. 5.1-9. Infrared Spectrum of Al in Ar + O<sub>2</sub> (a. After 1 Diffusion, b. After Several Diffusions).

trix completely diffused. It was easily noticed that the  $\text{Al}_2\text{O}_3 \nu_3$  disappeared entirely, the  $686 \text{ cm}^{-1}$  band grew slightly, and the others relative intensity varied with each diffusion probably indicating higher polymers of some species.

An experiment was attempted with 20 per cent  $\text{O}_2$  in a  $\text{N}_2$  matrix. The sample was deposited for 8 minutes at 1673 K. The only observable peaks were the  $\nu_3$  for  $\text{Al}_2\text{O}_3$  at  $988.8 \text{ cm}^{-1}$  and a weak band at  $1095.6 \text{ cm}^{-1}$  possibly corresponding to those seen earlier for the other "M +  $\text{O}_2$ " systems and the one at  $1116.0 \text{ cm}^{-1}$  seen in the first aluminum experiment.

Since the  $\text{Al}_2\text{O}_3 \nu_3$  absorption was detected in every deposition of metal into a mixed matrix, a blank run was made to deposit only metal in a pure Ar matrix. The sample was heated for 8 minutes at 1773 K. The spectrum showed one absorption at  $992.3 \text{ cm}^{-1}$  indicating that a small amount of  $\text{Al}_2\text{O}_3$  had effused from the cell. Since this had been completely outgassed and used for several experiments, it appeared that the Al was leaching oxygen from the zirconia cell walls to form  $\text{Al}_2\text{O}_3$ .

The high temperature cell was reloaded with  $\text{Al}_2\text{O}_3$  and Al. The degassed sample was heated at 1730 K for 8 minutes. The matrix was argon with 20 per cent oxygen. The spectrum, Fig. 5.1-10, demonstrates that there are no major differences from earlier spectra other than the stronger  $\text{Al}_2\text{O}_3$  absorption. However, the expected  $714 \text{ cm}^{-1}$  peak from the " $\text{Al}_2\text{O}_3$ " system did not appear. A list of absorptions is given in Table 5.1-4 along with an indication of the effect of several diffusions.

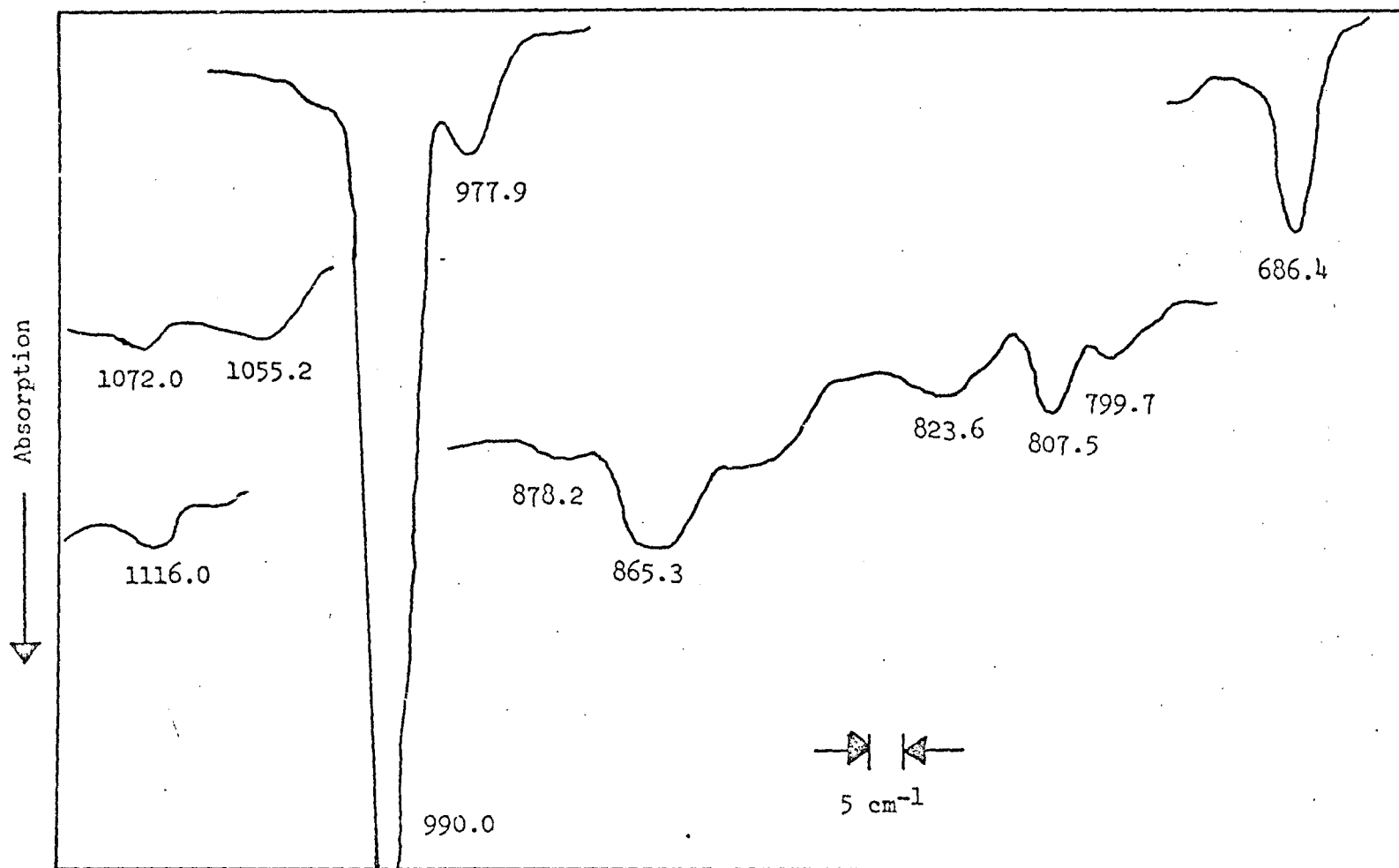


Fig. 5.1-10. Infrared Spectrum of Al + Al<sub>2</sub>O in Ar + O<sub>2</sub>.

Table 5.1-4. Infrared Frequencies ( $\text{cm}^{-1}$ ) of Al and  $\text{Al}_2\text{O}$  Matrix Reactions with  $\text{O}_2$  in Ar ( $\text{N}_2$ ).

Absorptions <sup>a</sup>	Initial Intensities <sup>b</sup>	Diffusion <sup>c</sup>	Precursor System
686.1	50	R	$\text{Al} + \text{O}_2$
782.5	12	D	$\text{Al} + \text{O}_2$
787.2	0	I	$\text{Al} + \text{O}_2$
795.4	3	I	$\text{Al} + \text{O}_2$
799.3	1	D	$\text{Al} + \text{O}_2$
809.5	12	I	$\text{Al} + \text{O}_2$
824.7	14	D	$\text{Al} + \text{O}_2$
836.1	10	I	$\text{Al} + \text{O}_2$
851.3	1	I	$\text{Al} + \text{O}_2$
862.6	35	D	$\text{Al} + \text{O}_2$
869.6	35	D	$\text{Al} + \text{O}_2$
878.2	7	I	$\text{Al} + \text{O}_2$
977.9	1	D	$\text{Al}_2\text{O}$
991.4 (988.8) <sup>d</sup>	100	D	$\text{Al}_2\text{O}$
1000.1	2	D	$\text{Al}_2\text{O}$
1039.6	6	D	$\text{Al}_2\text{O}$
1071.6	7	D	$\text{Al} + \text{O}_2$
1116.0 (1095.6) <sup>d</sup>	8	D	$\text{Al} + \text{O}_2$

a Accuracy considered better than  $\pm 1.0 \text{ cm}^{-1}$ .

Table 5.1-4. (Continued)

- 
- 
- b Relative intensities all normalized to the most intense peak.
- c I denotes an increase upon matrix warming, D a decrease, and R indicates that the intensity remained approximately constant.
- d Nitrogen + O<sub>2</sub> matrix.

## 5.2 Isotopic Investigation of the Suboxides

In order to obtain a definite picture as to the accuracy of the vibrational assignments for the suboxides, the investigator performed a series of experiments with aluminum and gallium sesquioxide isotopically enriched with oxygen -18. The oxygen atom is quite light as compared with most metal atoms and gives relatively large vibrational isotopic effects. For any system with both  $^{16}\text{O}$  and  $^{18}\text{O}$  present, a molecule containing one oxygen atom will have each of its vibrational modes appear as a doublet. However, a molecule containing two equivalent oxygens will have each absorption appear as a triplet. In either example, the pure oxygen -16 band will be at the highest energy and the oxygen -18 at the lowest.

### a) Aluminum Suboxide

Three satisfactory  $\text{Al}_2\text{O}$  experiments were performed with the mixture of Al and enriched  $\text{Al}_2\text{O}_3$ . In all cases the high temperature Knudsen cell was employed. In the first experiment the cell was heated to 1725 K for ten minutes to deposit 11 $\mu$  moles of  $\text{Al}_2\text{O}$  at an isolation ratio of 1000. Although the matrix flowed slightly, three absorptions were detected as shown in Fig. 5.2-1. The first at  $990.7\text{ cm}^{-1}$  corresponded to the  $\nu_3$  for  $\text{Al}_2\text{O}$  reported by Linevsky et al.<sup>15</sup>, Makowiecki,<sup>13,19</sup> and Snelson.<sup>17</sup> The second at  $946.6\text{ cm}^{-1}$  was the oxygen -18  $\nu_3$  of  $\text{Al}_2\text{O}$  found previously.<sup>15</sup> The third was a very weak side band at  $1012.2\text{ cm}^{-1}$ . Although the  $\text{Al}_2\text{O}_3$  was nominally 70 per cent enriched, the spectrum indicated only 35 per cent. There was no indication in this experiment of any absorption near the re-

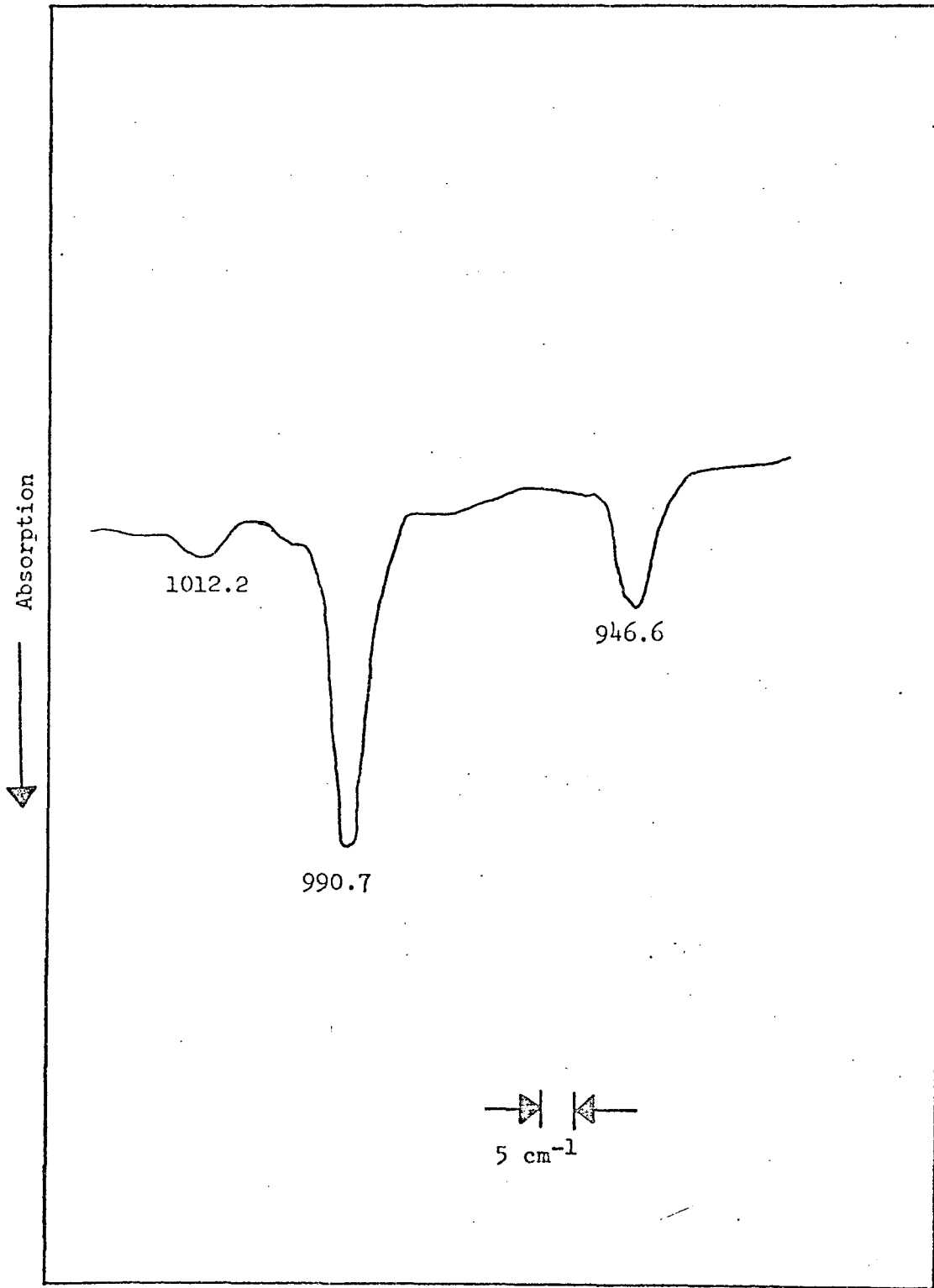


Fig. 5.2-1. Infrared Spectrum of <sup>18</sup>O Enriched Al<sub>2</sub>O in Ar.

ported  $\text{Al}_2\text{O}$   $\nu_1$  value of  $714 \text{ cm}^{-1}$ .

In the next experiment the cell was heated at 1750 K for five minutes. Approximately  $7\mu$  moles were deposited at an isolation ratio in excess of 1000. The IR-7 spectrum, illustrated in Fig. 5.2-2a, shows two strong absorptions at  $989.8$  and  $946.8 \text{ cm}^{-1}$  along with several side bands. These side bands corresponded to those seen by Linevsky in his heavier matrix deposits. There was also a small band at  $747.2 \text{ cm}^{-1}$  which showed no oxygen isotopic effect and disappeared rapidly upon annealing. With diffusion, three weak absorptions grew in at  $714.8$ ,  $700.0$ , and  $689.4 \text{ cm}^{-1}$  as shown in Fig. 5.2-2b. The first two corresponded to absorptions detected by Linevsky and assigned as  $\nu_1$  and  $\nu_1'$  for  $\text{Al}_2\text{O}$ . However, this assignment was now untenable as a triplet clearly indicated two equivalent oxygens. Also, these bands were not observed until after a diffusion experiment, indicating that they were due to an association process in the matrix and not to a direct deposition. The IR-11 spectrum showed no absorption near  $500 \text{ cm}^{-1}$  where the  $\text{Al}_2\text{O}$   $\nu_2$  had been reported.

In the third experiment the cell was heated to 1725 K, and approximately  $11\mu$  moles were deposited at an isolation ratio of 600. The recorded spectrum is shown in Fig. 5.2-3 before diffusion and in Fig. 5.2-4 after several diffusions. Initially the two major absorptions at  $989.9$  and  $947.8 \text{ cm}^{-1}$  had several side bands. There was a peak at  $747 \text{ cm}^{-1}$ , and again there was a triplet at  $714.8$ ,  $699.8$ , and  $688.4 \text{ cm}^{-1}$ . After several diffusions the triplet maintained its relative size as the doublet drastically decreased in intensity. The IR-11 spectrum again showed no bands although it had a mechanical

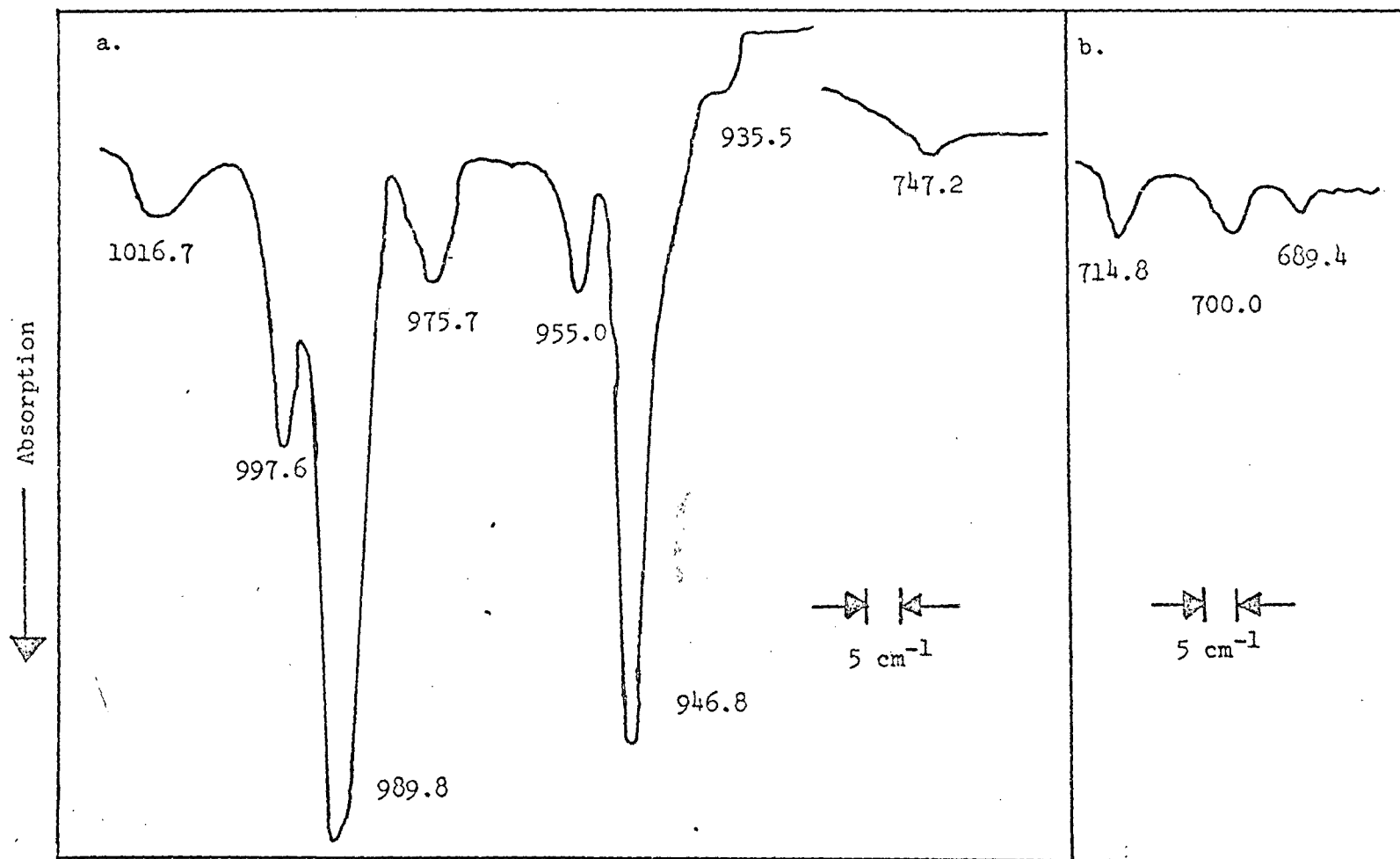


Fig. 5.2-2. Infrared Spectrum of  $^{18}\text{O}$  Enriched  $\text{Al}_2\text{O}$  in Ar (a. Before Diffusion, b. After Diffusion).

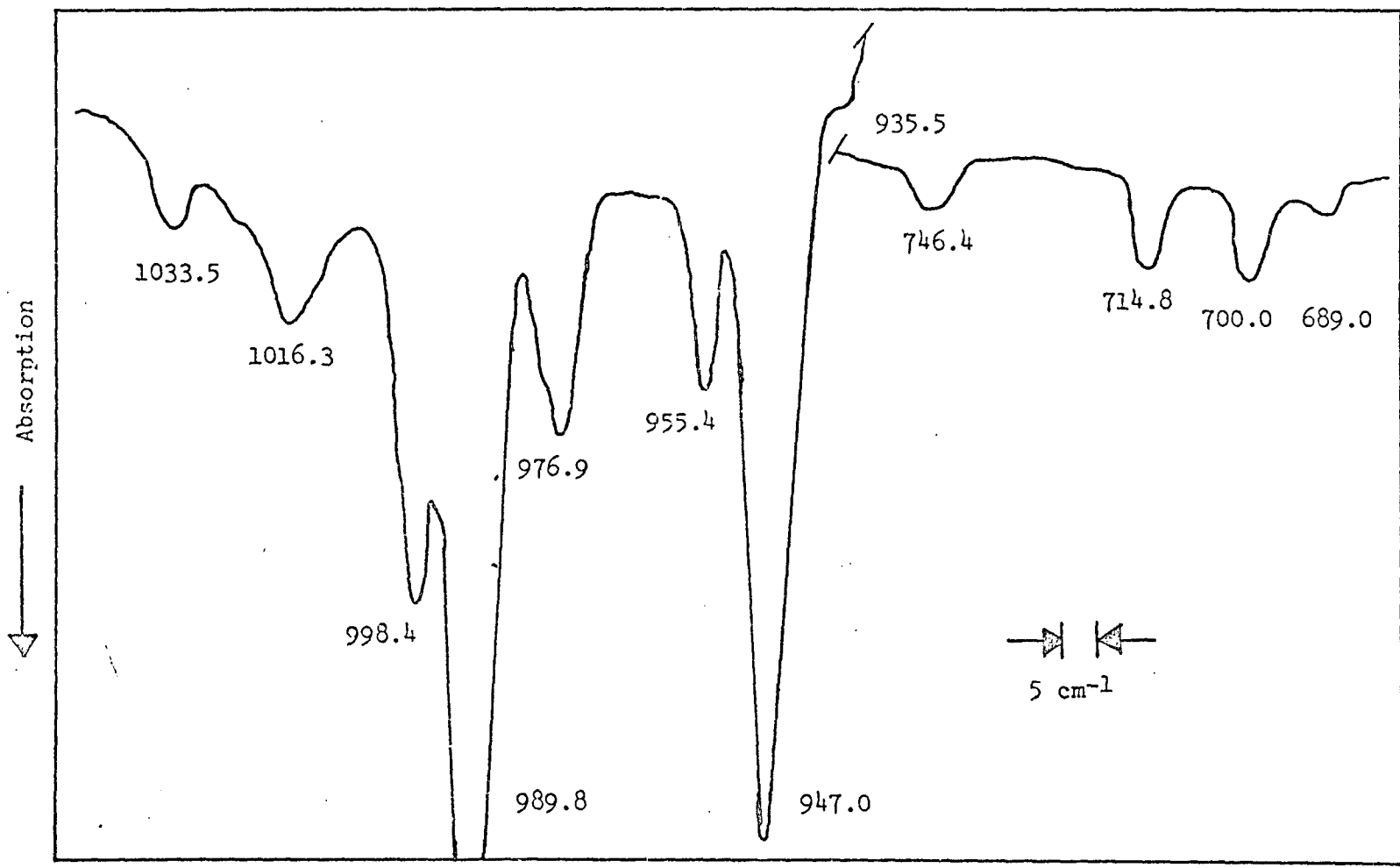


Fig. 5.2-3. Infrared Spectrum of <sup>18</sup>O Enriched Al<sub>2</sub>O<sub>3</sub> in Ar Before Diffusion.

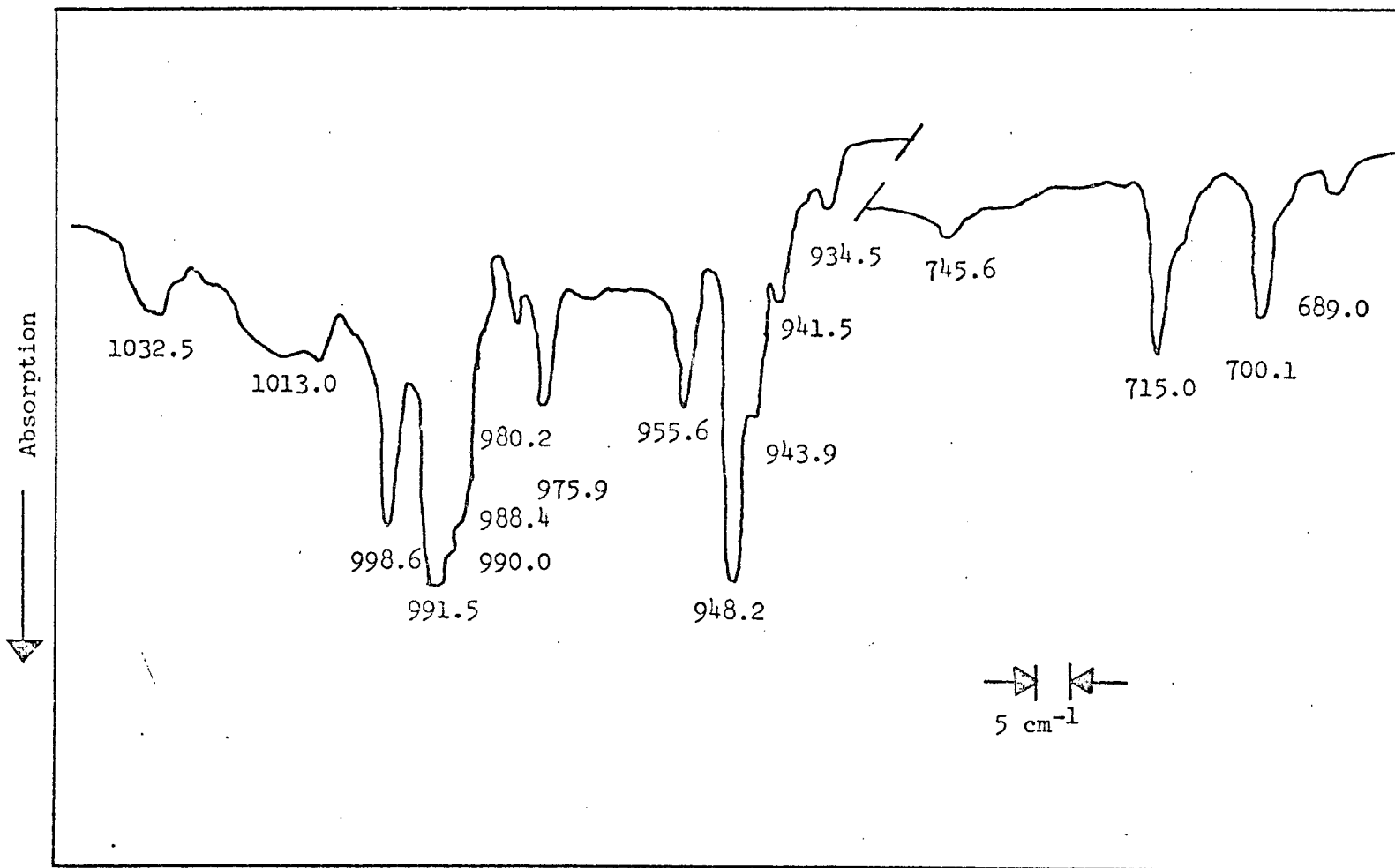


Fig. 5.2-4. Infrared Spectrum of <sup>18</sup>O Enriched Al<sub>2</sub>O<sub>3</sub> in Ar After Several Diffusions.

failure during the experiment. The dry air purge was broken, causing a loss in energy and the appearance of large water bands.

No other absorptions were seen during these experiments. The observed frequencies and their relative intensities are listed in Table 5.2-1.

b) Gallium Suboxide

Gallium suboxide was isolated several times in argon matrices and once in nitrogen. In the first experiment, the sample of Ga plus enriched  $\text{Ga}_2\text{O}_3$  was heated for 8 minutes at 1173 K to deposit  $3\mu$  moles of  $\text{Ga}_2\text{O}$  in argon at a M/R ratio of 1500. The IR-7 showed two main absorptions, each of which was a doublet at 822.1, 818.1 and at 781.3, 777.4  $\text{cm}^{-1}$ . The splitting of the  $\nu_3$  band in argon had been seen before for gallium, indium, and thallium suboxide and was expected. The two main peaks were the  $\nu_3$  and  $\nu_3'$  for  $\text{Ga}_2\text{O}$  as predicted.<sup>13</sup> The IR-11 spectrum, illustrated in Fig. 5.2-5, showed a triplet at 595.0, 579.5 and 567.5  $\text{cm}^{-1}$ . After diffusion, the two main absorptions, Fig. 5.2-6, had definitely decreased in intensity while the triplet had increased. This indicated that the previously assigned  $\nu_1$ <sup>13,19</sup> was incorrect and that this absorption belonged to another molecule.

In the next experiment,  $3\mu$  moles of  $\text{Ga}_2\text{O}$  were isolated in argon at a ratio of 5000. The spectrum, represented in Fig. 5.2-7, showed a triplet at 595.4, 579.4, and 568.1  $\text{cm}^{-1}$  as before. After several diffusions an original doublet at 416.3 and 407.9  $\text{cm}^{-1}$  was seen to actually be a triplet with the third absorption at 396.0  $\text{cm}^{-1}$

Table 5.2-1. Infrared Frequencies ( $\text{cm}^{-1}$ ) of Oxygen -18 Enriched  $\text{Al}_2\text{O}_3$  in Ar (Exp. 3.).

Absorptions <sup>a</sup>	Initial Intensities <sup>b</sup>	Diffusion <sup>c</sup>
689.0	3	I
700.0	10	I
714.8	10	I
746.4	5	D
935.5	3	D
947.0	80	D
955.4	25	D
976.9	30	D
989.8	100	D
998.4	45	D
1016.3	17	D
1033.5	10	D

a Accuracy considered better than  $\pm 1.0 \text{ cm}^{-1}$ .

b Relative intensities all normalized to the most intense peak.

c I denotes an increase upon matrix warming, D a decrease, and R indicates that the intensity remained approximately constant.

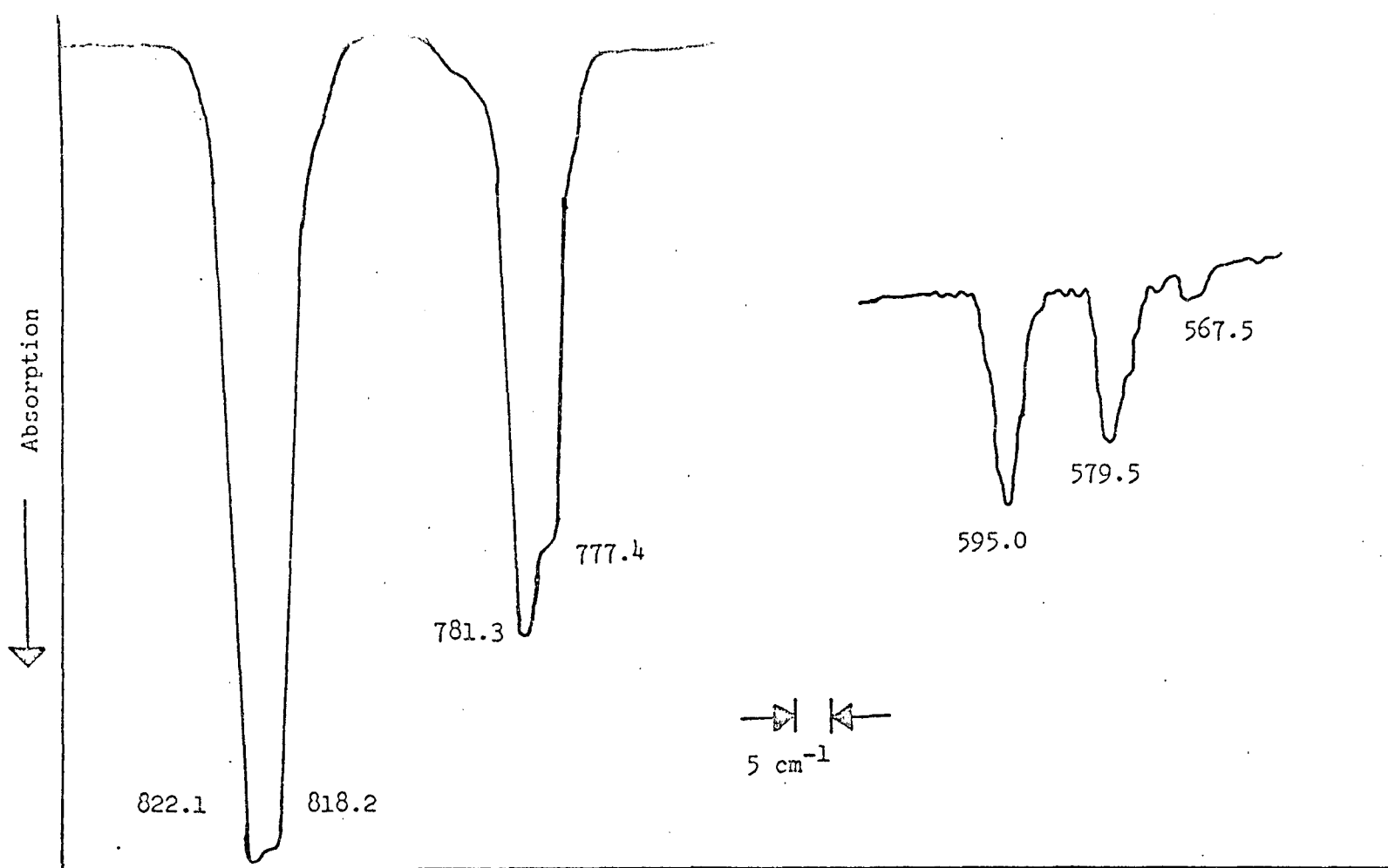


Fig. 5.2-5. Infrared Spectrum of  $^{18}\text{O}$  Enriched  $\text{Ga}_2\text{O}$  in Ar (Before Diffusion).

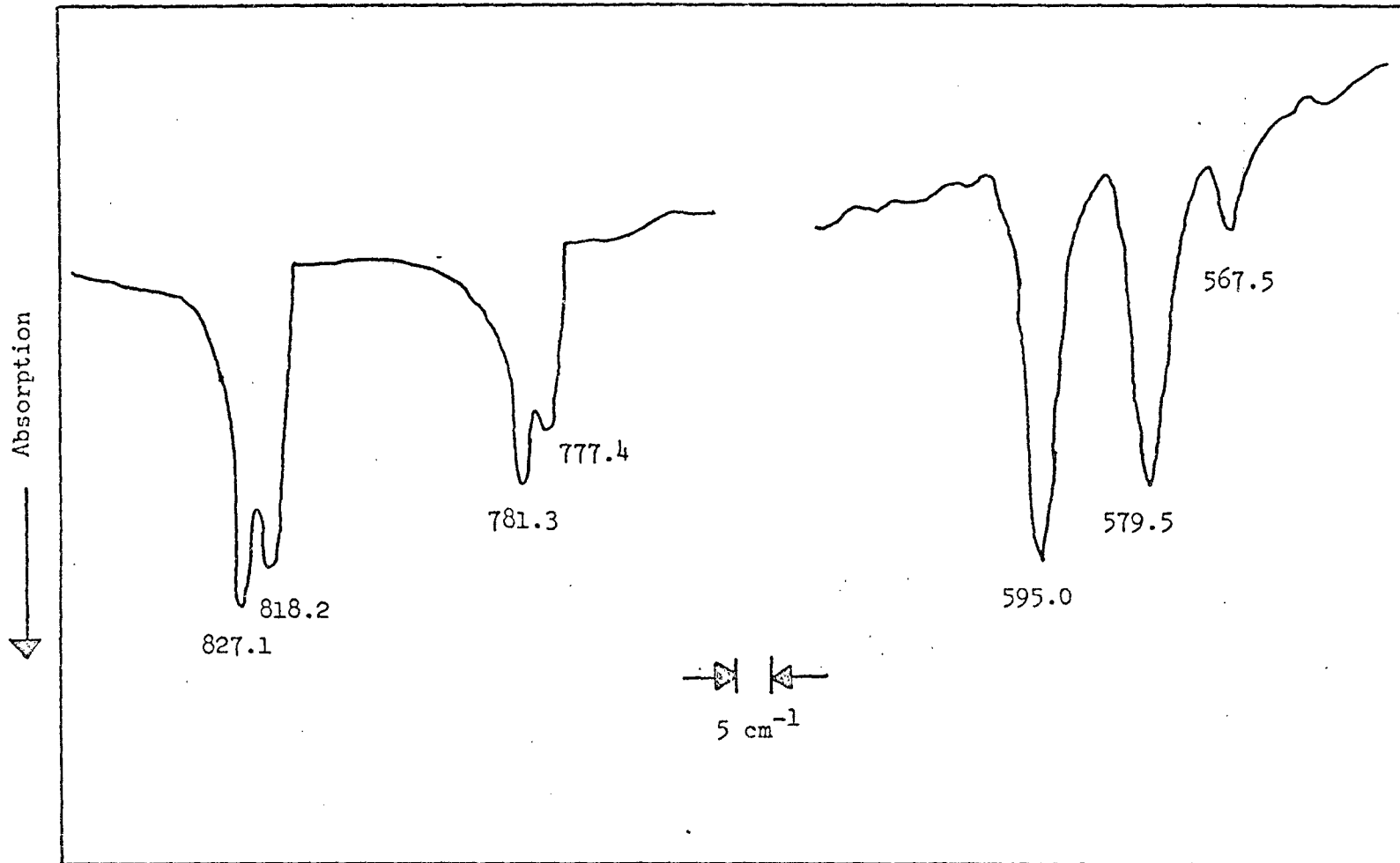


Fig. 5.2-6. Infrared Spectrum of  $^{18}\text{O}$  Enriched  $\text{Ga}_2\text{O}$  in Ar (After Diffusion).

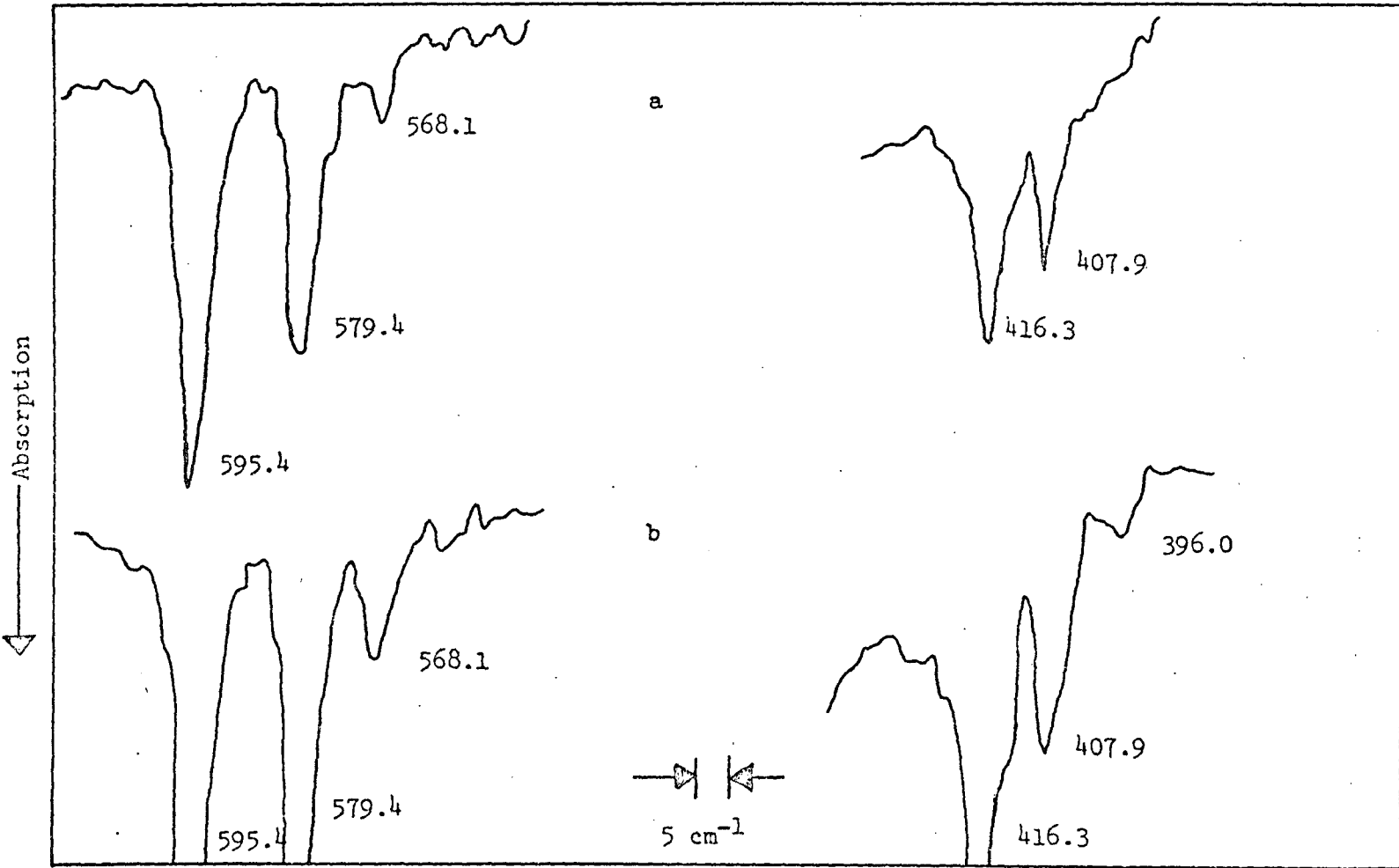


Fig. 5.2-7. Partial Infrared Spectrum of  $^{18}\text{O}$  Enriched  $\text{Ga}_2\text{O}$  in Ar (a. Before Diffusion, b. After Diffusion).

thus indicating the  $\nu_2$  assignment of Makowiecki was also incorrect. It was possible that both triplets were from the same molecule as both grew upon diffusion.

The same sample was reheated and  $7.7\mu$  moles of  $\text{Ga}_2\text{O}$  were deposited in a  $\text{N}_2$  matrix at a M/R ratio of 1500. A large doublet at 808.0 and 767.7  $\text{cm}^{-1}$ , shown in Fig. 5.2-8, corresponded to  $\nu_3$  and  $\nu_3'$  reported by Ogden<sup>16</sup> and Makowiecki.<sup>13,19</sup> There was definitely a triplet at 590.4, 574.7 and 567.8  $\text{cm}^{-1}$ . However, it was not until after diffusion, as shown in Fig. 5.2-9, that a triplet structure appeared with peaks at 425.3, 416.5, and 404.7  $\text{cm}^{-1}$ . The small absorptions at 881.4 and 751.3  $\text{cm}^{-1}$  were unassignable. The latter peak remained after several diffusions.

Additional experiments were undertaken with oxygen -18 enrichment of approximately 60 per cent. In Fig. 5.2-10 the spectrum is shown before diffusion. There was no doubt that  $\nu_3$  and  $\nu_3'$  were a doublet. The triplet near 595  $\text{cm}^{-1}$  was detected, but no bands were seen near 415  $\text{cm}^{-1}$ . After diffusion, as illustrated in Fig. 5.2-11, the triplet at 595  $\text{cm}^{-1}$  had increased in intensity, a new weak triplet was revealed around 415  $\text{cm}^{-1}$ , and the  $\nu_3$  doublet had decreased in intensity. This doublet did not show the normal 4  $\text{cm}^{-1}$  splitting because it was recorded at the upper limits of the IR-11, where some resolution is lost.

A summary of the observed frequencies is found in Table 5.2-2. The vibrational assignments of Makowiecki were definitely incorrect for the  $\nu_1$  and  $\nu_2$  modes of  $\text{Ga}_2\text{O}$ .

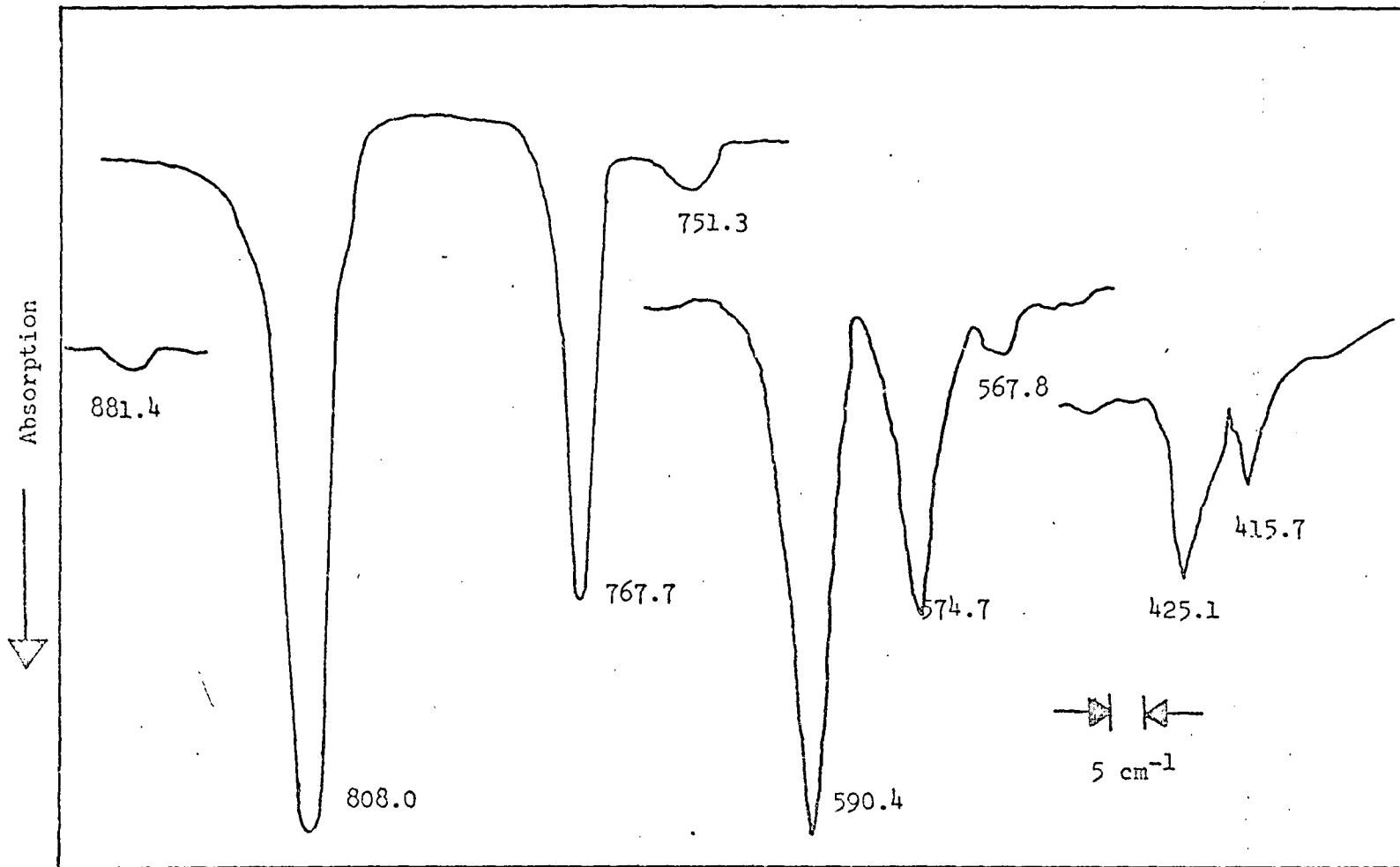


Fig. 5.2-8. Infrared Spectrum of  $^{18}\text{O}$  Enriched  $\text{Ca}_2\text{O}$  in  $\text{N}_2$  (Before Diffusion).

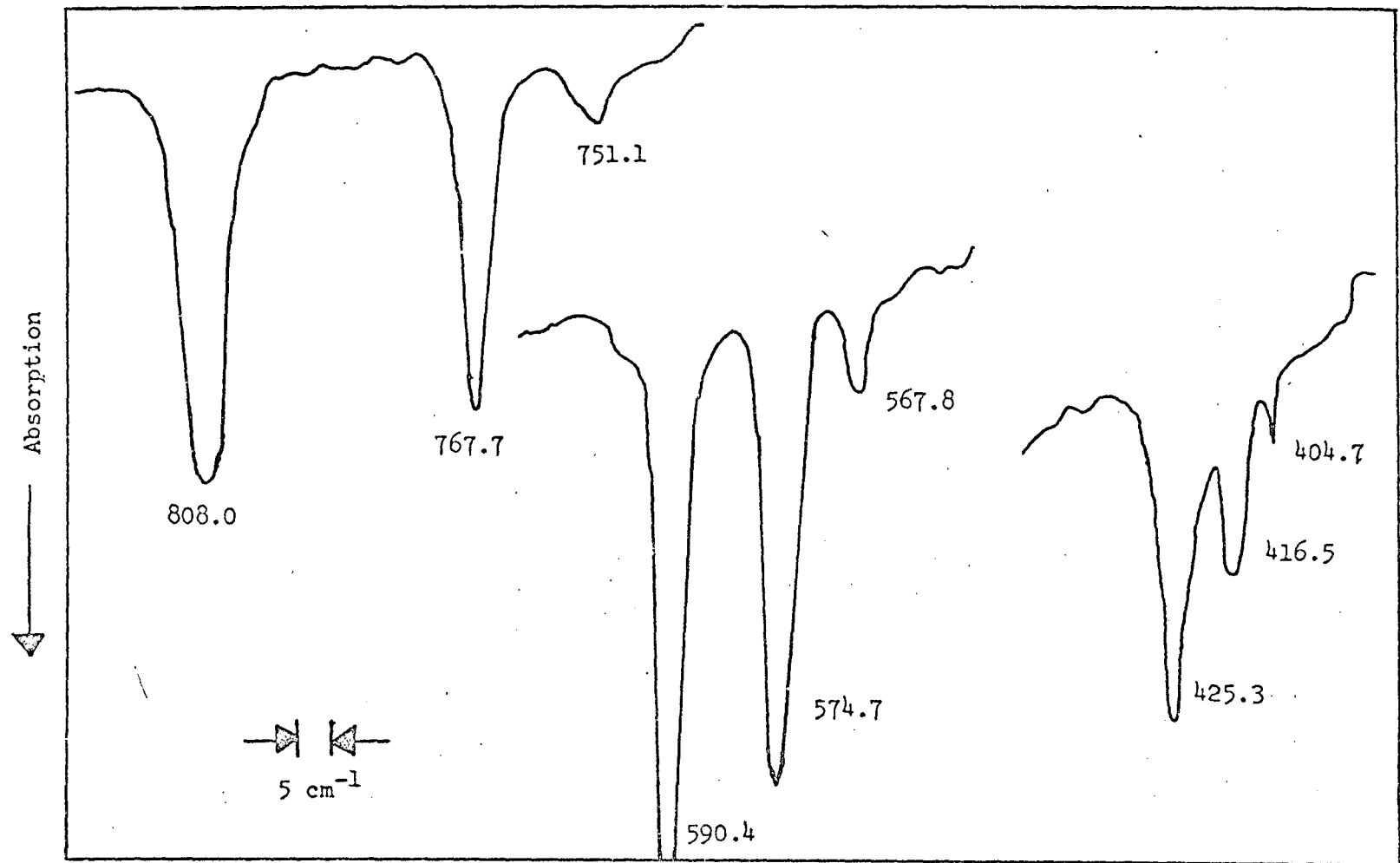


Fig. 5.2-9. Infrared Spectrum of <sup>18</sup>O Enriched Ga<sub>2</sub>O in N<sub>2</sub> (After Diffusion).

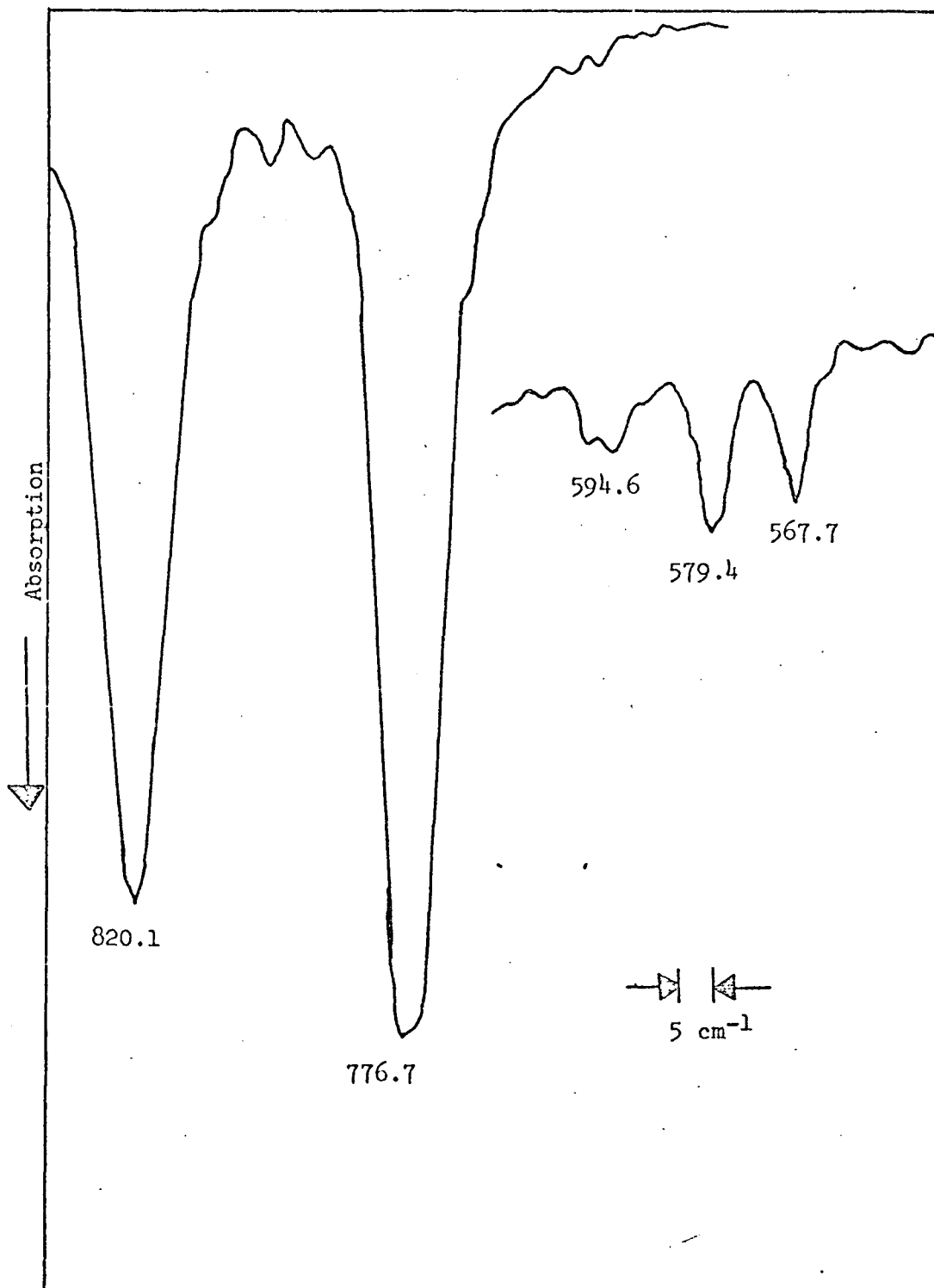


Fig. 5.2-10. Infrared Spectrum of  $^{18}\text{O}$  Enriched  $\text{Ga}_2\text{O}$  in Ar Before Diffusion.

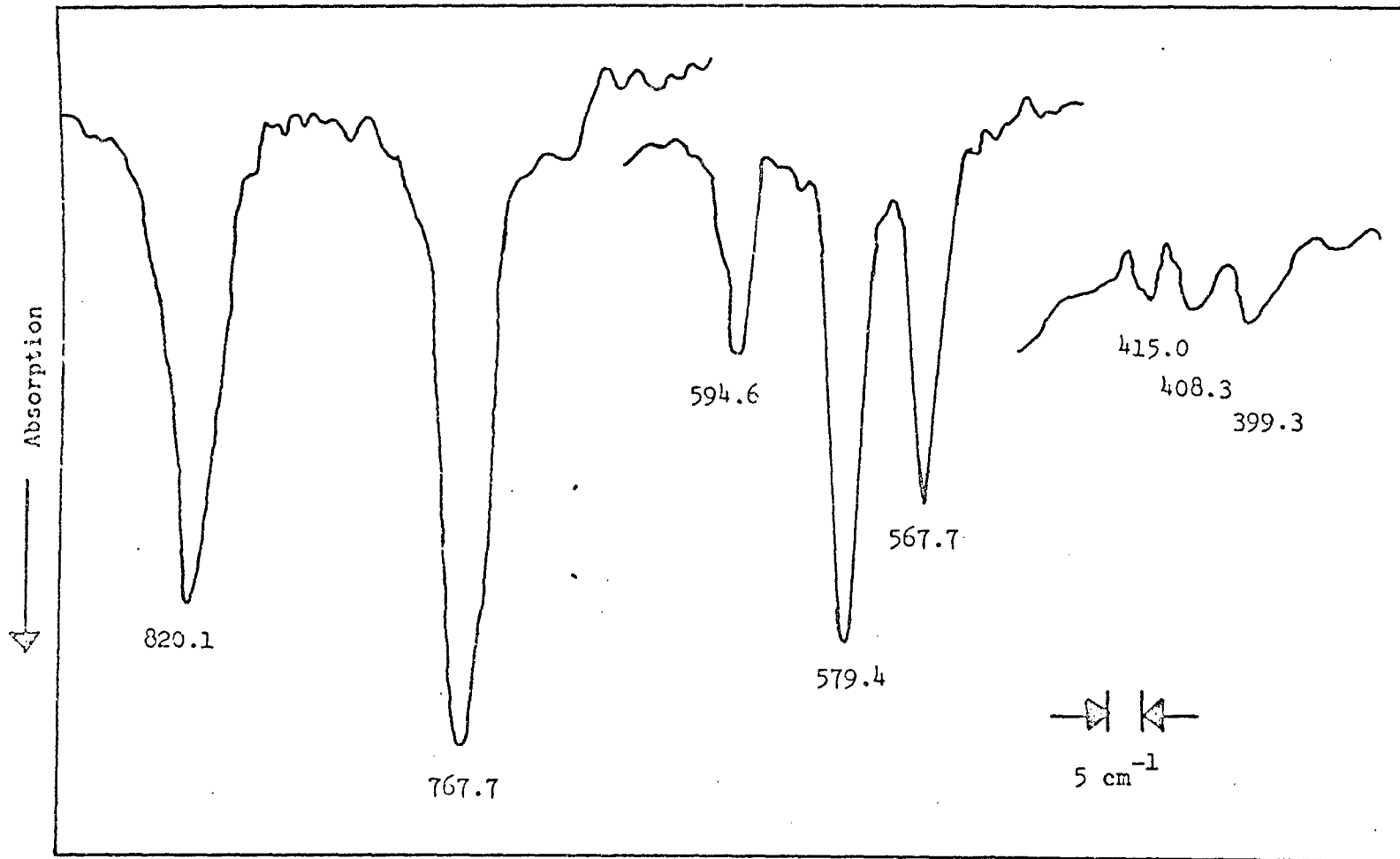


Fig. 5.2-11. Infrared Spectrum of <sup>18</sup>O Enriched Ga<sub>2</sub>O in Ar After Diffusion.

Table 5.2-2. Infrared Frequencies of Oxygen -18 Enriched Ga<sub>2</sub>O.

Absorptions <sup>a</sup>	Initial Intensities <sup>b</sup>	Diffusion <sup>c</sup>
Ar Matrix		
822.1	100	D
818.1	99	D
781.3	72	D
777.4	62	D
595.0	27	I
579.5	19	I
567.5	4	I
416.3	4	I
407.9	3	I
396.0	1	I
N <sub>2</sub> Matrix		
881.4	3	D
808.0	100	D
767.7	67	D
751.3	5	R
590.4	75	I
574.7	41	I
562.8	5	I
425.3	26	I
416.5	11	I
404.7	1	I

Table 5.2-2. (Continued)

- 
- 
- a Accuracy considered better than  $\pm 1.0 \text{ cm}^{-1}$ .
  - b Relative intensities all normalized to the most intense peak.
  - c I denotes an increase upon matrix warming, D a decrease, and R indicates that the intensity remained approximately constant.

c) Indium Gallium Suboxide

It was reported previously<sup>13,19</sup> that the molecule InGaO was produced as the predominant species when a mixture of In and Ga<sub>2</sub>O<sub>3</sub> was heated. At that time a spectrum was reported for the mixed system. Therefore, an attempt was made to isolate this molecule with the enriched Ga<sub>2</sub>O<sub>3</sub>. Since In<sub>2</sub>O and Ga<sub>2</sub>O are also found in this reaction, it was possible to carry out several studies at the same time.

The sample was heated to approximately 1280 K for ten minutes. The ratio of InGaO/In<sub>2</sub>O/Ga<sub>2</sub>O was calculated to be 1.0/0.9/0.3. A total of 2.5 μ moles were deposited at a total isolation ratio of 5000 in argon. The only discernable absorptions, shown in Fig. 5.2-12, were between 675 and 825 cm<sup>-1</sup>, which is the region of the antisymmetric stretching mode  $\nu_3$  of the three molecules. As seen with Ga<sub>2</sub>O, each absorption was split into a doublet apparently due to site splitting in the argon matrix. The spectrum showed the  $\nu_3$  for Ga<sub>2</sub>O at 820.4 and 816.7 cm<sup>-1</sup>. The  $\nu_3'$  was discernable only as the side band at 780.8 cm<sup>-1</sup>. The  $\nu_3$  for InGaO at 792.1 and 789.0 cm<sup>-1</sup> corresponded with the  $\nu_3'$  at 752.3 and 748.0 cm<sup>-1</sup>. Likewise, the  $\nu_3$  absorption of In<sub>2</sub>O was found at 739.8 and 732.7 cm<sup>-1</sup> while the  $\nu_3'$  was located at 700.7 and 694.1 cm<sup>-1</sup>. The only other discernable absorption was a small side band at 799.5 cm<sup>-1</sup>. There was a general absorption from 530-600 cm<sup>-1</sup> which was one of the regions where bands were expected. Unfortunately, it was never possible to resolve any detail in this region, probably because of many overlapping peaks anticipated from the oxygen -18 substitution. Table 5.2-3 contains a list of absorptions, relative intensities and assignments.

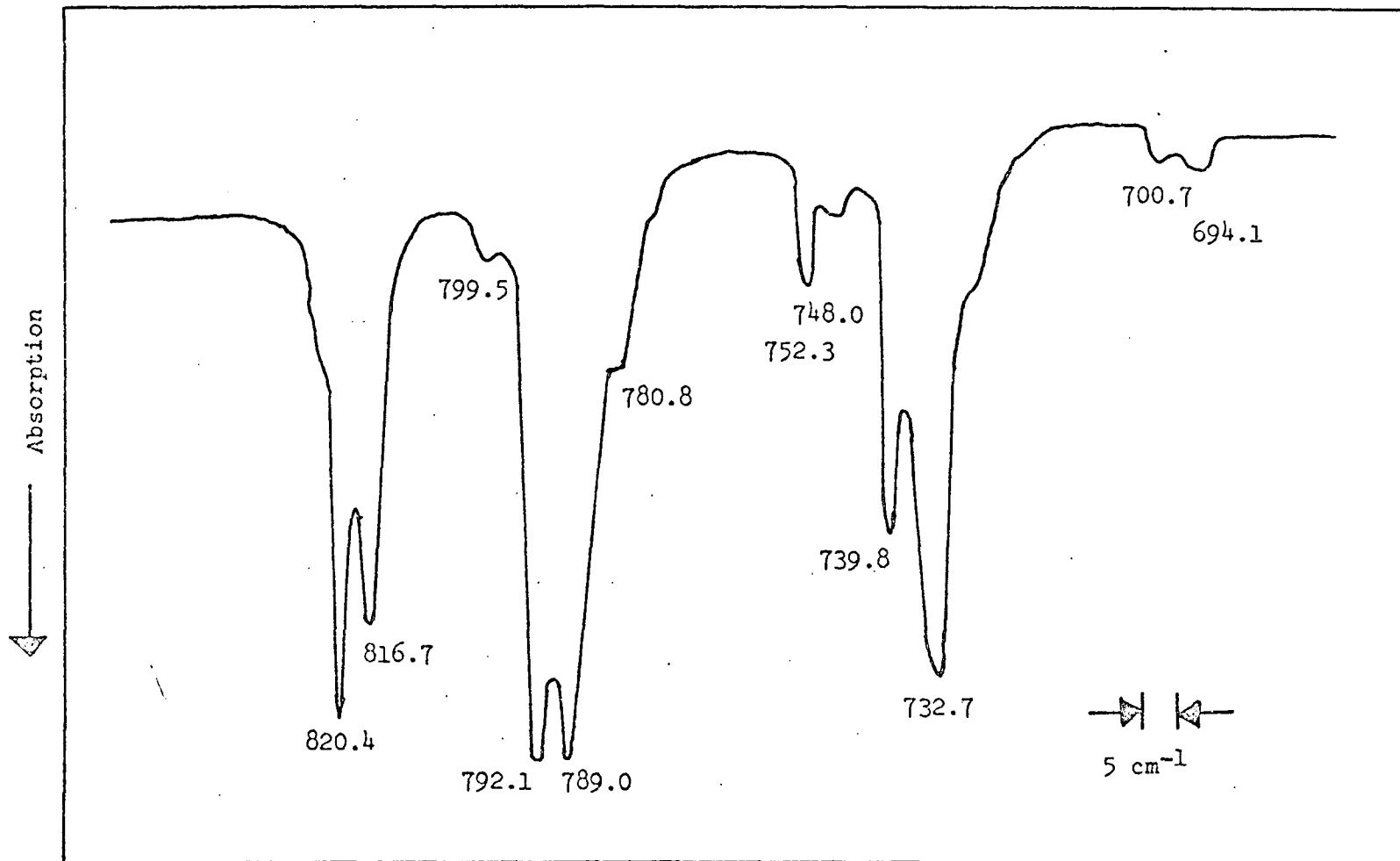


Fig. 5.2-12. Infrared Spectrum of <sup>18</sup>O Enriched Ga<sub>2</sub>O, InGaO, and In<sub>2</sub>O in Ar.

Table 5.2-3. Infrared Frequencies ( $\text{cm}^{-1}$ ) of Oxygen -18 Enriched  $\text{Ga}_2\text{O}$ ,  $\text{InGaO}$ , and  $\text{In}_2\text{O}$  in Ar.

Absorptions <sup>a</sup>	Intensities <sup>b</sup>	Assignment <sup>c</sup>
820.4	86	$\nu_3 \text{Ga}_2\text{O}$
816.7	72	
799.5	14	----
792.1	100	$\nu_3 \text{InGaO}$
789.0	100	
780.8	36	$\nu_3' \text{Ga}_2\text{O}$
757.3	21	$\nu_3' \text{InGaO}$
748.0	11	
739.8	64	$\nu_3 \text{In}_2\text{O}$
732.7	86	
700.7	7	$\nu_3' \text{In}_2\text{O}$
694.1	9	

a Accuracy considered better than  $\pm 1.0 \text{ cm}^{-1}$ .

b Relative intensities all normalized to the most intense peak.

c All doublets treated as a single absorption for assignment.

### 5.3 Additional Experiments and Review of Earlier Research

#### a) Aluminum Suboxide Diffusion Study

An experiment was carried out in an attempt to positively confirm that the  $714\text{ cm}^{-1}$  absorption was from a molecule forming in the matrix. A sample of Al and  $\text{Al}_2\text{O}_3$  was heated to 1780 K for 11 minutes. A heavy  $\text{Al}_2\text{O}$  deposit of  $30\mu$  moles was isolated in Ar at a ratio of 590. In Figs. 5.3-1, 5.3-2, and 5.3-3 the initial spectrum and two later diffusion spectra are shown. The  $714.6\text{ cm}^{-1}$  absorption grew dramatically as the one at  $991.3\text{ cm}^{-1}$  disappeared entirely. The small side bands near the  $\text{Al}_2\text{O } \nu_3$  remained almost to the end, indicating that they might also belong to some associated molecule. The  $749\text{ cm}^{-1}$  absorption again diffused rapidly. Earlier it was shown to have no oxygen isotopic effect and was an unknown species. Table 5.3-1 lists the behavior of all absorptions upon diffusion.

#### b) A New Look at the InGaO System

The oxygen -18 data definitely proved that earlier assignments of  $\nu_1$  and  $\nu_2$  for the suboxides were incorrect, as these absorptions grew while the  $\nu_3$  disappeared. Also, a triplet was detected in each case which indicated the presence of two equivalent oxygens. Therefore, it was interesting to reexamine previous spectra from the mixed molecule system studied by Makowiecki.<sup>13</sup> In Fig. 5.3-4a is given the partial spectrum of  $13\mu$  moles of the mixed system, deposited at 1273 K, and isolated in an Ar matrix with M/R = 940. The illustrated region was reported to contain the  $\nu_1$  for the three suboxide molecules in this system. After annealing and slight diffusion, as

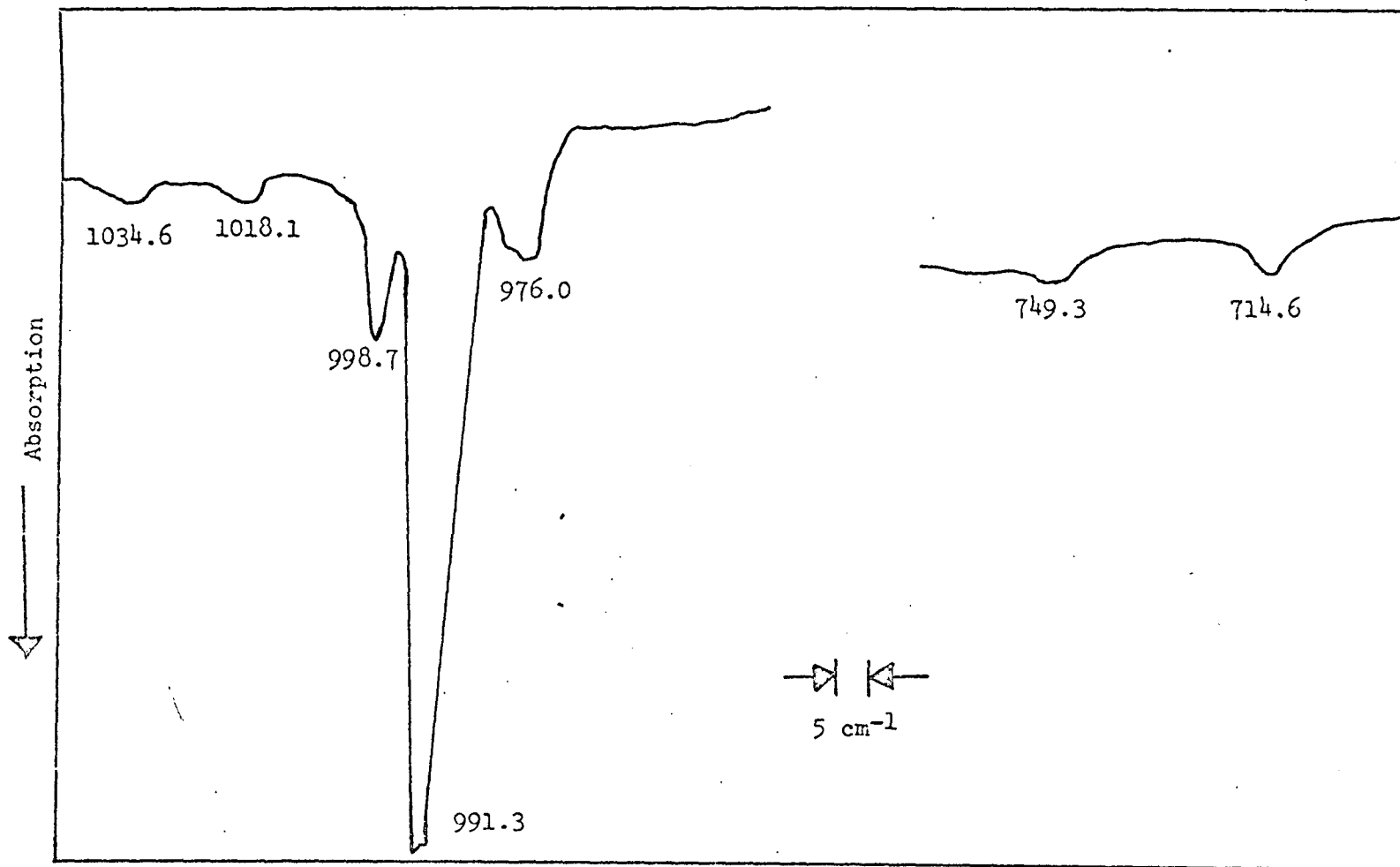


Fig. 5.3-1. Infrared Spectrum of Al<sub>2</sub>O in Ar Before Diffusion.

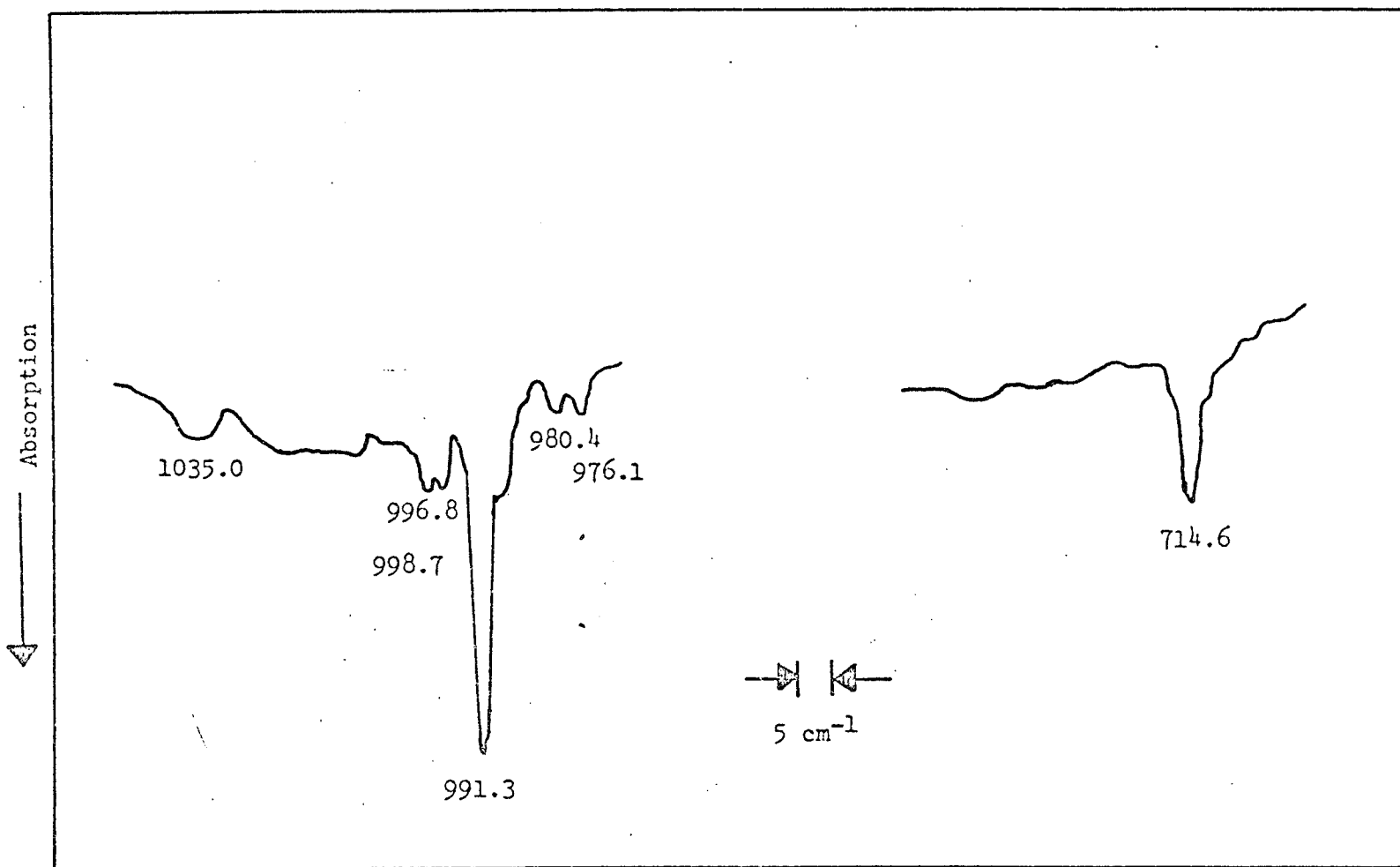


Fig. 5.3-2. Infrared Spectrum of Al<sub>2</sub>O<sub>3</sub> in Ar After Two Diffusions.

CR

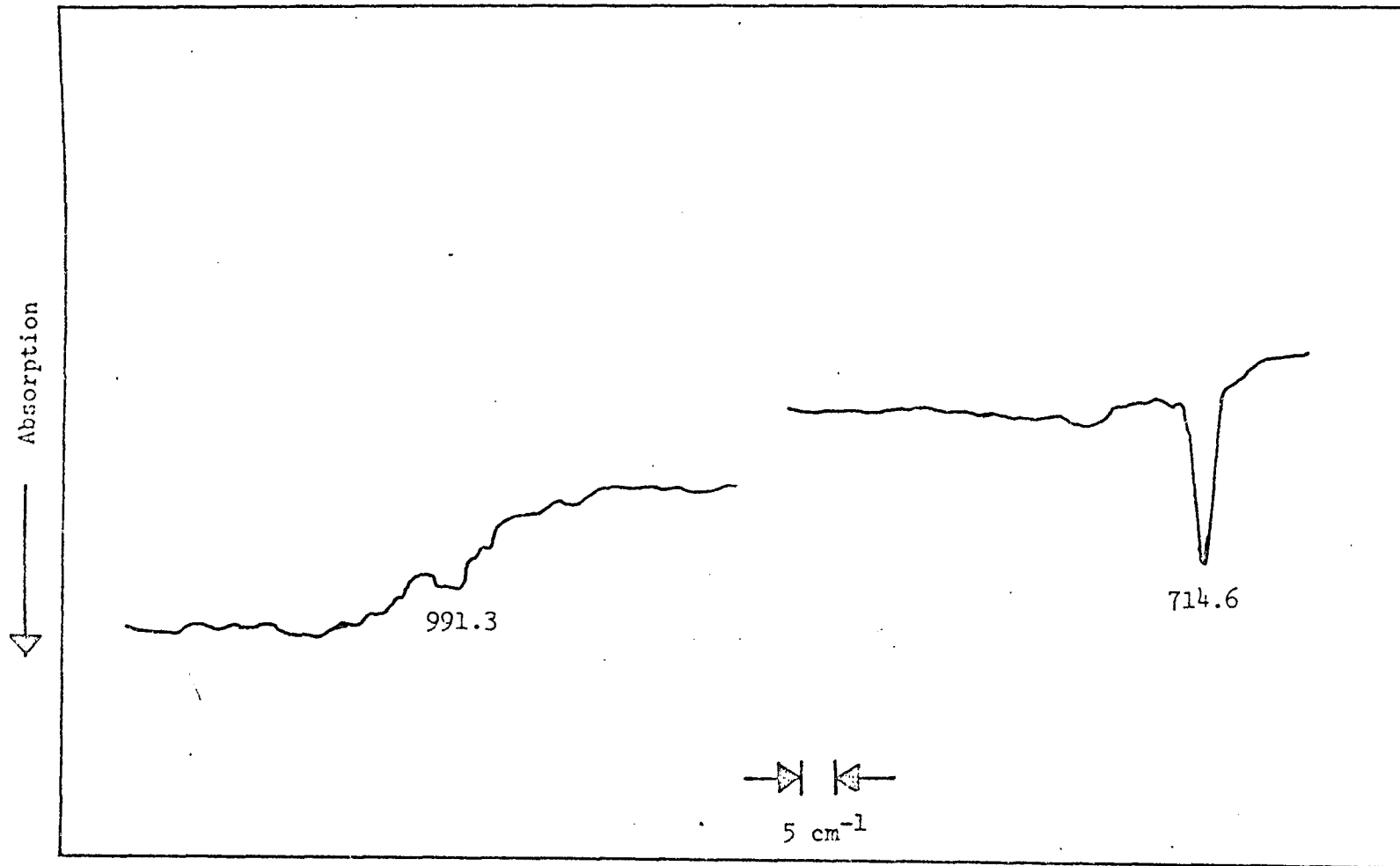


Fig. 5.3-3. Infrared Spectrum of Al<sub>2</sub>O in Ar After Four Diffusions.

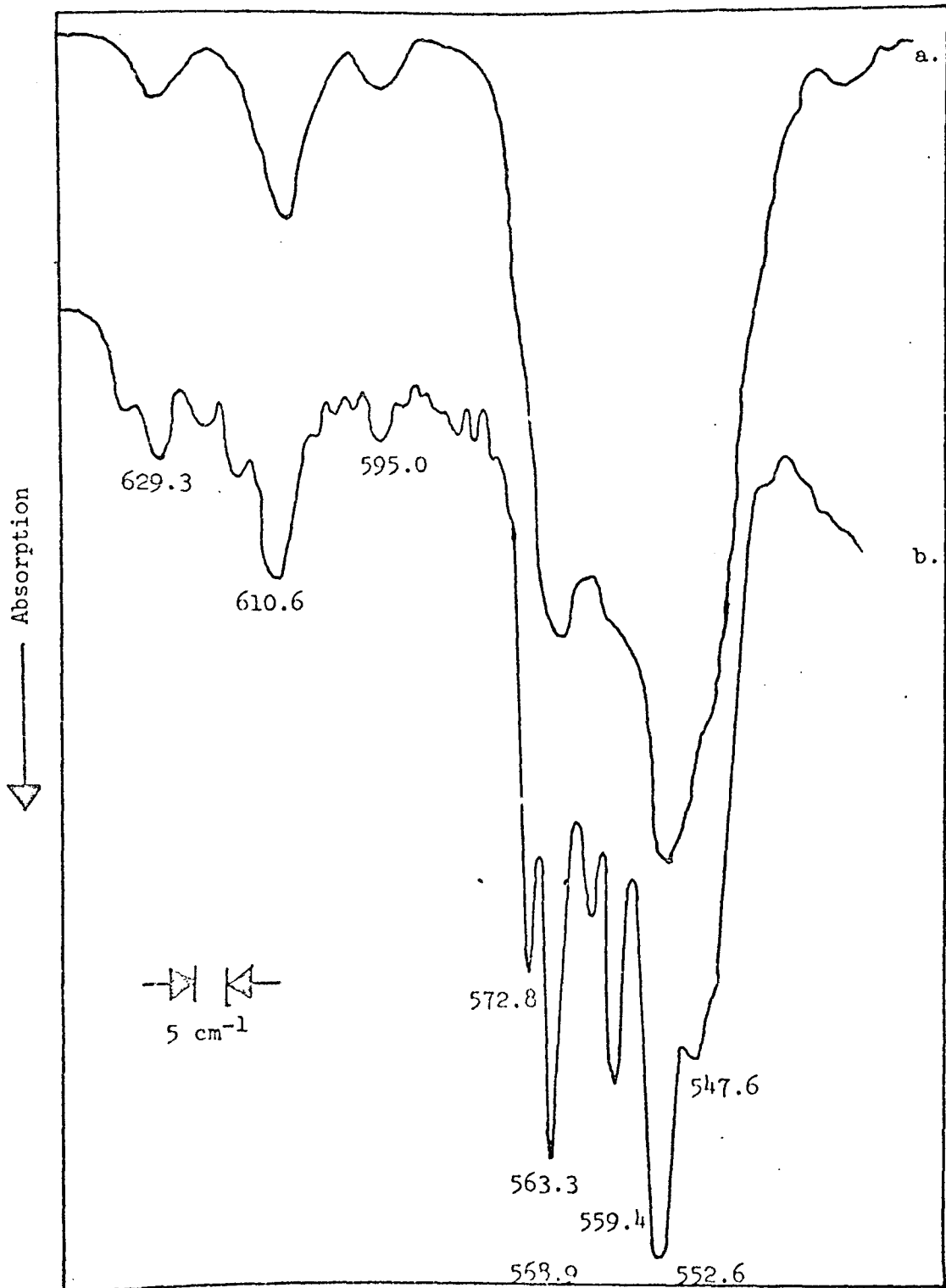


Fig. 5.3-4. Partial Infrared Spectrum of InGaO System in Ar (a. Before Diffusion, b. After Diffusion).

Table 5.3-1. Infrared Frequencies ( $\text{cm}^{-1}$ ) of  $\text{Al}_2\text{O}$  in Ar.

Absorptions <sup>a</sup>	Initial Intensities <sup>b</sup>	Diffusion <sup>c</sup>
714.6	5	I
749.3	3	D
976.0	19	D
991.3	100	D
998.7	26	D
1018.1	4	D
1034.6	3	R

a Accuracy considered better than  $\pm 1.0 \text{ cm}^{-1}$ .

b Relative intensities all normalized to the most intense peak.

c I denotes an increase upon matrix warming, D a decrease, and R indicates that the intensity remained approximately constant.

shown in Fig. 5.3-4b, there was an increase in definition in which several distinct absorptions now appeared. With further diffusion the intensities increased off scale, so that it was impossible to record the exact structure of the bands.

Similarly, another experiment was performed in a nitrogen matrix. The sample was heated to 1235 K and 5 $\mu$  moles of suboxide were isolated at a ratio of 1800. Again more absorptions were detected than would be expected from only three suboxide molecules as illustrated in Fig. 5.3-5. The instrument resolution for this matrix was slightly less than that for argon, but the same general features were apparent.

Table 5.3-2 lists the absorptions for each experiment with their relative intensities. Since it was previously known that the  $\nu_3$  modes were split into doublets by an argon matrix, the additional peaks were explained as matrix effects. However, this could not have been the case for  $N_2$  as no site splittings had been observed for the suboxides in this type of matrix. Therefore, the original assignments are in error and must be reevaluated in view of this investigation.

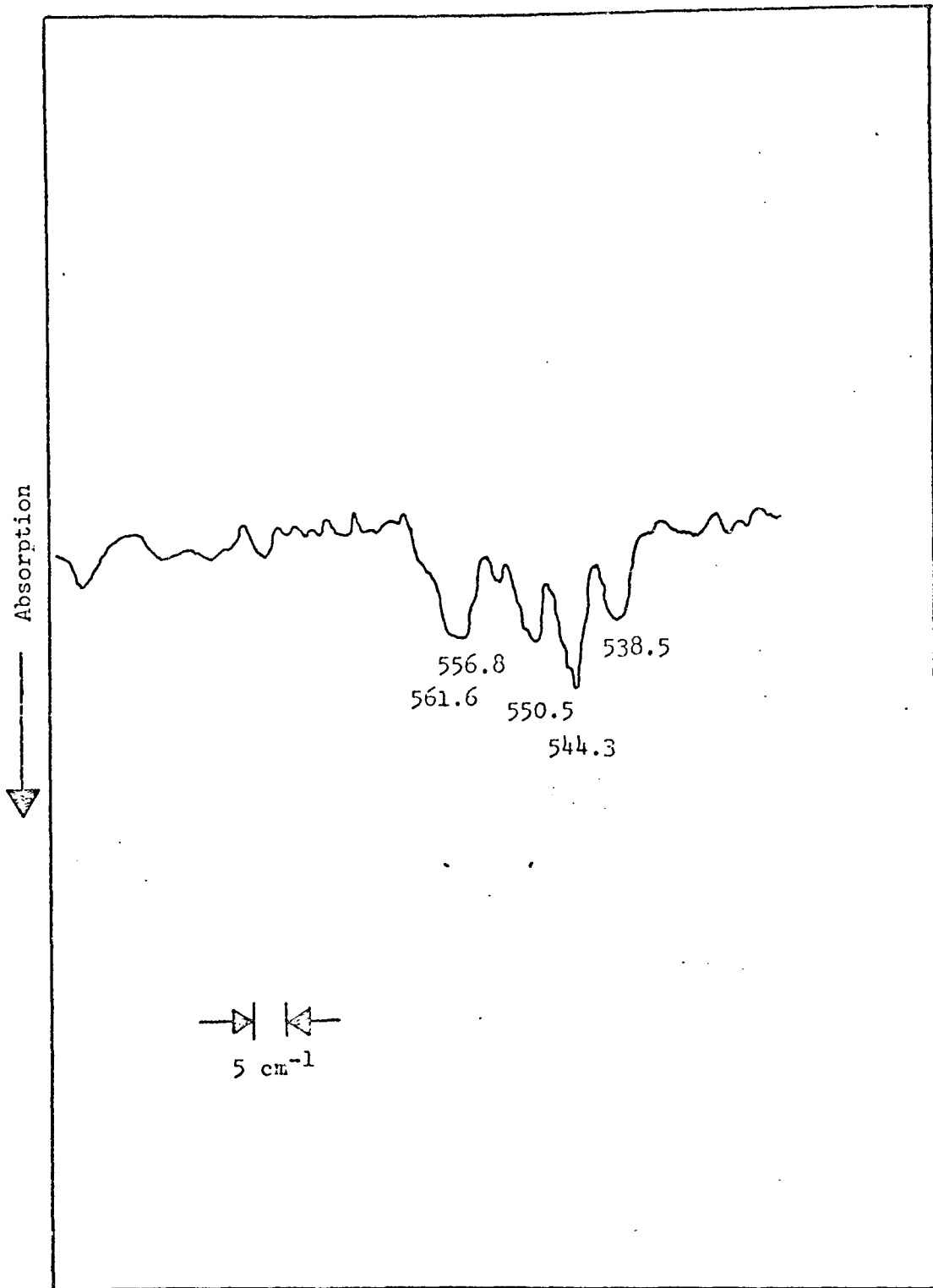


Fig. 5.3-5. Partial Infrared Spectrum of InGaO System in  $\text{N}_2$ .

Table 5.3-2. Infrared Frequencies ( $\text{cm}^{-1}$ ) of the InGaO System From 500-640  $\text{cm}^{-1}$ .

Ar	Absorptions <sup>a</sup>		Intensities <sup>b</sup>	
	Ar	N <sub>2</sub>	Ar	N <sub>2</sub>
547.6	538.5		76	50
552.6	544.3		100	100
559.4	550.5		82	75
563.3	556.8		62	38
568.9	561.6		92	80
572.8			67	
595.0			6	
610.6			19	
629.3			8	

a Accuracy considered better than  $\pm 1.0 \text{ cm}^{-1}$ .

b Relative intensities all normalized to the most intense peak.

## CHAPTER 6

### VIBRATIONAL ASSIGNMENTS AND STRUCTURAL ANALYSIS

In a complete infrared analysis it is necessary to assign the observed frequencies to particular species. This is accomplished either by analogy with similar molecules or by a careful study of vibrational intensities with a change in concentration. Also, monomer absorptions are usually separated from those of associated species by studying the effect of several diffusion experiments. These frequencies are then assigned to definite vibrational modes of each molecule for a normal coordinate analysis. In several of the systems investigated here only tentative assignments may be made without further isotopic investigations.

#### 6.1 Assignment of $M + O_2$ Frequencies

The first reactions to be considered are those involving the matrix reaction of  $M$  with  $O_2$ . In each experiment several absorptions were observed. As was pointed out in Chapter 2, the metal superoxide is expected to be the predominant species formed in these experiments. The isosceles triangle structure was found previously for the alkali metal superoxides and apparently is also found here. The basis for this conclusion is the observation of weak absorptions between 1116 and  $1080\text{ cm}^{-1}$  which disappear rapidly upon matrix warming. This spectral region is close to the estimated value of the vibrational frequency of  $O_2^{-1}$  at  $1090\text{ cm}^{-1}$ .<sup>21</sup>

Although Andrews<sup>20-23</sup> found several other species in the alkali metal reactions, such as the rhombohedral  $M_2O_2$ ,  $M-M-O-O$ ,  $(MO_2)_2$ , and

$O_2MO_2$ , it is doubtful that these molecules would be detected in large quantities during these experiments because of the relatively high  $O_2/M$  ratios and the short deposition times. However, the rhombohedral  $M_2O_2$  molecule, which is apparently formed by diffusion of another metal into the  $MO_2$  framework in such a way as to minimize any ionic repulsion, may be detected in the diffusion experiments since its absorptions should grow slightly as more molecules are formed.

The  $MO_2$  species have three infrared active modes. The oxygen-oxygen stretching frequency, near  $1090\text{ cm}^{-1}$ , is the  $\nu_1$  mode and is expected to be quite weak. The  $\nu_2$  and  $\nu_3$  (symmetric and antisymmetric) M-O stretching modes are expected to occur at lower energies. The  $\nu_2$  mode has been shown to have a slightly stronger intensity in the other systems, but either one may be at the lowest energy. Unfortunately, the metals (Ga, Tl) are too heavy to give large isotopic shifts to help with molecular identification. Also, the absorptions are rather broad, which precludes any possibility of the small splittings being observed. Therefore, isotopic oxygen data would be required for a definite structural determination.

a) Tl +  $O_2$

The bands at  $1082.1$ ,  $432.9$ ,  $428.4$ , and  $295.9\text{ cm}^{-1}$  disappeared rapidly upon matrix annealing. The doublet at  $432.9$  and  $428.4\text{ cm}^{-1}$  was probably only a single broad band, as it showed no definite splittings either before, during, or after annealing. The  $1082.1$  peak was quite weak and near the known superoxide absorption value. It was assigned as the  $\nu_1$  for  $TlO_2$ . Likewise, both the ab-

sorptions at 432.9 and 295.9  $\text{cm}^{-1}$  were from this same molecule. The latter value was chosen as  $\nu_2$  because of its strong relative intensity. The former, therefore, was assigned as  $\nu_3$ . The other two bands at 1022.0 and 1035.7  $\text{cm}^{-1}$  probably belong to the rhombohedral  $\text{M}_2\text{O}_2$  species, for they stayed fairly constant in intensity until just before the matrix was lost. This doublet might also arise from association of  $\text{O}_2$  and  $\text{M}_2\text{O}$  since they were detected in an experiment in which  $\text{M}_2\text{O}$  was present. No further assignments may be made at this time.

b) In +  $\text{O}_2$

The three bands at 1082.3, 456.4, and 332.2  $\text{cm}^{-1}$  disappeared rapidly upon diffusion. They are therefore assigned to  $\text{InO}_2$ . The 1082.3  $\text{cm}^{-1}$  band was quite weak as in the thallium example and was assigned as  $\nu_1$ . The 332.2 and 456.4  $\text{cm}^{-1}$  peaks were determined from intensity considerations and a similarity with the previous example to be  $\nu_2$  and  $\nu_3$ , respectively. The last absorption at 1006.0  $\text{cm}^{-1}$  was similar to the doublet near 1025  $\text{cm}^{-1}$  in the thallium system. It was also observed in an experiment in which only a very weak band near 332  $\text{cm}^{-1}$  was detected, indicating that the 1006  $\text{cm}^{-1}$  peak was not an absorption of  $\text{InO}_2$ . No definite assignment can be made as to the origin of this band.

c) Ga +  $\text{O}_2$

The Ga +  $\text{O}_2$  reaction produced results slightly different from the two previous examples. Only two absorptions were detected and both disappeared rapidly upon annealing the matrix. The first at

1088.4  $\text{cm}^{-1}$  was quite weak and apparently is the  $\nu_1$  for  $\text{GaO}_2$ . The second at 383.3  $\text{cm}^{-1}$  was fairly intense and appeared to be related to the 295.9 and 332.2  $\text{cm}^{-1}$  absorptions seen earlier. Therefore, it was assigned as the  $\nu_2$ . The  $\nu_3$  mode was not observed. An estimated value of 487  $\text{cm}^{-1}$  was made from central force field calculations to be discussed later in this chapter.

d)  $\text{Al} + \text{O}_2$

The reaction of  $\text{Al} + \text{O}_2$  produced many peaks. However, the data were quite difficult to analyze since  $\text{Al}_2\text{O}$  was present in the matrix during each experiment and was also reacting. Furthermore, the IR-11 was inoperable during these experiments which precluded any attempt to detect the expected lower lying  $\text{AlO}_2$  modes. The 1116.0  $\text{cm}^{-1}$  peak was apparently related to those near this value for the other  $\text{MO}_2$  species and was assigned as the  $\nu_1$  for  $\text{AlO}_2$ . This same mode was detected at 1095.6  $\text{cm}^{-1}$  in  $\text{N}_2 + \text{O}_2$ . In both experiments this absorption disappeared immediately during all attempts at annealing the matrix. No other absorption disappeared as rapidly. The 686  $\text{cm}^{-1}$  band remained fairly constant in intensity after initially growing and was probably from the bridged  $\text{Al}_2\text{O}_2$  molecule. The other absorptions were apparently related either to higher polymer species or to reactions of  $\text{Al}_2\text{O}$  with  $\text{Al} + \text{O}_2$ , but it was impossible to make positive identifications. The other two absorptions for  $\text{AlO}_2$  should be detected below 650  $\text{cm}^{-1}$  from comparison with the other systems. The  $\text{AlO}_2$  molecule formed in this type of reaction was probably not the same as that observed mass spectrometrically which was assumed to be linear.

Table 6.1-1 summarizes the assignments for the absorptions from the  $M + O_2$  reactions.

## 6.2 Force Constants and Bond Angles for the Superoxides

An analysis was undertaken to determine the force constants, bond angles and internuclear distances for the superoxides. Although several possible potentials could be used, two were chosen because of the ring structure of the  $MO_2$  species. These are listed in Table 6.2-1 along with the equations for the determination of the frequencies from the force constants and bond angles. The first is the simple central force field potential<sup>58</sup> for an  $XY_2$  molecule. The second is a slightly simplified version of one given by Kohlrausch<sup>59</sup> for an  $XY_2$  ring structure.

Calculations were made for  $InO_2$  and  $TlO_2$  using the central force field approximation. The results are listed in Table 6.2-2 along with data from a similar calculation for  $LiO_2$ . It was found that with this potential the best relative agreement between calculated and observed values for  $InO_2$  and  $TlO_2$  occurred near an O-M-O bond angle of  $90^\circ$  which would imply a relatively long O-O internuclear distance. However, it must be remembered that the central force field calculations give relatively poor results for a bond angle determination. The Kohlrausch potential gave essentially the same results since the potential is nearly the same. The force constants are only slightly changed by the additional bending constant, and again the bond angle data are inconclusive. The values of the force constants and internuclear separations for several molecules includ-

Table 6.1-1. Vibrational Assignments for the MO<sub>2</sub> Molecules.

Molecule	$\nu_1$	$\nu_2$	$\nu_3$
AlO <sub>2</sub>	1116.0 (1095.6) <sup>a</sup>		
GaO <sub>2</sub>	1088.4	383.3	
InO <sub>2</sub>	1082.3	332.2	456.4
TlO <sub>2</sub>	1082.1	295.9	432.9

a Nitrogen matrix.

Table 6.2-1. Potential Functions Applied to the Group III A Super-oxides.

Central Forces<sup>a</sup>

$$2V = a_{11} (Q_1^2 + Q_2^2) + a_{33} Q_3^2$$

$$\lambda_3 = 4\pi^2 \nu_3^2 = \left(1 + \frac{2M_o}{M_m} \sin^2(\alpha/2)\right) \frac{a_{11}}{M_o}$$

$$\lambda_1 + \lambda_2 = 4\pi^2 (\nu_1^2 + \nu_2^2) = 2 \frac{a_{33}}{M_o} + \frac{a_{11}}{M_o} \left(1 + \frac{2M_o}{M_m} \cos^2(\alpha/2)\right)$$

$$\lambda_1 \lambda_2 = 16\pi^4 \nu_1^2 \nu_2^2 = 2 \left(1 + \frac{2M_o}{M_m} \cos^2(\alpha/2)\right) \frac{a_{11} a_{33}}{M_o^2}$$

Mixture of Valence and Central Forces<sup>b</sup>

$$2V = k_1 (Q_1^2 + Q_2^2) + k_2 Q_3^2 + k_\delta \delta^2$$

$$\lambda_3 = 4\pi^2 \nu_3^2 = \left(1 + \frac{2M_o}{M_m} \sin^2(\alpha/2)\right) \frac{k_1}{M_y}$$

Table 6.2-1. (Continued)

$$\lambda_1 + \lambda_2 = 4\pi^2 (v_1^2 + v_2^2) = \frac{1}{M_o} [k_1 (1 + \frac{2 M_o}{M_m} \cos^2 (\alpha/2)) + 2k_2 + 2k_\delta (1 + \frac{2 M_o}{M_m} \sin^2 (\alpha/2) ) ]$$

$$\lambda_1 \lambda_2 = 16\pi^4 v_1^2 v_2^2 = \frac{2}{M_o} [ 1 + \frac{2 M_o}{M_m} ] [k_1 k_\delta + k_2 k_1 \cos^2 (\alpha/2) + 2k_2 k_\delta \sin^2 (\alpha/2) ]$$

- a G. Herzberg, Molecular Spectra and Molecular Structure II. Infra-red and Raman Spectra of Polyatomic Molecules, (D. Van Nostrand and Co., Princeton, N.J., 1945), p. 160.
- b K. W. Kohlrausch, Der Smekal-Raman-Effekt, (J. Springer, Berlin, 1938), p. 65.

Table 6.2-2. Force Constants of In and Tl Superoxides Under the Assumption of a Central Force Field<sup>a</sup> and Modified Central Force Field<sup>c</sup>.

Molecule	Apex Angle (deg)	Central Force Field		q (v <sub>1</sub> <sup>2</sup> + v <sub>2</sub> <sup>2</sup> )	
		a <sub>11</sub> (m dynes/Å)	a <sub>33</sub>	Observed	Calc.
InO <sub>2</sub>	90	1.72	5.21	77500	77400
TlO <sub>2</sub>	90	1.63	4.81	74100	71100
LiO <sub>2</sub>	90	.66	14.1	103508	191715
LiO <sub>2</sub>	45 <sup>b</sup>	1.36	4.03	103508	97591

Table 6.2-2. (Continued)

Molecule	Modified Central Force Field			$k_{\delta}$
	Apex Angle (deg)	$k_1$	$k_2$ (m dynes/Å)	
InO <sub>2</sub>	90	1.72	5.02	.229
TiO <sub>2</sub>	90	1.61	4.98	.814

- a G. Herzberg, Molecular Spectra and Molecular Structure II. Infra-red and Raman Spectra of Polyatomic Molecules, (D. Van Nostrand and Co., Princeton, N.J., 1945), p. 160.
- b Experimental bond angle.
- c K. W. Kohlrausch, Der Smekal-Raman-Effekt, (J. Springer, Berlin, 1938), p. 65.

ing those calculated above for  $\text{InO}_2$  and  $\text{TlO}_2$  are listed in Table 6.2-3. The internuclear M-O separations were determined from the appropriate Laurie-Herschbach<sup>60</sup> equation and from the trigonometric relationship

$$r_{\text{O-O}} = 2r_{\text{M-O}} \sin (\alpha/2) \quad (6.2-1)$$

It is immediately obvious that the oxygen-oxygen internuclear distance is too great to support any significant bonding, although the force constants and the M-O bond distances are apparently reasonable. Upon reexamining the normal coordinate data, the author noted that although the convergence is not satisfactory, the force constants and internuclear separations are more appropriate for an apex angle of  $40^\circ$  for  $\text{InO}_2$  and  $\text{TlO}_2$ . These results are shown in Table 6.2-4. The force constants are still reasonable and there is much better agreement with known internuclear distances.

In order to obtain a positive structural determination, oxygen isotopic data are required, but there is a great similarity between the superoxides of the alkali and group III A metals. The M-O stretching force constants for all the superoxides are slightly more than half that of the suboxides. The oxygen stretching mode is also slightly less than that of the isolated superoxide anion. The M-O bond distances are slightly elongated over those of the suboxides, as would be expected for a weakly bound molecule, and the internuclear oxygen distances are reasonable although slightly larger than expected for  $\text{InO}_2$ . Therefore, the bonding for the group III A superoxides probably involves the metal cation bonded symmetrically to the superoxide anion as was the case for the alkali metals.

Table 6.2-3. Metal-Oxygen and Oxygen Stretching Force Constants and Bond Lengths.

Molecule	$F_{M-O}$ or $F_{O-O}$ (m dyne/Å)	Estimated $r_{M-O}$ or $r_{O-O}$ (Å)	Ref. k/l
$In_2O$	2.67	2.04	a/a
$Tl_2O$	2.12	2.19	a/a
$InO_2$	1.72	2.18	This work
$TlO_2$	1.63	2.29	This work
$Li_2O$	2.14	1.59	b/b
$LiO_2$	1.18	1.77	b/b
$O_2^+$	16.0	1.12	b/b
$O_2$	11.4	1.20	b/b
$O_2^-$	5.59	1.33	b/b
$LiO_2$	5.59	1.33	b/b
$InO_2$	5.21	3.12	This work
$TlO_2$	4.81	3.24	This work

a A. J. Hinchcliffe and J. S. Ogden, Chem. Comm. 18, 1053 (1969).

b L. Andrews, J. Chem. Phys. 50, 4288 (1969).

Table 6.2-4. Corrected Superoxide Force Constants and Bond Lengths.

Molecule	Apex Angle (deg)	$F_{M-O}$ or $F_{O-O}$ (m dyne/Å)	Estimated $r_{M-O}$ or $r_{O-O}$ (Å)
InO <sub>2</sub>	90	1.72	2.18
InO <sub>2</sub>	40	1.90	2.15
TlO <sub>2</sub>	90	1.63	2.29
TlO <sub>2</sub>	40	1.73	2.26
O <sub>2</sub> <sup>-</sup>	--	5.59	1.33
InO <sub>2</sub>	90	5.21	3.12
InO <sub>2</sub>	40	2.67	1.65
TlO <sub>2</sub>	90	4.81	3.24
TlO <sub>2</sub>	40	2.57	1.32

### 6.3 Analysis for M<sub>2</sub>O in Ar + O<sub>2</sub>

For all experiments in which the suboxide molecule was deposited in the mixed matrices, the same frequencies were detected as those reported earlier by Makowiecki.<sup>13</sup> These modes are therefore not due to a reaction of free metal with oxygen. There was a slight shift of 2-5 cm<sup>-1</sup> for the three modes, except in the case of aluminum, but this was relatively small considering the unusual matrix combination. It was interesting that the reported  $\nu_1$  and  $\nu_3$  were shifted to lower energy and  $\nu_2$  to a higher value. The degree of change was found to be dependent upon the M<sub>2</sub>O rather than O<sub>2</sub> concentration. The reason for this is unknown, but it may be related to the distortion of the Ar matrix by both O<sub>2</sub> and M<sub>2</sub>O. Previous investigations<sup>13,51</sup> had shown that the modes observed in pure Ar are closest to the gas phase values. The degree of variance from these values was related to the molecular weight of the matrix gas. The mixture of O<sub>2</sub> and Ar was expected to shift the absorptions because of the change in the average molecular weight of the matrix gas.

The mixed matrix provided an interesting insight into the site splitting (matrix effect) observed by Makowiecki for the  $\nu_3$  mode of Ga<sub>2</sub>O, In<sub>2</sub>O, and Tl<sub>2</sub>O. During the experiments reported here, each doublet became a single rounded absorption, although a CO<sub>2</sub> peak was observed in the Tl<sub>2</sub>O experiments next to the  $\nu_3$  band. It was noted that the single rounded peak was closest to the value, assigned by Makowiecki as the correct one, in all cases except Ga<sub>2</sub>O where the results were inconclusive. Apparently the oxygen molecule distorted the argon matrix in such a way that the second trapping site for the

suboxide was no longer available.

#### 6.4. Assignment of $^{18}\text{O}$ Suboxide Frequencies

In the previous chapter it was shown that the  $\nu_3$  assignments were correct for  $\text{Al}_2\text{O}$ ,  $\text{Ga}_2\text{O}$ ,  $\text{In}_2\text{O}$ , and  $\text{InGaO}$ . This was demonstrated by the presence of only two absorptions when both  $\text{M}_2^{16}\text{O}$  and  $\text{M}_2^{18}\text{O}$  were in the same matrix. It was therefore possible to calculate the M-O-M bond angle for these suboxides and to compare them with the literature values. The results are listed in Table 6.4-1. The only major discrepancy with previous data was in the case of  $\text{Ga}_2\text{O}$  where an angle near  $125^\circ$  was determined in both Ar and  $\text{N}_2$  matrices. The nature of this difference is unknown. However, it must be pointed out that the primary objective of these experiments was the investigation of the reported  $\nu_1$  and  $\nu_2$  values. Therefore, relatively heavy suboxide deposits were employed which made the  $\nu_3$  modes quite intense and difficult to measure to the required accuracy. The major importance of these calculations was the verification of the bent structure for the suboxides because the previous isotopic  $\nu_3$  data<sup>16</sup> had been questioned.<sup>18</sup>

The oxygen-18 investigation did prove that the  $\nu_1$  assignments for both  $\text{Al}_2\text{O}$  and  $\text{Ga}_2\text{O}$  and  $\nu_2$  for  $\text{Ga}_2\text{O}$  were incorrect. The triplet structure representing  $^{16}\text{O}-^{16}\text{O}$ ,  $^{16}\text{O}-^{18}\text{O}$ , and  $^{18}\text{O}-^{18}\text{O}$  indicated the presence of two equivalent oxygens. Also, the diffusion studies in Sections 5.2 and 5.3 demonstrated that these modes grew dramatically upon diffusion at the expense of the suboxide  $\nu_3$ . Since it was shown earlier<sup>13</sup> that the  $\nu_1$  and  $\nu_2$  frequencies for all the suboxides

Table 6.4-1. Bond Angles Calculated from Isotopic Data.

Molecule	$\nu_3$	$\nu_3'$	Bond Angle	
	( $\text{cm}^{-1}$ )	( $\text{cm}^{-1}$ )	Calc. (deg)	Lit. (deg)
$\text{Al}_2\text{O}$	989.8	947.8	143	145 <sup>a</sup>
$\text{Ga}_2\text{O}$	822.1 (808.0) <sup>b</sup>	781.3 (767.7) <sup>b</sup>	124 (126) <sup>b</sup>	143 <sup>c</sup>
$\text{In}_2\text{O}$	732.7	694.1	133	135 <sup>c</sup>
$\text{InGaO}$	792.1	752.3		

a M. J. Linevsky, D. White, and D. E. Mann, J. Chem. Phys. 41, 542 (1964).

b Nitrogen matrix.

c A. J. Hinchcliffe and J. S. Ogden, Chem. Comm. 18, 1053 (1969).

were related to the same type of molecule, these assignments must be considered to be from another type of molecule formed in each suboxide experiment. Therefore, all  $\nu_1$  and  $\nu_2$  assignments by Makowiecki for the suboxides are incorrect.

An investigation was made to determine which molecules were responsible for the absorptions. The mass spectrometric results had indicated that no other parent species was present in the vapor phase to any appreciable extent. Therefore, the new molecule must be formed by an aggregation of species already present in the matrix. Of these,  $M_2O$  and  $M$  were in a large predominance and should be the precursors. The triplet isotopic effect immediately made it possible to rule out any molecules of the  $M_xO$  type. The only possible species must be of the form  $M_xO_2$  where the oxygens are equivalent. In the previous section we have demonstrated that  $MO_2$  could not possibly be responsible for such absorptions. The mass spectrometric results indicated that under certain conditions  $M_2O_2$ ,  $M_3O_2$ , and  $M_4O_2$  are stable vapor species. It was possible to eliminate the first two molecules since a stable  $M-O$  species would be required for diffusion. It has been shown that the  $M-O$  concentration is below  $\sim 5 \times 10^{-6}$  the suboxide value. Also,  $Tl-O$  has never been detected as a stable monomer. There is also no reason to believe the suboxide dissociates to form the monoxide since a stable  $Tl_2O$  solid exists at room temperature. The  $M_4O_2$  molecule is the suboxide dimer. It was shown to exist in the gas phase for the  $In_2O$  system and it was found in an earlier investigation in the  $Tl_2O$  system.<sup>12</sup> Since the suboxide was the pre-

dominant vapor species, it was not unusual to expect dimer formation upon diffusion. The presence of the dimer before diffusion was unexpected, but is explained by the fast deposition rates employed which greatly increased the possibility of molecular interactions before reaching the matrix. No other molecules could be produced in sufficient concentrations in the matrix to account for the isotopic data.

A further attempt was made to locate the correct  $\nu_1$  and  $\nu_2$  suboxide modes. Both the suboxide and matrix gas concentrations were varied over a wide range, but no absorptions were observed consistently. Therefore, values were estimated for these modes from a simple valence force calculation.<sup>61</sup> The results are listed in Table 6.4-2. The  $\nu_1$  calculated for the  $Tl_2O$  does not correspond to the value reported by Brom *et al.*<sup>18</sup> but their data still may be questionable because of the weak intensity of the  $^{18}O$   $\nu_1$  mode.

### 6.5. Structural Analysis of $M_4O_2$

The single  $\nu_3$  mode for  $InGaO$  and the oxygen isotopic data clearly indicates that the suboxide molecules possess  $C_{2v}$  symmetry. The possibility remains that a weak bond also exists between the metals, but this is not the major concern. There is no evidence that one of the M-O bonds is broken during dimer formation with a corresponding increase in the metal-metal bond strength. Consequently, only symmetric suboxide molecules should be available for dimer formation. The possible dimer structures are illustrated in Fig. 6.5-1. In each example the oxygens are also equivalent as required by the

Table 6.4-2. Estimated Vibrational Frequencies for the Group III A Suboxides.

Molecule	Bond Angle (deg)	$\nu_3$	$\nu_2$ ( $\text{cm}^{-1}$ )	$\nu_1$	$k_1$	$\frac{k_\delta^a}{l^2}$ (m dynes/ $\text{\AA}^2$ )
$\text{Al}_2\text{O}$	145 <sup>b</sup>	988 <sup>b</sup>	367	611	3.8	.38
$\text{Ga}_2\text{O}$	143 <sup>c</sup>	809 <sup>c</sup>	219	472	3.1	.31
$\text{In}_2\text{O}$	135 <sup>c</sup>	722 <sup>c</sup>	153	451	2.7	.27
$\text{Tl}_2\text{O}$	131 <sup>c</sup>	625 <sup>c</sup>	101	404	2.1	.21

a  $k_\delta$  estimated to be 0.1  $k_1$ .

b M. J. Linevsky, D. White, and D. E. Mann, J. Chem. Phys. 41, 542 (1964).

c A. J. Hinchcliffe and J. S. Ogden, Chem. Comm. 18, 1053 (1969).

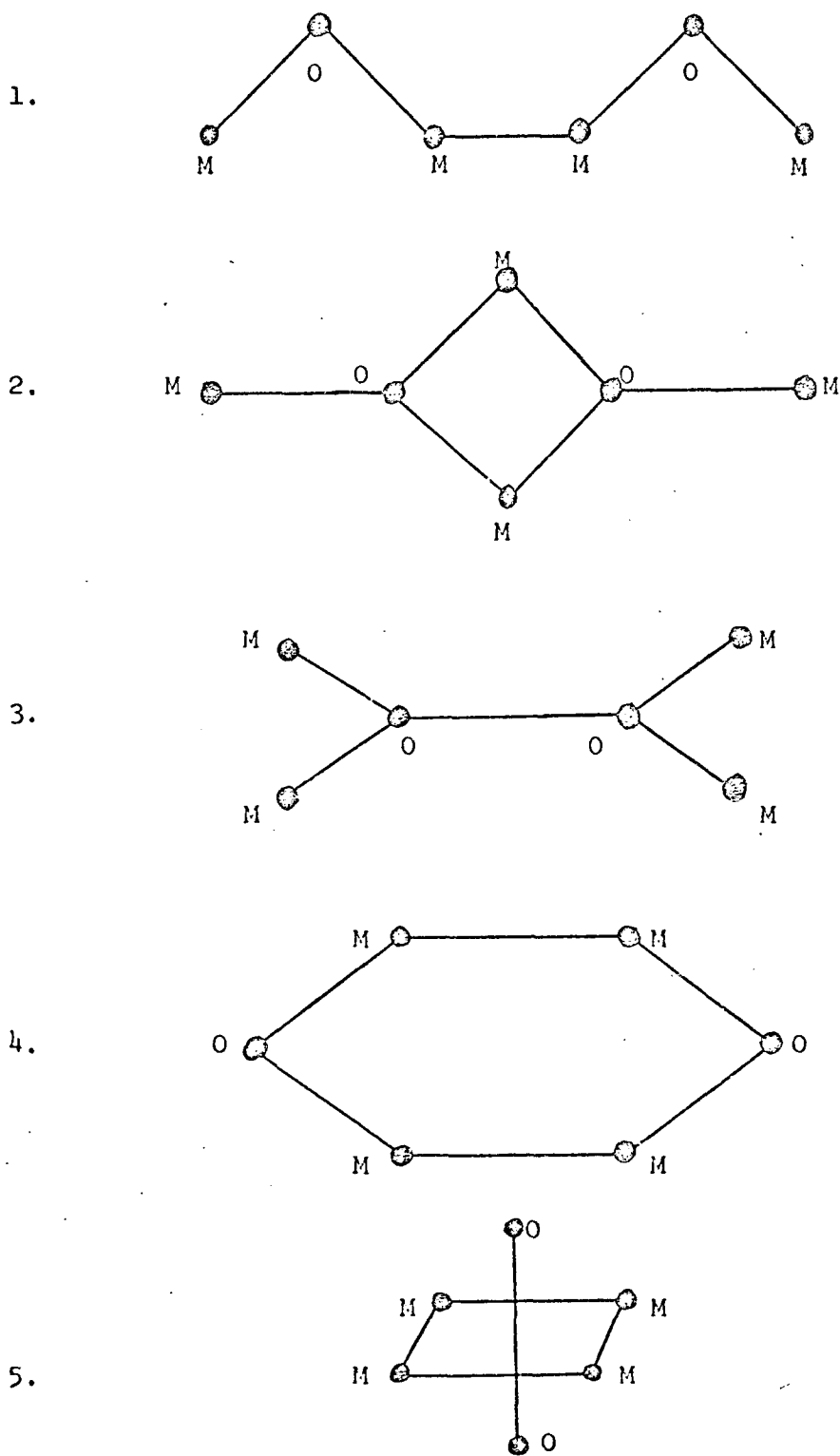


Fig. 6.5-1. Possible  $M_4O_2$  Structures.

isotopic data.

The first structure may be ruled out immediately. Although a chain structure is not unusual, it is inconceivable that only a dimer would form. It should be equally probable that higher polymers would be present, but the infrared spectra do not indicate their presence even after extensive diffusion.

The second model is similar to the one proposed for the transition metal dihalides.<sup>51</sup> The bonding of the oxygen is somewhat questionable and preliminary normal coordinate calculations rule out this type of structure.

The third possibility also involves unusual oxygen bonding, but the results of a Tl plus O<sub>2</sub> reaction reported by Ogden<sup>29</sup> indicates that at least the 510 cm<sup>-1</sup> band of Tl<sub>4</sub>O<sub>2</sub> can be found by a non-dissociative reaction of metal with enriched oxygen. However, simple calculations indicate that this structure is unlikely.

The fourth proposed model may be close to the true structure. With this model there is no chance of higher polymer formation. The metal-metal bonding is not unrealistic since similar bonding is predicted for the suboxide molecules and all valencies can be satisfied with normal bonding.

With further examination it was decided that this planar model was probably too restrictive. Therefore, the true structure is felt to lie between the fourth structure and the fifth which is an octahedral model with oxygen atoms at opposite ends of the major axis. This structure would allow for maximum metal-metal and metal-oxygen overlap. It was also seen that the third structure could be trans-

formed into the last one if the terminal metals were flipped up on one end and down on the other. This would satisfy the requirements of the Ogden paper.

For a non-linear molecule with six atoms, there are twelve vibrational modes of which six are infrared active. In order to carry out a vibrational analysis, the model proposed by Ramsay<sup>62</sup> for the chair form of dioxane was employed. There are three Au and three Bu modes which are infrared active. The necessary equations are given in Appendix I.

It was necessary to make several assumptions for the calculations. The M-O-M bond angles were set at the values determined by the isotopic data and the M-O internuclear distances were also taken from the literature. The M-M bond lengths were taken as slightly longer than that found in the pure metals.<sup>13</sup> The M-O stretching force constants were taken from the literature and were varied by tenths of their value from 0.1 to 1.0. Similarly, the M-M force constants were varied from  $8 \times 10^4$  to  $4.0 \times 10^5$  m dynes/Å by units of  $8 \times 10^4$ . The bending force constants were chosen as 1/20 the sum of the stretching constants for the adjacent bonds.

The results of the calculations are given in Table 6.5-1. The agreement is better for the heavier elements as might be expected since the aluminum suboxide was the most difficult to form and also has the shortest metal-oxygen bond lengths. This should make it difficult for the four aluminums to be in a plane. The available isotopic data are consistent with this type of structure, although the agreement could be better. The point group of this dimer is  $C_{2h}$

Table 6.5-1. Calculations for Group III A Metal Suboxide Dimers.

Molecule	Frequencies (cm <sup>-1</sup> )								Bond Angle (deg)	F <sub>M-O</sub> (m dynes/Å)	F <sub>O-O</sub>	r <sub>M-O</sub> (Å)	r <sub>M-M</sub> (Å)
	Observed		Calculated										
	<sup>16</sup> O <sub>2</sub>	<sup>18</sup> O <sub>2</sub>	<sup>16</sup> O <sub>2</sub>	<sup>18</sup> O <sub>2</sub>	<sup>16</sup> O <sub>2</sub>	<sup>18</sup> O <sub>2</sub>	<sup>16</sup> O <sub>2</sub>	<sup>18</sup> O <sub>2</sub>					
Al <sub>4</sub> O <sub>2</sub>	714.8	689.0	503.0 <sup>a</sup>		748	738	508	489	145 <sup>b</sup>	1.53 <sup>c</sup>	3.2	1.66 <sup>b</sup>	3.00 <sup>d</sup>
Ga <sub>4</sub> O <sub>2</sub>	595.0	567.5	416.3	396.0	598	572	375	358	143 <sup>e</sup>	1.57 <sup>f</sup>	3.2	1.86 <sup>e</sup>	2.50 <sup>d</sup>
In <sub>4</sub> O <sub>2</sub>	555.1 <sup>a</sup>		404.3 <sup>a</sup>		577	547	395	374	135 <sup>e</sup>	1.66 <sup>g</sup>	3.2	2.04 <sup>e</sup>	3.40 <sup>d</sup>
Tl <sub>4</sub> O <sub>2</sub>	510.1 <sup>a</sup>		381.5 <sup>a</sup>		504	477	372	352	131 <sup>e</sup>	1.35 <sup>h</sup>	4.0	2.19 <sup>e</sup>	3.50 <sup>d</sup>

a D. M. Makowiecki, D. A. Lynch, Jr., and K. D. Carlson, J. Phys. Chem. 75, 1963 (1971).

b M. J. Linevsky, D. White, and D. E. Mann, J. Chem. Phys. 41, 542 (1964).

c  $F_{M-O} = 0.4 \times F_{Al_2O}$ .

d Estimated.

e A. J. Hinchcliffe and J. S. Ogden, Chem. Comm. 18, 1053 (1969).

f  $F_{M-O} = 0.5 \times F_{Ga_2O}$ .

g  $F_{M-O} = 0.6 \times F_{In_2O}$ .

h  $F_{M-O} = 0.6 \times F_{Tl_2O}$ .

which would not allow doubly excited overtone bands. However, since these modes have been observed previously,<sup>13</sup> one concludes that the actual structure is distorted from this symmetry type.

There were several absorptions between 500 and 610  $\text{cm}^{-1}$  for the InGaO system. Seven structures are possible for the  $C_{2h}$  structure, as shown in Fig. 6.5-2. However, the relative intensities do not agree with what was predicted. This discrepancy could not be accounted for, and no other structures could be found which would give the observed splittings. There must be several trapping sites or some other matrix perturbation occurring, such as a structural distortion, which produces this variance.

The proposed model gives excellent agreement with the experimental frequencies. While a more sophisticated potential should give an even better correlation, the dimer structure has been shown to have a three dimensional distorted octahedral structure. The three dimensional treatment of a dimer molecule in a matrix is unusual, but merits an even closer consideration for the suboxide molecules.

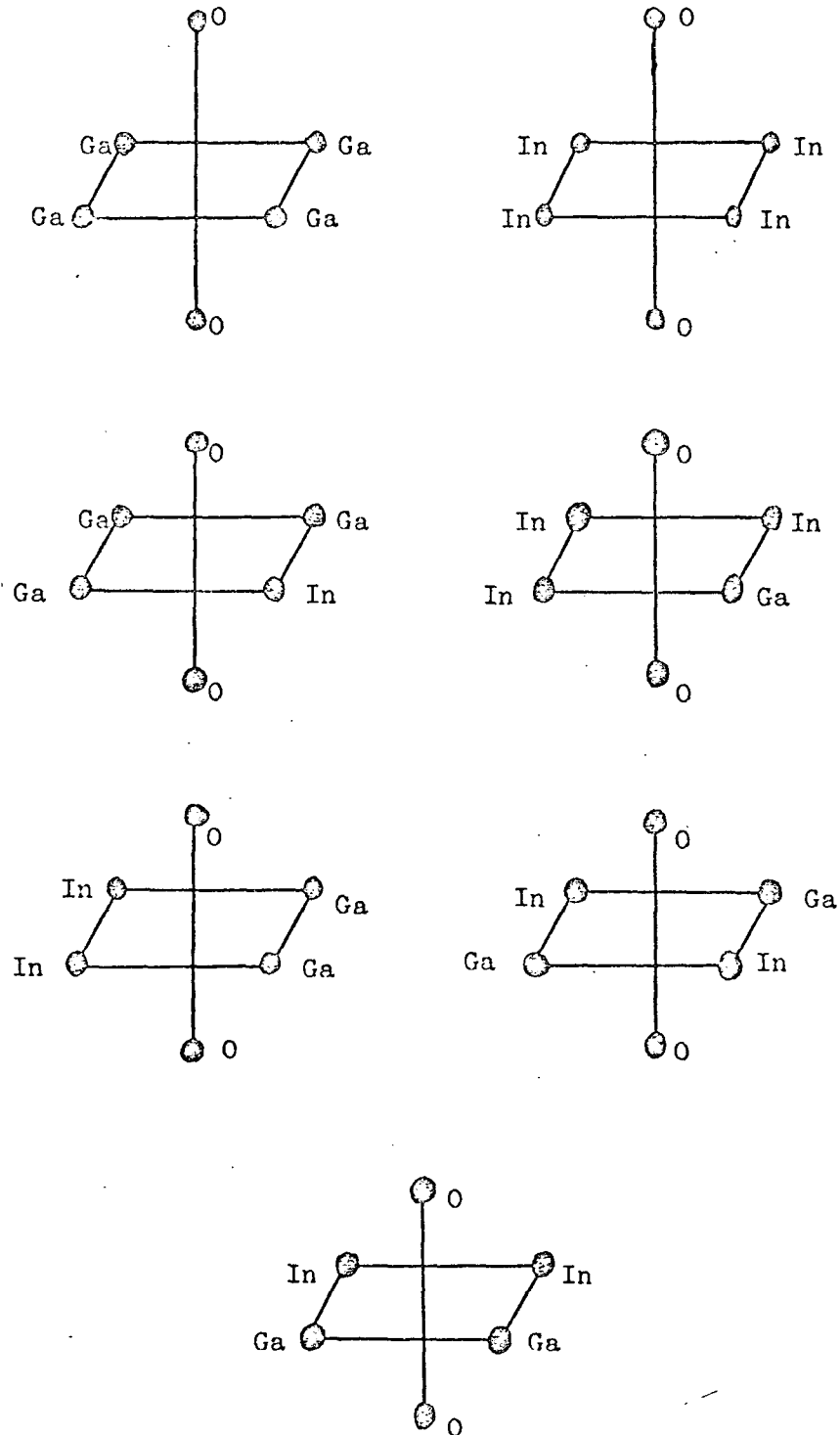


Fig. 6.5-2. InGaO System Dimers.

## CHAPTER 7

## DISCUSSION OF THE RESULTS

The experiments and analyses in the previous chapters have provided a variety of new and interesting information concerning the group III A metal oxides. Three independent investigations gave corroborating evidence for the conclusions reached in the last chapter.

During the mass spectrometric study several new molecules, including  $\text{Al}_3\text{O}_2$ ,  $\text{Ga}_3\text{O}$ ,  $\text{In}_3\text{O}$ ,  $\text{In}_4\text{O}_2$ ,  $\text{InTaO}$ ,  $\text{InTaO}_2$ , and  $\text{In}_2\text{WO}_4$ , were discovered in low concentrations. The  $\text{In}_4\text{O}_2$  molecule is the dimer of the suboxide, and it was important to considerations in the present investigations. It was also shown that the stable M-O species did not exist in the vapor phase above the metal and metal sesquioxide except for the aluminum system where it was found in very low concentrations.

Similarly, it was determined that the group III A metals do react with  $\text{O}_2$  in an inert matrix to form the metal superoxide with  $\text{C}_{2v}$  symmetry. The three vibrational modes were detected for  $\text{InO}_2$  and  $\text{TlO}_2$  in which  $\nu_1 > \nu_3 > \nu_2$ . The data were incomplete for  $\text{AlO}_2$  and  $\text{GaO}_2$ . Each molecule was found to have one absorption near that of an isolated  $\text{O}_2^{-1}$  species. This indicated that the bonding was highly ionic. The molecule may be considered as a metal cation bonded to the superoxide anion by Coulombic forces. It was difficult to determine an apex angle since the central force field approximation is unreliable for obtaining this information. However, in consideration of the force constants and internuclear separations, an O-M-O angle of  $\sim 40^\circ$  was chosen for both  $\text{InO}_2$  and  $\text{TlO}_2$ . It would be necessary to

perform reactions with enriched  $O_2$  to verify the angles and force constants.

The results of the metal reaction experiments were useful in analyzing the isotopic study of the suboxides. Here, the  $\nu_3$  modes were verified as belonging to the suboxides, and bond angles were calculated and found to be in agreement with the literature values for  $Al_2O$  and  $In_2O$ . There was an unexplainable but consistent discrepancy for  $Ga_2O$ .

The previously assigned  $\nu_1$  and  $\nu_2$  modes for  $Al_2O$  and  $Ga_2O$  were found to be absorptions from another species which formed upon diffusion and had two equivalent oxygens. Further attempts at determining the  $\nu_1$  and  $\nu_2$  modes for the suboxides were unsuccessful and it was possible only to estimate their values. With the aid of the mass spectrometric and superoxide investigation, it was determined that the suboxide dimer  $M_4O_2$  was being formed in the matrix and was responsible for the two unassigned bands in each system. This was verification of the report of Brom *et al.*<sup>18</sup> on  $Tl_2O$  and the recent conjecture of Knight and Weltner<sup>39</sup> for the  $Al_2O$  system. During the final preparation of this thesis, a note by Hinchcliffe and Ogden<sup>63</sup> was published. These authors had investigated the  $Ga_2O$  and  $In_2O$  systems and had drawn the same conclusion, as reported here, that the two absorptions found by Makowiecki were from the  $M_4O_2$  dimer. Their isotopic data for  $(Ga_2^{18}O)_2$  are equivalent to that reported in Chapter 5. Their  $(In_2^{18}O)_2$  data are consistent with the values calculated in Chapter 6. None of the above authors made a prediction of the dimer structure.

APPENDIX 1

EQUATIONS FOR  $M_4O_2$  VIBRATIONS

This appendix presents the details of the method used to correlate the experimentally determined vibrational frequencies for  $M_4O_2$  with force constants and structural parameters. The method was adapted from that of Ramsay<sup>62</sup> for an analysis of dioxane.

The vibrational equations for the  $C_{2h}$  configuration of  $M_4O_2$  have been obtained using the vector method applied previously to the chair configuration of the dioxane molecule. The dimer molecule was treated as six mass points situated at the vertices of a puckered hexagon as illustrated in Fig. A.1-1. All bond angles were assumed to be equal for ease of calculation. A simple valence force field was applied to the molecule with the potential energy  $V$  expressed by the equation

$$2V = \sum_{ij} k_{ij} q_{ij}^2 + \sum_i c_i \alpha_i^2 \quad (\text{A.1-1.})$$

where  $q_{ij}$  is the change in the bond length  $s_{ij}$  and  $\alpha_i$  is the change in the bond angle  $\gamma_i$ .

The normal vibrations, obtained by using symmetry relations and the property that all normal vibrations must be mutually orthogonal, and the symmetry co-ordinates are illustrated in the text by Ramsay.<sup>62</sup>

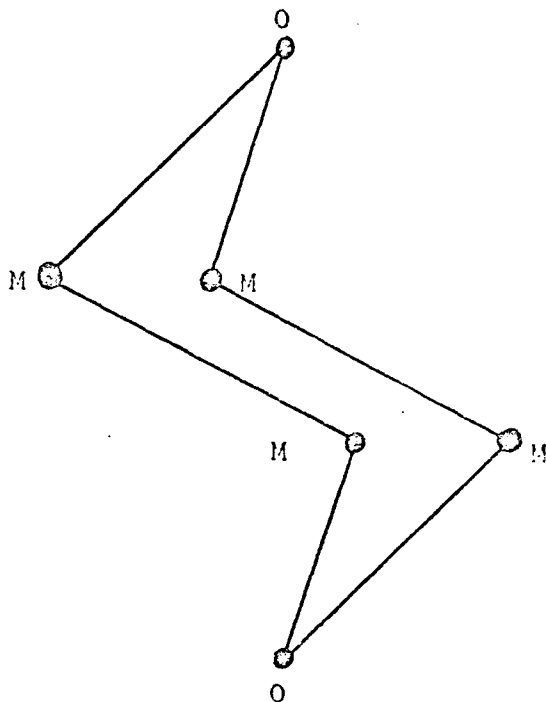
The following abbreviations were made to simplify the equations:

$$c = \cos \gamma, \quad s = \sin \gamma, \quad M = \frac{1}{m_a} + \frac{1}{m_b}$$

$$L_1 = \frac{1}{m_a s_a^2}, \quad L_2 = \frac{1}{m_b s_a^2}, \quad L_3 = \frac{1}{m_b s_b^2}, \quad L_4 = \frac{1}{m_b s_a s_b},$$

$$M_1 = 2s_a^2 L_2, \quad M_2 = 1/2cM_1, \quad M_3 = -sL_1 s_a, \quad M_4 = -sL_2 s_a,$$

$$M_5 = M + cL_1 s_a^2, \quad M_6 = M - cL_1 s_a^2, \quad M_7 = -1/2s(L_1 + L_4) s_a,$$



Definitions:

$m_a$  = mass of O atom

$m_b$  = mass of M atom

$s_a$  = length of M-O bond

$s_b$  = length of M-M bond

$k_a$  = stretching constant of M-O bond

$k_b$  = stretching constant of M-M bond

$c_a$  = deformation constant of M-O-M bond angle

$c_b$  = deformation constant of O-M-M bond angle

Fig. A.1-1.  $M_4O_2$  dimer structure.

$$\begin{aligned}
M_8 &= 1/2s (L_1 - L_4) s_a, & M_9 &= M_7 - sL_4 s_a, & M_{10} &= M_8 - sL_4 s_a, \\
M_{11} &= 2(1-c) L_1 + 2L_2, & M_{12} &= (2L_1 + L_2 + L_3) + 1/2 c (L_1 - 2L_4), \\
M_{13} &= -1/2 (L_1 + L_2 + 2L_4 - cL_1), & M_{14} &= M_{12} - (2 + c) L_1, \\
M_{15} &= M_{13} + (2 + c) L_4, & M_{16} &= M_{14} + 2(L_3 - cL_4), \\
M_{17} &= M_{16} + (2 + c) L_1.
\end{aligned}$$

The symmetry co-ordinates were substituted into the equations of motion and the vibration equations were obtained. These may be expressed in the determinantal form as follows:

$$\text{Class } A_g, \quad \begin{vmatrix} (k_a M_5 - v^2) & k_b M_2 & c_a M_3 & c_b M_8 \\ 2k_a M_2 & (k_b M_1 - v^2) & -c_a M_4 & 2c_b M_4 \\ 2k_a M_3 & -k_b M_4 & (c_a M_{11} - v^2) & 2c_b M_{15} \\ k_a M_8 & k_b M_4 & c_a M_{15} & (c_b M_{12} - v^2) \end{vmatrix} = 0.$$

$$\text{Class } A_u, \quad \begin{vmatrix} (k_a M_6 - v^2) & k_b M_2 & c_b M_m \\ 2k_a M_2 & (k_b M_1 - v^2) & 2c_b M_4 \\ k_a M_m & k_b M_4 & (c_b M_{14} - v^2) \end{vmatrix} = 0.$$

$$\text{Class } B_g, \quad \begin{vmatrix} (k_a M_6 - v^2) & c_b M_9 \\ k_a M_9 & (c_b M_{16} - v^2) \end{vmatrix} = 0.$$

$$\text{Class } B_u, \quad \begin{vmatrix} (k_a M_5 - v^2) & c_a M_3 & c_b M_{10} \\ 2k_a M_3 & (c_a M_{11} - v^2) & 2c_b M_{13} \\ k_a M_{10} & c_a M_{13} & (c_b M_{17} - v^2) \end{vmatrix} = 0.$$

The  $A_u$  and  $B_u$  modes are infrared active and the  $A_g$  and  $B_g$  modes are Raman active.

## APPENDIX 2

## THERMODYNAMIC FUNCTIONS FOR TWO

## GROUP III A METAL SUPEROXIDES

Thermodynamic functions are tabulated in Tables A.2-1 and A.2-2 for the ideal gaseous molecules  $\text{InO}_2$  and  $\text{TlO}_2$ . These properties were calculated from statistical mechanical equations given by Stull and Prophet<sup>64</sup> with the use of molecular parameters based on this research and other sources as given in Section 6.3. The twofold degeneracy appropriate to the unpaired electron spin has been included in the entropy and free energy functions. It is assumed that there are no excited electronic states at sufficiently low energy to contribute significantly.

Table A.2-1. Thermodynamic Functions for  $\text{InO}_2$ .

$\text{InO}_2$  Ideal triatomic gas  
 Molecular weight 146.8181 gm/mole  
 Point group  $C_{2v}$   $\sigma = 2$

Vibrational Frequencies and Degeneracies ( $\text{cm}^{-1}$ )

1082.3 (1)  
 332.2 (1)  
 456.4 (1)

Internuclear distances In-O = 2.15 Å  
 and angles  $\angle$  O-In-O =  $40^\circ$

Moments of inertia  $I_A = 16.959 \times 10^{-39}$  gm  $\text{cm}^2$   
 $I_B = 2.873 \times 10^{-39}$  gm  $\text{cm}^2$   
 $I_C = 19.833 \times 10^{-39}$  gm  $\text{cm}^2$

<u>T(K)</u> <u>(deg)</u>	<u><math>H_T^0 - H_0^0</math></u> <u>(cal/mole)</u>	<u><math>S_T^0</math></u> <u>(cal/mole deg)</u>	<u><math>-(G_T^0 - H_0^0) / T</math></u> <u>(cal/mole deg)</u>
100	8.05	56.07	48.03
200	8.69	64.47	53.78
298.15	9.35	66.73	57.38
400	9.92	70.14	60.21
500	10.38	72.86	62.48
600	10.76	75.16	64.40
700	11.07	77.16	66.09
800	11.33	78.91	67.58
900	11.55	80.47	68.93
1000	11.73	81.89	70.16
1500	12.35	87.39	75.04
2000	12.70	91.35	78.65

Table A.2-2. Thermodynamic Functions for  $\text{TlO}_2$ .

$\text{TlO}_2$  Ideal triatomic gas  
 Molecular weight 236.88 gm/mole  
 Point group  $C_{2v}$   $\sigma = 2$

Vibrational Frequencies and Degeneracies ( $\text{cm}^{-1}$ )

1082.1 (1)  
 295.9 (1)  
 432.9 (1)

Internuclear distances  $\text{Tl-O} = 2.26 \text{ \AA}$   
 and angles  $\angle \text{O-Tl-O} = 40^\circ$

Moments of inertia  $I_A = 20.718 \times 10^{-39} \text{ gm cm}^2$   
 $I_B = 3.174 \times 10^{-39} \text{ gm cm}^2$   
 $I_C = 23.892 \times 10^{-39} \text{ gm cm}^2$

$T(\text{K})$ (deg)	$H_T^\circ - H_0^\circ$ (cal/mole)	$S_T^\circ$ (cal/mole deg)	$-(G_T^\circ - H_0^\circ) / T$ (cal/mole deg)
100	8.09	58.04	49.95
200	8.81	64.58	55.77
298.15	9.49	68.91	59.42
400	10.05	72.34	62.29
500	10.50	75.08	64.58
600	10.86	77.39	66.53
700	11.16	79.39	68.23
800	11.41	81.15	69.73
900	11.62	82.71	71.09
1000	11.80	84.13	72.32
1500	12.40	89.64	77.24
2000	12.74	93.59	80.85

## BIBLIOGRAPHY

1. W. Klemperer, J. Chem. Phys. 24, 353 (1955).
2. W. Klemperer and L. Lindeman, J. Chem. Phys. 25, 397 (1956).
3. A. Büchler and W. Klemperer, J. Chem. Phys. 29, 121 (1958).
4. A. M. Bass and H. P. Broida, eds., The Formation and Trapping of Free Radicals, Academic Press, New York, (1960).
5. W. Weltner, Proc. Int. Symp. Condensation and Evaporation of Solids, p. 243 (1964).
6. A. J. Barnes and H. E. Hallam, Quarterly Review 23, 392 (1969).
7. L. Brewer and A. W. Searcy, J. Am. Chem. Soc. 73, 5308 (1951).
8. C. J. Frosch and D. C. Thurmond, J. Phys. Chem. 66, 877 (1962).
9. S. A. Shchukarev, G. A. Semenov, and I. A. Ratkovskii, Russ. J. Inorg. Chem. 14, 1 (1969).
10. C. N. Cochran and L. M. Foster, J. Electrochem. Soc. 109, 144 (1962).
11. D. Cubicciotti, High Temp. Sci. 1, 11 (1969).
12. D. Cubicciotti, High Temp. Sci. 2, 213 (1970).
13. D. M. Makowiecki, "Infrared Spectra of the Group III A Metal Suboxides," Ph.D. Thesis, Case Western Reserve University, January, 1971.
14. A. A. Mal'tsev and V. F. Shevel'kov, Teplofiz. Vysok. Temp. 2, 650 (1964).
15. M. J. Linevsky, D. White, and D. E. Mann, J. Chem. Phys. 41, 542 (1964).
16. A. J. Hinchcliffe and J. S. Ogden, Chem. Comm. 18, 1053 (1969).
17. A. Snelson, J. Phys. Chem. 74, 2574 (1970).
18. J. M. Brom, Jr., T. Devore, and H. F. Franzen, J. Chem. Phys. 54, 2742 (1971).
19. D. M. Makowiecki, D. A. Lynch, Jr., and K. D. Carlson, J. Phys. Chem. 75, 1963 (1971).

20. L. Andrews, *J. Am. Chem. Soc.* 90, 7368 (1968).
21. L. Andrews, *J. Chem. Phys.* 50, 4288 (1969).
22. L. Andrews, *J. Phys. Chem.* 73, 3922 (1969).
23. L. Andrews, *J. Chem. Phys.* 54, 4935 (1971).
24. N. G. Rambidi and S. M. Tolmachev, *Teplofiz. Vysok Temp.* 3, 487 (1965).
25. N. G. Rambidi and YW. S. Ezhov, *Zhur. Strukt. Khim.* 9, 363 (1968).
26. A. Büchler, J. L. Stauffer, W. Klemperer, and L. Wharton, *J. Chem. Phys.* 39, 2299 (1963).
27. G. Herzberg, Molecular Spectra and Molecular Structure. II. Infrared and Raman Spectra of Polyatomic Molecules, (D. Van Nostrand and Co., Princeton, N. J., 1945), p. 228.
28. F. P. Coheur and B. Rosen, *Bull. Soc. Roy. Sci. (Liège)* 10, 405 (1941).
29. J. S. Ogden, A. J. Hinchcliffe, and J. S. Anderson, *Nature* 226, 940 (1970).
30. V. F. Shevel'kov, N. A. Klyuev, and A. A. Malt'sev, *Vestn. Mosk. Univ. Khim.* 24, 32 (1969).
31. R. P. Burns, *J. Chem. Phys.* 44, 3307 (1966).
32. R. P. Burns, G. DeMaria, J. Drowart, and M. G. Inghram, *J. Chem. Phys.* 38, 1035 (1963).
33. S. Antkiv and V. H. Dibeler, *J. Chem. Phys.* 21, 1890 (1953).
34. M. Farber, R. D. Srivastava, and O. M. Uy, *J. Chem. Phys.* 55, 4142 (1971).
35. J. W. C. Johns, *Can. J. Phys.* 39, 1738 (1961).
36. A. Sommer, D. White, M. J. Linevsky, and D. E. Mann, *J. Chem. Phys.* 38, 87 (1963).
37. A. D. Walsh, *J. Chem. Soc.* 1953, 2266.
38. L. Brewer and G. M. Rosenblatt, "Dissociation Energies and Free Energy Functions of Gaseous Monoxides," in Advances in High Temperature Chemistry, v.2, L. Eyring, ed., (Academic Press, New York, 1969), p. 1.

39. L. B. Knight, Jr. and W. Weltner, Jr., *J. Chem. Phys.* 55, 5066 (1971).
40. O. M. Uy and J. Drowart, *Trans. Faraday Soc.* 67, 1293 (1971).
41. R. T. Grimley, "Mass Spectrometry" in The Characterization of High Temperature Vapors, J. L. Margrave, ed., (John Wiley and Sons, New York, 1967), p. 195.
42. J. Drowart and P. Goldfinger, *Angew. Chemie Int. Ed.* 6, 581 (1967).
43. M. G. Inghram and J. Drowart, in High Temperature Technology, (McGraw-Hill, New York, 1960), pp. 219-240.
44. C. A. Stearns and F. J. Kohl, NASA TN D-5027 (1969).
45. F. J. Kohl and C. A. Stearns, NASA TN D-5646 (1970).
46. R. W. Kiser, Introduction to Mass Spectrometry (Prentice-Hall, New York, 1965).
47. J. Drowart, G. DeMaria, R. P. Burns, and M. G. Inghram, *J. Chem. Phys.* 32, 1366 (1960).
48. J. Dewar, *Proc. Roy. Soc. (London)* 68, 360 (1901).
49. E. B. Whittle, D. A. Dows, and G. C. Pimentel, *J. Chem. Phys.* 22, 1943 (1954).
50. M. J. Linevsky, *J. Chem. Phys.* 34, 587 (1961).
51. K. R. Thompson, "Infrared Spectra of Some Transition Metal Dihalide Molecules," Ph.D. Thesis, Case Western Reserve University, June, 1968.
52. K. D. Carlson, "The Knudsen Effusion Method," loc. cit., ref. 41, p. 115.
53. J. Gaffney and J. R. Clement, *Rev. Sci. Instr.* 26, 620 (1955).
54. D. Bhogeswara Rao and K. Motzfeldt, *Acta. Chem. Scand.* 24, 2796 (1970).
55. R. Multgren, R. L. Orr, P. D. Anderson, and K. K. Kelley, Selected Values of Thermodynamic Properties of Metals and Alloys, John Wiley and Sons, Inc., (1963).
56. M. Hoch and R. Ramakrishnan, AFML-TR-68-60.